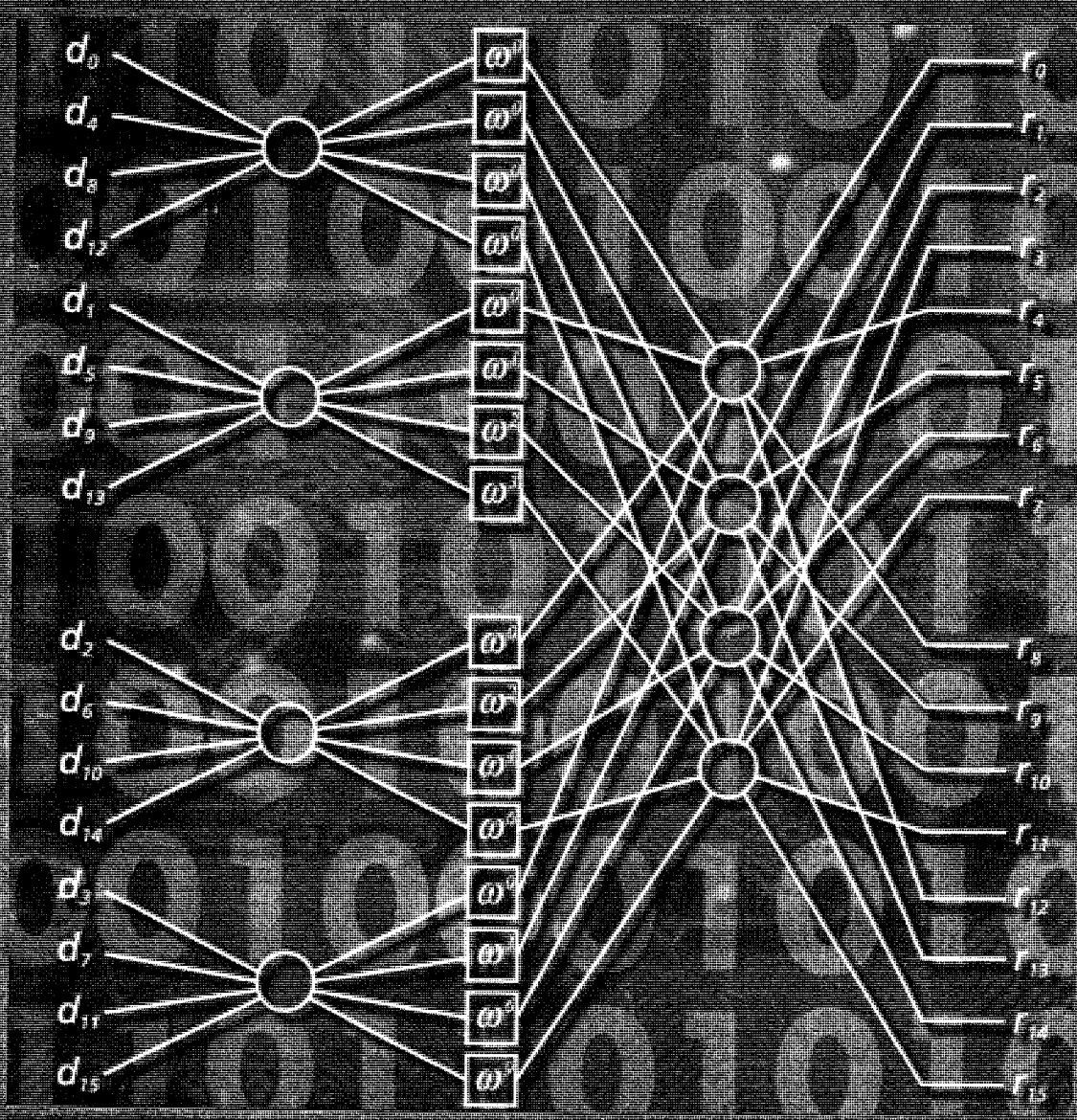


OFDM FOR WIRELESS MULTIMEDIA COMMUNICATIONS



RICHARD VAN NEE
RAMJEE PRASAD

OFDM FOR WIRELESS
MULTIMEDIA COMMUNICATIONS

VAN NEE
PRASAD



Rao S.

OFDM for Wireless Multimedia Communications

For a listing of recent titles in the *Artech House Universal Personal Communications Series*, turn to the back of this book.

OFDM for Wireless Multimedia Communications

Richard van Nee
Ramjee Prasad



Artech House
Boston • London

Library of Congress Cataloging-in-Publication Data

van Nee, Richard.

OFDM for wireless multimedia communications / Richard van Nee, Ramjee Prasad.
p. cm. — (Artech House universal personal communications library)

Includes bibliographical references and index.

ISBN 0-89006-530-6 (alk. paper)

1. Wireless communication systems. 2. Multimedia systems. 3. Multiplexing.

I. Prasad, Ramjee. II. Title. III. Series.

TK5103.2.N44 2000

621.3845—dc21

99-052312

CIP

British Library Cataloguing in Publication Data

van Nee, Richard

OFDM for wireless multimedia communications. — (Artech House
universal personal communications library)

1. Wireless communication systems 2. Multimedia systems

I. Title II. Prasad, Ramjee

621.3'82

ISBN 0-89006-530-6

Cover design by Igor Valdman

© 2000 Richard van Nee and Ramjee Prasad

All rights reserved. Printed and bound in the United States of America. No part of this book may be reproduced or utilized in any form or by any means, electronic or mechanical, including photocopying, recording, or by any information storage and retrieval system, without permission in writing from the authors.

All terms mentioned in this book that are known to be trademarks or service marks have been appropriately capitalized. Artech House cannot attest to the accuracy of this information. Use of a term in this book should not be regarded as affecting the validity of any trademark or service mark.

International Standard Book Number: 0-89006-530-6

Library of Congress Catalog Card Number: 99-052312

10 9 8 7 6 5 4 3

*To my wife Iris, to our son Floris, to our daughters Roselinde and Mirrelijn, and to our
newly born baby
—Richard van Nee*

*To my wife Jyoti, to our daughter Neeli, and to our sons Anand and Rajeev
—Ramjee Prasad*

Contents

Preface		xiii
Acknowledgments		xvii
Chapter 1	Introduction	1
1.1	Standardization and Frequency Bands	4
1.2	Multimedia Communications	7
1.2.1	The Need for High Data Rates	8
1.2.2	Services and Applications	9
1.2.3	Antennas and Batteries	9
1.2.4	Safety Considerations	10
1.2.5	ATM-Based Wireless (Mobile) Broadband Multimedia Systems	12
1.3	Multipath Propagation	15
1.3.1	Multipath Channel Models	16
1.3.2	Delay Spread Values	17
1.4	Time Variation of the Channel	19
1.5	History of OFDM	20
1.6	Preview of the Book	24
References		25
Chapter 2	OFDM Basics	33
2.1	Introduction	33
2.2	Generation of Subcarriers using the IFFT	33
2.3	Guard Time and Cyclic Extension	39
2.4	Windowing	42
2.5	Choice of OFDM Parameters	46
2.6	OFDM Signal Processing	47
2.7	Implementation Complexity of OFDM Versus Single Carrier Modulation	48

References	51
Chapter 3	Coding and Modulation 53
3.1	Introduction 53
3.2	Forward Error Correction Coding 54
3.2.1	Block Codes 54
3.2.2	Convolutional Codes 55
3.2.3	Concatenated Codes 58
3.3	Interleaving 59
3.4	Quadrature Amplitude Modulation 60
3.5	Coded Modulation 62
References	70
Chapter 4	Synchronization 73
4.1	Introduction 73
4.2	Sensitivity to Phase Noise 74
4.3	Sensitivity to Frequency Offset 77
4.4	Sensitivity to Timing Errors 78
4.5	Synchronization using the Cyclic Extension 80
4.6	Synchronization using Special Training Symbols 86
4.7	Optimum Timing in the Presence of Multipath 88
References	92
Chapter 5	Coherent and Differential Detection 95
5.1	Introduction 95
5.2	Coherent Detection 95
5.2.1	Two Dimensional Channel Estimators 96
5.2.2	One Dimensional Channel Estimators 103
5.2.3	Special Training Symbols 104
5.2.4	Decision Directed Channel Estimation 106
5.3	Differential Detection 107
5.3.1	Differential Detection in the Time Domain 107

5.3.2	Differential Detection in the Frequency Domain	112
5.3.3	Differential Amplitude and Phase Shift Keying	115
References		117
Chapter 6	The Peak Power Problem	119
6.1	Introduction	119
6.2	Distribution of the Peak-to-Average Power Ratio	120
6.3	Clipping and Peak Windowing	123
6.3.1	Required Backoff with a Non-Ideal Power Amplifier	127
6.3.2	Coding and Scrambling	130
6.4	Peak Cancellation	131
6.5	PAP Reduction Codes	138
6.5.1	Generating Complementary Codes	141
6.5.2	Minimum Distance of Complementary Codes	144
6.5.3	Maximum Likelihood Decoding of Complementary Codes	145
6.5.4	Suboptimum Decoding of Complementary Codes	147
6.5.5	Large Code Lengths	150
6.6	SYMBOL Scrambling	150
References		153
Chapter 7	Basics of CDMA	155
7.1	Introduction	155
7.2	CDMA: Past, Present, and Future	156
7.3	CDMA Concepts	157
7.3.1	Pure CDMA	161
7.4	Basic DS-CDMA Elements	171
7.4.1	RAKE Receiver	171
7.4.2	Power Control	172
7.4.3	Soft Handover	173
7.4.4	Interfrequency Handover	175
7.4.5	Multiuser Detection	175

References	176
Chapter 8	Multi - Carrier CDMA
8.1	Introduction
8.2	Channel Model
8.3	DS-CDMA and MC-CDMA Systems
8.3.1	DS-CDMA System
8.3.2	MC-CDMA System
8.4	MC-CDMA System Design
8.5	BEP LOWER Bound
8.5.1	DS-CDMA System
8.5.2	MC-CDMA System
8.5.3	BEP Lower Bound Equivalence
8.6	Numerical Results
8.6.1	MC-CDMA System Design
8.6.2	Down - Link BEP Performance
8.6.3	Up - Link BER Performance
8.7	Conclusions
Appendix 8A	
References	
Chapter 9	Orthogonal Frequency Division Multiple Access
9.1	Introduction
9.2	Frequency Hopping OFDMA
9.3	Differences between OFDMA and MC-CDMA
9.4	OFDMA System Description
9.4.1	Channel Coding
9.4.2	Modulation
9.4.3	Time and Frequency Synchronization
9.4.4	Initial Modulation Timing Synchronization
9.4.5	Initial Frequency Offset Synchronization

9.4.6	Synchronization Accuracy	222
9.4.7	Power Control	223
9.4.8	Random Frequency Hopping Operation	224
9.4.9	Dynamic Channel Allocation (Fast DCA)	225
9.4.10	Dynamic Channel Allocation (Simple DCA)	227
9.4.11	Capacity of OFDMA	227
9.5	Conclusions	227
References		228
Chapter 10	Applications of OFDM	229
10.1	Introduction	229
10.2	Digital Audio Broadcasting	229
10.3	Terrestrial Digital Video Broadcasting	231
10.4	Magic WAND	233
10.4.1	Magic WAND Physical Layer	234
10.4.2	Coding	236
10.4.3	Simulated Error Probabilities	236
10.4.4	Effects of Clipping	237
10.4.5	Magic WAND Medium Access Control Layer	238
10.5	IEEE 802.11, HIPERLAN/2, and MMAC Wireless LAN Standards	241
10.5.1	OFDM Parameters	243
10.5.2	Channelization	244
10.5.3	OFDM Signal Processing	245
10.5.4	Training	246
10.5.5	Differences between IEEE 802.11, HIPERLAN/2 and MMAC	249
10.5.6	Simulation Results	250
References		252
About the Authors		255
Index		257

Preface

सर्वद्वारेषु देहेऽस्मिन् प्रकाश उपजायते ।
ज्ञानं यदा तदा विद्याद् विवृद्धं सत्त्वमित्युत

*sarva-dvāreṣu dehe 'smin
prakāśa upajāyate
jñānaṁ yadā tadā vidyād
vivṛddhaṁ sattvam ity uta*

**The manifestations of the mode of goodness can be experienced when all
the gates of the body are illuminated by knowledge**

The Bhagavad Gita (14.11)

During the joint supervision of a Master's thesis "The Peak-to-Average Power Ratio of OFDM," of Arnout de Wild from Delft University of Technology, The Netherlands, we realized that there was a shortage of technical information on orthogonal frequency division multiplexing (OFDM) in a single reference. Therefore, we decided to write a comprehensive introduction to OFDM. This is the first book to give a broad treatment to OFDM for mobile multimedia communications. Until now, no such book was available in the market. We have attempted to fill this gap in the literature.

Currently, OFDM is of great interest by the researchers in the Universities and research laboratories all over the world. OFDM has already been accepted for the new wireless local area network standards from IEEE 802.11, High Performance Local Area Network type 2 (HIPERLAN/2) and Mobile Multimedia Access Communication (MMAC) Systems. Also, it is expected to be used for the wireless broadband multimedia communications.

OFDM for Wireless Multimedia Communications is the first book to take a comprehensive look at OFDM, providing the design guidelines one needs to maximize benefits from this important new technology. The book gives engineers a solid base for assessing the performance of wireless OFDM systems. It describes the new OFDM-based wireless LAN standards; examines the basics of direct-sequence and frequency-hopping CDMA, helpful in understanding combinations of OFDM and CDMA. It also looks at applications of OFDM, including digital audio and video broadcasting, and wireless ATM. Loaded with essential figures and equations, it is a must-have for practicing communications engineers, researchers, academics, and students of communications technology.

Chapter 1 presents a general introduction to wireless broadband multimedia communication systems (WBMCS), multipath propagation, and the history of OFDM. A part of this chapter is based on the contributions of Luis Correia from the Technical University of Lisbon, Portugal, Anand Raghawa Prasad from Lucent Technologies, and Hiroshi Harada from the Communications Research Laboratory, Ministry of Posts and Telecommunications, Yokosuka, Japan.

Chapters 2 to 5 deal with the basic knowledge of OFDM including modulation and coding, synchronization, and channel estimation, that every post-graduate student as well as practicing engineers must learn. Chapter 2 contains contributions of Rob Kopmeiners from Lucent Technologies on the FFT design.

Chapter 6 describes the peak-to-average power problem, as well as several solutions to it. It is partly based on the contribution of Arnout de Wild.

Basic principles of CDMA are discussed in Chapter 7 to understand multi carrier CDMA and frequency-hopping OFDMA, which are described in Chapters 8 and 9. Chapter 8 is based on the research contributions from Shinsuke Hara from the University of Osaka, Japan, a postdoctoral student at Delft University of Technology during 1995–96. Chapter 9 is based on a UMTS proposal, with main contributions of Ralf Böhnke from Sony, Germany, David Bhatoolaul and Magnus Sandell from Lucent Technologies, Matthias Wahlquist from Telia Research, Sweden, and Jan-Jaap van de Beek from Lulea University, Sweden.

Chapter 10 was written from the viewpoint of top technocrats from industries, government departments, and policy-making bodies. It describes several applications of OFDM, with the main focus on wireless ATM in the Magic WAND project, and the new wireless LAN standards for the 5 GHz band from IEEE 802.11, HIPERLAN/2 and MMAC. It is partly based on contributions from Geert Awater from Lucent Technologies, and Masahiro Morikura and Hitoshi Takanashi from NTT in Japan and California, respectively.

We have tried our best to make each chapter quite complete in itself. This book will help generate many new research problems and solutions for future mobile multimedia communications. We cannot claim that this book is errorless. Any remarks to improve the text and correct any errors would be highly appreciated.

Acknowledgments

The material in this book originates from several projects at Lucent Technologies and research activities at Delft University of Technology, The Netherlands. A great deal of OFDM-knowledge was acquired during the Magic WAND project, in which several companies jointly managed to build a wireless ATM network demonstrator based on OFDM. We wish to thank all Magic WAND members who were involved in the design of the OFDM modem, in particular Geert Awater, James Hopper, Rob Kopmeiners, Erik Busking, Han Schmitz, Theo Kleijne, Martin Janssen, Jan Kruys, Urs Bernhard, Urs Lott, Alex Grant, James Aldis, Thomas Mark, Rodolfo Mannpelz, and Ari Vaisanen. Another fruitful source of information was the OFDM-based proposal for UMTS, with main contributions coming from Ralf Böhnke, David Bhatoaul, Magnus Sandell, and Jan-Jaap van de Beek.

Richard wishes to thank Masahiro Morikura and Hitoshi Takanashi for all their contributions and the pleasant cooperation on the joint OFDM proposal for the IEEE 802.11 wireless LAN standard. All members of IEEE 802.11 and HiperLAN/2 are thanked for numerous contributions, that greatly improved the quality of the final standards and helped to gain more insight in various OFDM techniques.

Geert Awater and Rob Kopmeiners made contributions and corrected numerous mistakes. Neeli Rashmi Prasad helped to prepare the complete manuscript, freeing us from the enormous burden of editorial requirements. Shinsuke Hara from the University of Osaka, Japan, Hiroshi Harada from the Communications Research Laboratory, Ministry of Posts and Telecommunications, Yokosuka, Japan, Luis Correia from the Technical University of Lisbon, Portugal, Anand Raghawa Prasad from Lucent Technologies, and Arnout de Wild from Siemens, The Netherlands, are deeply acknowledged for their valuable contributions.

After the Magic WAND project, we studied several OFDM options for new high-rate wireless LAN products. A circle was completed by the selection of OFDM for the high rate extension of the IEEE 802.11 wireless LAN standard in July 1998. We hope this book will help to gain insight in the principles and design of OFDM-based systems, in particular the new OFDM-based wireless LAN standards.

*Richard van Nee
Ramjee Prasad
October 1999*

Chapter 1

Introduction

The spectacular growth of video, voice, and data communication over the Internet, and the equally rapid pervasion of mobile telephony, justify great expectations for mobile multimedia. Research and development are taking place all over the world to define the next generation of wireless broadband multimedia communications systems (WBMCS) that may create the “global information village.” Figure 1.1 illustrates the basic concept of the global information village, which consists of various components at different scales ranging from global to picocellular size. As we know, the demand for wireless (mobile) communications and Internet/multimedia communications is growing exponentially. Therefore, it is imperative that both wireless and Internet/multimedia should be brought together. Thus, in the near future, wireless Internet Protocol (IP) and wireless asynchronous transfer mode (ATM) will play an important role in the development of WBMCS.

While present communications systems are primarily designed for one specific application, such as speech on a mobile telephone or high-rate data in a wireless local area network (LAN), the next generation of WBMCS will integrate various functions and applications. WBMCS is expected to provide its users with customer premises services that have information rates exceeding 2 Mbps. Supporting such large data rates with sufficient robustness to radio channel impairments, requires careful choosing of modulation technique. The most suitable modulation choice seems to be orthogonal frequency division multiplexing (OFDM). Before going into the details of OFDM, however, first we give some background information on the systems that will be using it.

The theme of WBMCS is to provide its users a means of radio access to broadband services supported on customer premises networks or offered directly by public fixed networks. WBMCS will provide a mobile/movable wireless extension to

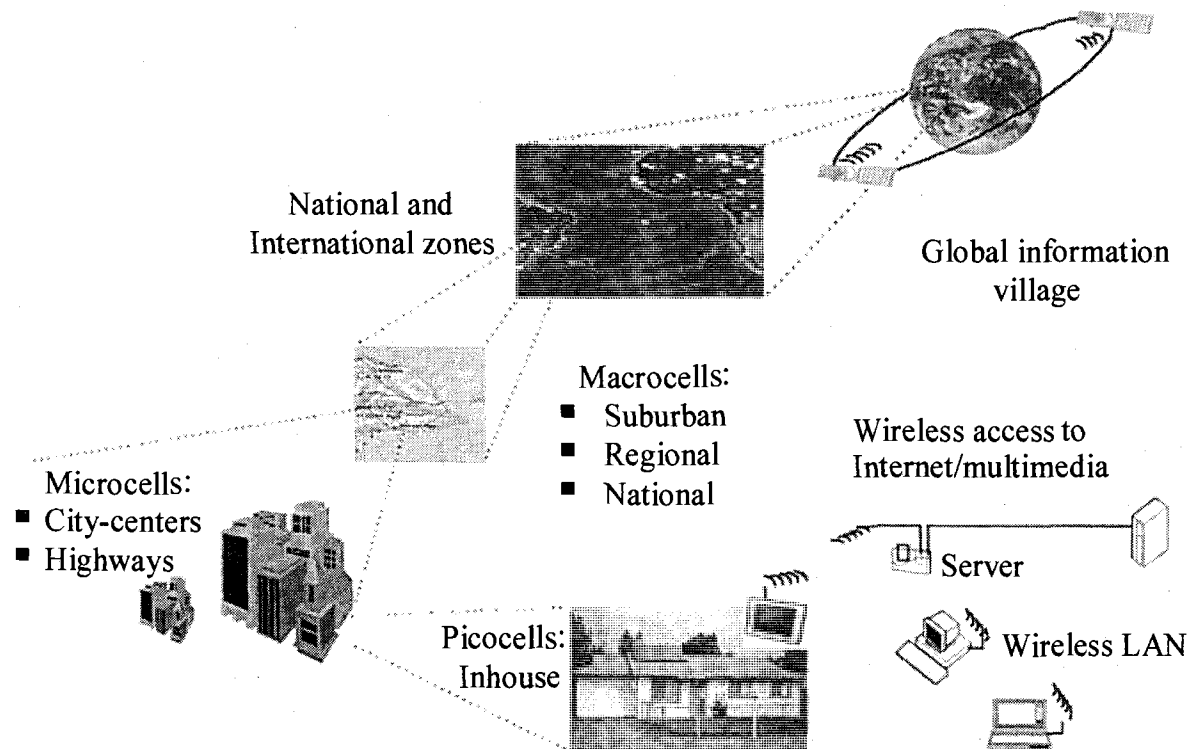


Figure 1.1 Global information village.

WBMCS is under investigation in North America, Europe, and Japan in the microwave and millimeter-wave bands to accommodate the necessary bandwidth. The research in the field of WBMCS has drawn much attention because of the increasing role of multimedia and computer applications in communications. There is a major thrust in three research areas: (1) microwave and millimeter-wave bands for fixed access in outdoor, public commercial networks, (2) evolution of WLAN for inbuilding systems, and (3) use of LAN technology outdoors rather than indoors. In short, WBMCS will provide novel multimedia and video mobile communications services, also related to wireless customer premises network (WCPN) and wireless local loop (WLL).

To implement the wireless broadband communication systems, the following challenges must be considered:

- Frequency allocation and selection;
- Channel characterization;
- Application and environment recognition, including health hazard issues;
- Technology development;
- Air interface multiple access techniques;
- Protocols and networks; and
- Systems development with efficient modulation, coding, and smart antenna techniques.

- Protocols and networks; and
- Systems development with efficient modulation, coding, and smart antenna techniques.

A significant number of research and development (R&D) projects are set up in the area of WBMCS. Within the European Advanced Communication Technologies and Services (ACTS) program are four European Union-funded R&D projects, namely Magic Wand (Wireless ATM Network Demonstrator), ATM Wireless Access Communication System (AWACS), System for Advanced Mobile Broadband Applications (SAMBA), and wireless broadband CPN/LAN for professional and residential multimedia applications (MEDIAN) [1–17]. Table 1.1 summarizes the European projects [11].

In the United States, seamless wireless network (SWAN) and broadband adaptive homing ATM architecture (BAHAMA), as well as two major projects in Bell Laboratories and a wireless ATM network (WATMnet), are being developed in the computer and communications (C&C) research laboratories of Nippon Electric Company (NEC) in the United States [2–6].

In Japan, Communication Research Laboratory (CRL) is working on several R&D projects, such as a broadband mobile communication system in the super high frequency (SHF) band (from 3 to 10 GHz) with a channel bit rate up to 10 Mbps and an indoor high speed WLAN in SHF band with a target bit rate of up to 155 Mbps [12].

In the Netherlands, Delft University of Technology has been busy with a multi-disciplinary research project, “Mobile Multimedia Communication (MMC),” since April 1996. The team consists of experts from the telecommunications and traffic control and information theory groups of the department of Electrical Engineering, the Product Ergonomics group of the department of Industrial Design Engineering, and the Organizational Psychology group of the department of Technology and Society.

The MMC has the following objectives to achieve at 60 GHz:

- Wireless access of 155 Mbps using OFDM;
- Both indoor and outdoor use;
- Less complex, inexpensive mobile stations by moving most functionality to the access points;
- Modified OFDM; and
- Constant bit rate (CBR), variable bit rate (VBR), and available bit rate (ABR) services.

Table 1.1
Summary of European ACTS Projects.

ACTS project	WAND	AWACS	SAMBA	MEDIAN
Parameter				
Frequency	5 GHz	19 GHz	40 GHz	61.2 GHz
Data rate	20 Mbps	70 Mbps	34 Mbps	155 Mbps
Modulation	OFDM, 16 subcarriers with 8-PSK (phase shift keying)	offset quadrature PSK (OQPSK)	OQPSK	OFDM, 512 carriers, differential QPSK (DQPSK)
Cell radius	20–50m (omnidirectional antennas)	50–100m (directional antennas, line-of-sight only)	10–50m (directional antennas at access point)	10m (directional antennas)
Radio access	time division multiple access/ time division duplex (TDMA/TDD)	TDMA/TDD	time division multiple access /frequency division duplex (TDMA/FDD)	TDMA/TDD

1.1 STANDARDIZATION AND FREQUENCY BANDS

There are three main forums for the standardization of wireless broadband communication systems; namely, IEEE 802.11 [18], European Telecommunication Standards Institute Broadband Radio Access Networks (ETSI BRAN) [19], and Multimedia Mobile Access Communications (MMAC) [20]. IEEE 802.11 made the first WLAN standard for the 2.4-GHz Industrial, Scientific, and Medical band (ISM). It specifies the medium access control and three different physical layers—direct-sequence spread spectrum, frequency hopping, and infrared—which give a data rate of 2 Mbps. Products based on this standard became available in 1998. Figure 1.2 shows an example of an IEEE 802.11 modem in a PCMCIA card. Following the initial 1- and 2-Mbps standard, IEEE 802.11 developed two new physical layer standards. One delivers data rates of up to 11 Mbps in the 2.4-GHz band, using complementary code keying [21,22]. Products based on this standard—with the old 1 and 2 Mbps as fallback rates—are available since mid 1999. An industry alliance called the Wireless Ethernet Compatibility Alliance (WECA) has been established to promote the high rate IEEE

available since mid 1999. An industry alliance called the Wireless Ethernet Compatibility Alliance (WECA) has been established to promote the high rate IEEE 802.11 technology and to certify interoperability of products from different vendors [23]. The second IEEE 802.11 standard extension targets a range of data rates from 6 up to 54 Mbps using OFDM in the 5-GHz band [24]. The OFDM standard was developed jointly with ETSI BRAN and MMAC, making OFDM effectively a worldwide standard for the 5-GHz band.

Table 1.2 lists the main characteristics of the IEEE 802.11 and the ETSI High Performance Local Area Network type 2 (HIPERLAN/2) standards. More details about these standards can be found in Chapter 10.

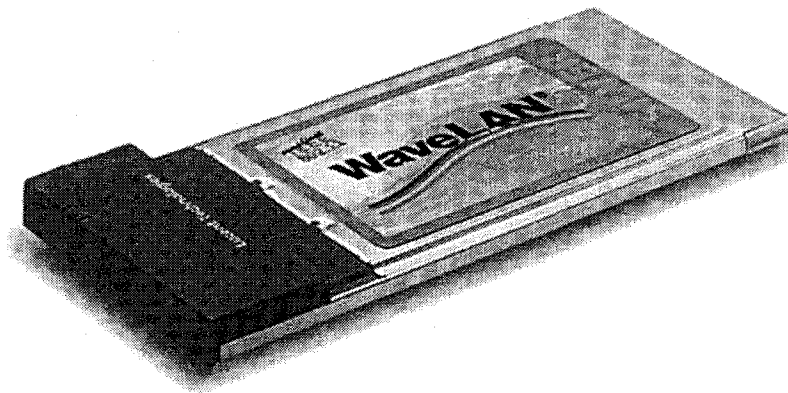


Figure 1.2 IEEE 802.11 modem for the 2.4-GHz band (WaveLAN™ from Lucent Technologies [25]).

Figure 1.3 shows that 2-, 5- and 60-GHz are the commercially important frequency bands because of geographically wide spectrum allocations in Europe, the United States (U.S.), and Japan for the wireless broadband multimedia communications networks. The 2.4-GHz band is an ISM band, which can be used for many types of transmission systems as long as they obey certain power, spectral density, and spreading gain requirements. The 5-GHz band is designated specifically for WBMCS. In Europe, only HIPERLAN devices are currently allowed in this band. HIPERLAN actually consists of a family of standards, one of which is an OFDM-based standard that is very similar to the IEEE 802.11 5-GHz standard. In Japan, MMAC supports both the IEEE 802.11 and the HIPERLAN standards. Notice that Japan only has 100 MHz available in the 5-GHz band, while the United States and Europe provide 300 and 455 MHz, respectively. In Europe, extra spectrum for HIPERLAN is available in the 17-GHz band, while Japan has allocated spectrum from 10- to 16-GHz to mobile broadband systems (MBS). An analysis of the propagation aspects at the bands foreseen for WBMCS microwaves, millimeterwaves, and infrared is presented in [26–31].

Table 1.2
Comparison of IEEE and HIPERLAN standards.

Parameter	IEEE 802.11 2 GHz	IEEE 802.11 5 GHz	HIPERLAN/2
Configurations	Centralized system with access points connected to wired network, or peer-to-peer networking	Centralized system with access points connected to wired network, or peer-to-peer networking	Centralized system with access points connected to wired network
Range	Up to 60m at 11 Mbps and up to 100m at 2 Mbps with omnidirectional antennas	Up to 30m at 24 Mbps and up to 60m at 6 Mbps with omnidirectional antennas	Up to 30m at 24 Mbps and up to 60m at 6 Mbps with omnidirectional antennas
Channel access	CSMA/CA, variable size data packets (up to 8192 bytes)	CSMA/CA, variable size data packets (up to 8192 bytes)	Reservation based access, scheduled by access point. Contention slots for making slot reservations
Frequency bands	2.4-2.4835 GHz	5.150-5.350 GHz; 5.725-5.825 GHz	5.150-5.350 GHz; 5.470-5.725 GHz;
Duplexing	TDD	TDD	TDD
Data rate	1, 2 Mbps (BPSK/QPSK) 5.5, 11 Mbps (CCK)	6, 9 Mbps (BPSK) 12, 18 Mbps (QPSK) 24, 36 Mbps (16-QAM) 54 Mbps (64-QAM)	6, 9 Mbps (BPSK) 12, 18 Mbps (QPSK) 24, 36 Mbps (16-QAM) 54 Mbps (64-QAM)

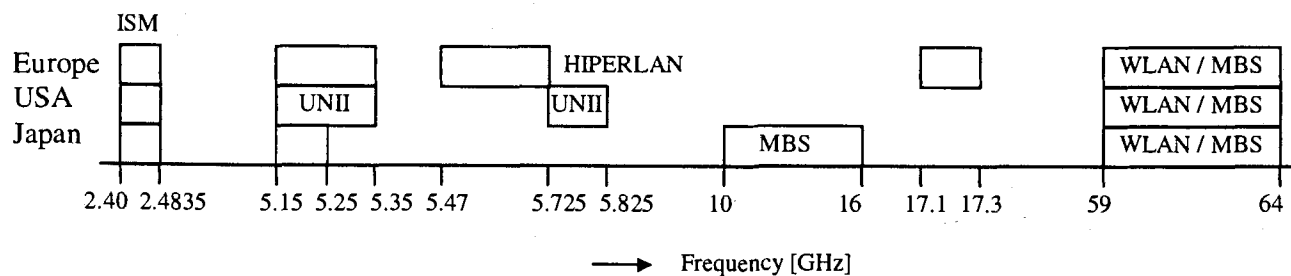


Figure 1.3 Frequency band for wireless broadband communications.

1.2 MULTIMEDIA COMMUNICATIONS

Multimedia and computer communications are playing an increasing role in today's society, creating new challenges to those working in the development of telecommunications systems. Besides that, telecommunications is increasingly relying upon wireless links. Thus, the pressure for wireless systems to cope with increasing data rates is enormous, and WBMCSs with data rates higher than 2 Mbps are emerging rapidly, even if at this moment applications for very high transmission rates do not exist.

Several WBMCSs are being considered for different users with different needs. They may accommodate data rates ranging between 2 and 155 Mbps; terminals can be mobile (moving while communicating) or portable (static while communicating); moving speeds can be as high as that of a fast train; users may or may not be allowed to use more than one channel if their application requires so; the system bandwidth may be fixed, or dynamically allocated according to the user's needs; communication between terminals may be direct or must go through a base station; possible ATM technology use; and so on. Many other cases can be listed as making the difference between various perspectives of a WBMCS, but two major approaches are emerging: WLANs directed to communication among computers, from which IEEE 802.11 [16, 18] and HIPERLAN [19, 20] are examples, with MBS [17] intended as a cellular system providing full mobility to B-ISDN users.

The different requirements imposed by the various approaches to WBMCSs have consequences on system design and development. The tradeoffs between maximum flexibility on one hand and complexity and cost on the other are always difficult to decide, as they have an impact not only on the deployment of a system, but also on its future evolution and market acceptance. GSM is a good example of a system foreseen to accommodate additional services and capacities to those initially offered, and the fact that operators are already implementing phase 2+ is proof of that.

This means that many decisions must be made on the several WBMCSs that will appear on the market. For IEEE 802.11, for example, those decisions have already been made, as the system will be commercialized in the very near future, but for other systems there are still many undecided aspects. Of course this depends on what are the applications intended to be supported by the systems, and whether these applications are targeted to the mass market or only to some niches. The former (from which mobile telephones are a good example) will certainly include WLANs, because the expansion of personal computers will dictate this application as a great success in WBMCSs; the latter will possibly have television broadcasters among their users (to establish links between HDTV cameras and the central control room).

Not only are market aspects at stake in the development and deployment of WBMCSs, but many technical challenges are posed as well. The transmission of such high data rates over radio in a mobile environment creates additional difficulties,

compared with that of existing systems; these difficulties are augmented by the fact that frequencies higher than UHF are needed to support the corresponding bandwidths, thus pushing mobile technology challenges (size and weight among other things) to frequencies where these aspects were not much considered until now. However, additional challenges are posed to those involved in WBMCSs development: in today's world, where consumers are in the habit of using a communications system that is available in different places (e.g., GSM roaming capability, because users can make and receive telephone calls in an increasing number of countries worldwide), or being able to exchange information among different systems (e.g., the exchange of files between different computer applications and systems), for future use it does not make sense to consider systems that offer a high data rate but do not support these capabilities to some extent.

1.2.1 Need for High Data Rates

Data rate is really what broadband is about. For example, the new IEEE and HIPERLAN standards specify bit rates of up to 54 Mbps, although 24 Mbps will be the typical rate used in most applications. Such high data rates impose large bandwidths, thus pushing carrier frequencies for values higher than the UHF band: HIPERLAN has frequencies allocated in the 5- and 17-GHz bands; MBS will occupy the 40- and 60-GHz bands; and even the infrared band is being considered for broadband WLANs. Many people argue whether there is a need for such high-capacity systems, however, bearing in mind all the compression algorithms developed and the type of applications that do require tens of megabits per second. We can examine this issue from another perspective.

The need for high-capacity systems is recognized by the "Visionary Group" [32], put together by the European Commission, to give a perspective of what should be the hot topics in the telecommunications for research in the next European programs (following R&D in Advanced Communications Technologies for Europe (RACE) and ACTS). In this visionary perspective, to meet the needs of society in the years to come as far as communications is concerned, capacity is one of the major issues to be developed because of the foreseen increase in demand for new services (especially those based on multimedia). Along with this, mobility will impose new challenges to the development of new personal and mobile communications systems.

We can conclude the following: even if at a certain point it may look academic to develop a system for a capacity much higher than what seems reasonable (in the sense that there are no applications requiring such high capacity), it is worthwhile to do so, as almost certainly in the future (which may be not very far off) applications will need those capacities and even more. The story of fiber optics is an example.

1.2.2 Services and Applications

The system concept of a WLAN such as IEEE 802.11 and of a mobile broadband cellular system such as MBS is totally different: each is directed to services and applications that differ in many aspects. A comparison of several systems, based on two of the key features (mobility and data rate), is shown in Figure 1.4 [33], where it is clear that no competition exists between the different approaches.

The applications and services of the various systems are also different. IEEE 802.11 is mainly intended for communications between computers (thus being an extension of wired LANS); nevertheless, it can support real-time voice and image signals, and users are allowed some mobility and can have access to public networks.

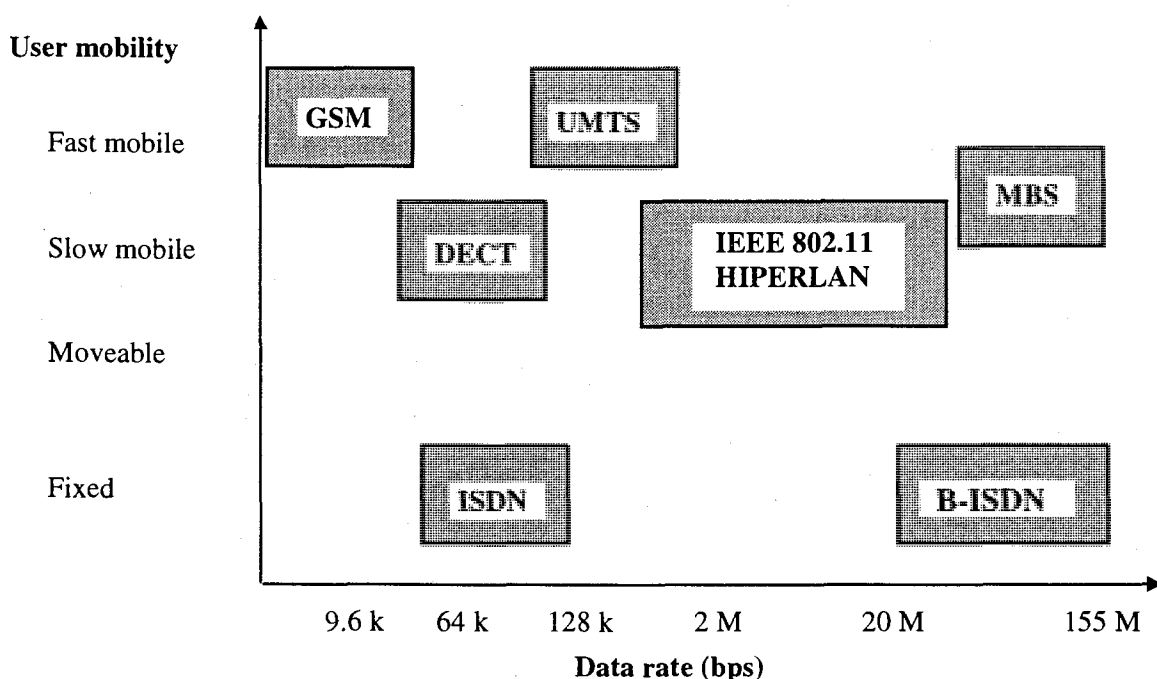


Figure 1.4 Comparison of mobility and data rates for several systems.

1.2.3 Antennas and Batteries

Antennas and batteries play a key role in wireless systems. With the advent of microelectronics and signal processing, antennas and batteries tend to impose the size and weight of mobile terminals. Of course, the higher one goes in frequency, the less developed the technology, and many problems are still found in size and weight at the millimeter-wave band. Power consumption is one example. Though these are likely to be solved in the near future. The number of hours battery-powered equipment can work or operate on stand by, and the percentage of its weight corresponding to the battery, is

not a specific problem of WBMCS. Laptop computers and cellular telephones are the most common terminals relying on batteries these days. This technology continues to demand huge R&D, to extend working time and reduce weight. Although a 100g mobile telephone battery corresponding to several hours of continuous work and a few days on standby is already on the market, users still want more. Mobile multimedia terminals, certainly those to be used in some applications of WBMCSs, will be an extension of the current cellular telephones. Therefore, we foresee that the current problems associated with batteries will be transposed on WBMCS terminals; the same applies to laptops.

Antennas (size, type, technology, etc.) are not a specific problem of WBMCSs as well, but again they are very much related to the type of systems that will be made available for users. It does not make sense to impose restrictions (e.g., pointing in a certain direction or avoiding someone to pass in between) on the type of mobility a mobile terminal can have. Even for portable terminals (e.g., computers), these restrictions make no sense. Hence, there are only two options as far as antennas are concerned: either an omnidirectional antenna (dipole type) or an adaptive array antenna is used. Either way, patch antennas seem a very promising solution for general use in WBMCS. For the frequency bands we consider, isolated patches or adaptive arrays (with many elements) can be made with a small size (e.g., a credit card), thus enabling the terminal not to be limited in size by the antenna system.

The role of antenna radiation patterns is not negligible when discussing system performance, nor is their influence on parameters associated with wave propagation. Although the tradeoff between an omnidirectional and a narrowbeam antenna is not particular of WBMCS, it assumes particular importance at microwave and millimeter waves because of the characteristics of wave propagation at these bands. Using an omnidirectional antenna means a lower gain, but also the possibility of receiving signals from various directions, without the requirement for knowing where the base station is, and allowing the received rays coming from reflections on the propagation scenario. On the other hand, the use of a very directive antenna provides a higher gain, but it must be pointed at the base station and does not receive reflected waves coming from directions very different from the one to which it is pointed. The need for pointing it can be very discouraging, if not a drawback, when a line of sight does not exist. On the other hand, omnidirectional antennas lead to high values of delay spread, but they may ensure that the link still exists, relying on reflections if the line of sight is lost.

1.2.4 Safety Considerations

Until a few years ago, the analysis of possible harmful effects of electromagnetic radiation on people was devoted mainly to power lines and radars, because of the huge power levels involved in those systems. Even when mobile telephone systems appeared, there was no major concern, as the antennas were installed on the roofs of cars. With

the development of personal communication systems, in which users carry mobile telephones inside their coat pockets, and the antenna radiates a few centimeters from the head, safety issues gained great importance and a new perspective. Much research in the literature focuses not only on the absorption of power inside the head, but also on the influence of the head on the antenna's radiation pattern and input impedance. However, these works have addressed only the frequency bands used in today's systems; that is, up to 2-GHz (mainly on the 900- and 1,800-MHz bands), and only very few references are made to systems working at higher frequencies, as it is in the case of WBMCSs.

The problems associated with infrared are different from those posed by microwaves and millimeter waves. Eye safety, rather than power absorption inside the head, is the issue here, because the eye acts as a filter to the electromagnetic radiation, allowing only light and near-frequency radiation to enter into it, and the amount of power absorption inside the human body is negligible. Exposure of the eye to high levels of infrared radiation may cause cataractlike diseases, and the maximum allowed transmitter power seems to limit the range to a few meters [31]. If this is the case, safety restrictions will pose severe limitations to the use of infrared in WBMCSs, as far as general applications are concerned. The question in this case is not that there are always problems during system operation (e.g., mobile telephones), but the damage that may be caused if someone looks at the transmitter during operation.

Microwaves and millimeter waves have no special effect on eyes, other than power absorption. In WLANs, antennas do not radiate very near (1 or 2 cm) to the user as in the mobile telephone case, thus enabling power limitations to be less restrictive; also if mobile multimedia terminals are used as they are in PDAs. But if terminals are used in the same form as mobile telephones, then maximum transmitter powers have to be established, similar to those for the current personal communication systems. The standards for safety levels have already been set in the United States and Europe, as the ones used for UHF extend up to 300 MHz (IEEE/ANSI and CENELEC recommendations are the references). Thus, it is left to researchers in this area to extend their work to higher frequencies, by evaluating SAR (the amount of power dissipated per unit of mass) levels inside the head (or other parts of the human body very near the radiating system), from which maximum transmitter powers will be established. This may not be as straightforward as it seems, however, because the calculation of SAR is usually done by solving integral or differential equations using numerical methods (method of moments or finite difference), which require models of the head made of small elements (e.g., cubes) with dimensions of the order of a tenth of the wavelength. This already requires powerful computer resources (in memory and CPU time) for frequencies in the high UHF band, and may limit the possibility of analyzing frequencies much higher than UHF. On the other hand, the higher the frequency, the smaller the penetration of radio waves into the human body, hence making it possible to have models of only some centimeters deep. This is an area for further research.

1.2.5 ATM-Based Wireless (Mobile) Broadband Multimedia Systems

Recent study of MBS, ATM, and ATM-oriented MBS has drawn the attention of several researchers [34–44]. With enormous complexity of managing and operating the many different types of networks now in use, the door is open for finding a common platform—a network on which all established services can be supported and which will allow new services to be introduced without needing new networks on which to run them. The answer seems to be ATM. This is the technology being defined and standardized for B-ISDN. Thus, ATM, when adequately modified, is also an answer for the future mobile wireless broadband multimedia systems.

ATM is a packet-oriented transmission scheme. The transmission path of the packets of constant length, the so-called ATM cells, is established during connection setup between the two endpoints by assigning a virtual channel. At this time, the necessary resources are provided and the logical channels are assigned. All packets of a virtual channel are carried over the same path. The transmission capacity of the virtual channel is characterized by the parameters, mean bit rate and peak bit rate during connection setup. ATM cells are generated according to the need of the data source. Thus, ATM is a very good method to meet the dynamic requirements of connections with variable data rates.

MBS is the interface between the fixed ATM net at the base station side and mobile ATM net at the mobile station side. Normally, the ATM net at the mobile station side only consists of one end system. For every end station, it is possible to operate several virtual channels with different data rates at the same time.

A conceptual view of the ATM-type broadband communications network is shown in Figure 1.5. The most important benefit of ATM is its flexibility; it is used for the new high bit rate services, which are either VBR or burst traffic. Several factors that tend to favor the use of ATM cell transport in MBS are as follows:

- Flexible bandwidth allocation and service-type selection for a range of applications;
- Efficient multiplexing of traffic from bursty data and multimedia sources;
- End-to-end provisioning of broadband services over wired and wireless networks;
- Suitability of available ATM switching for intercell switching;
- Improved service reliability with packet-switching techniques; and
- Ease of interfacing with wired B-ISDN systems.

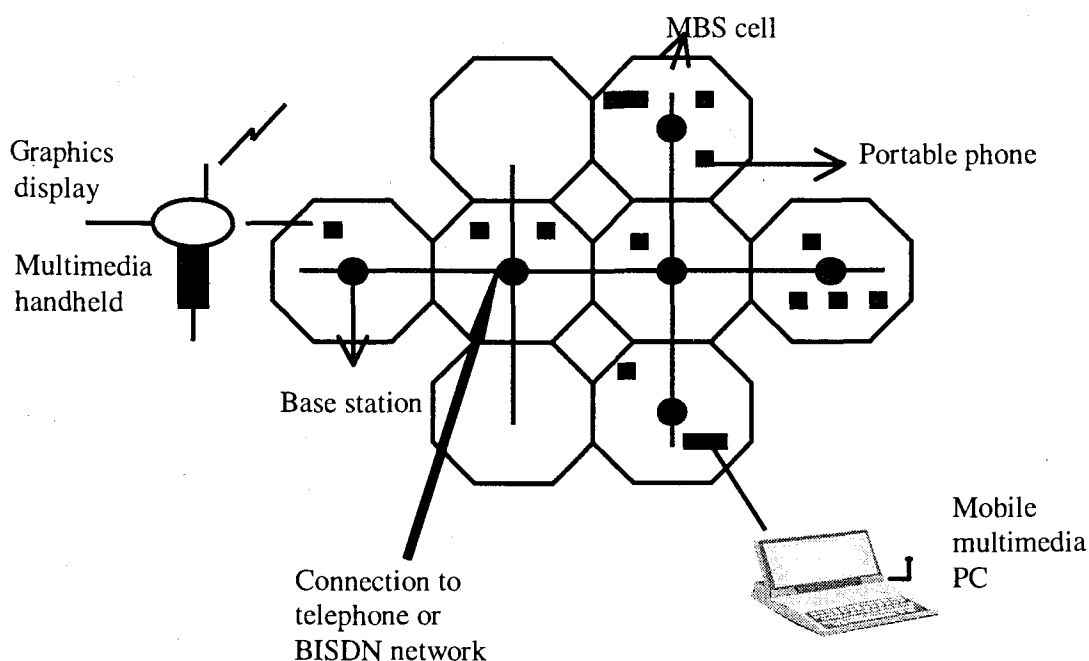


Figure 1.5 Conceptual view of MBS.

Taking the above points into consideration, adoption of ATM-compatible, fixed-length, cell-relay format for MBS is recommended. A possible ATM-compatible MBS approach is shown in Figure 1.6. With this approach, the 48-byte ATM cell payload becomes the basic unit of data within the MBS network. Within MBS, specific protocol layers (e.g., data link and medium-access control layer) are added to the ATM payload as required, and replaced by ATM headers before entering the fixed network [41]. The use of ATM switching for intercell traffic also avoids the crucial problem of developing a new backbone network with sufficient throughput to support intercommunication among large numbers of small cells. ATM multiplexers are used to combine traffic from several base stations into a single ATM port.

For a seamless internetworking mechanism with the wired broadband network, it is vital to have the MBS protocol layering harmonized with the ATM stack. Figure 1.7 shows a protocol reference model. In this approach, new wireless channel-specific physical, medium-access control, and data link layers are added below the ATM network layer. This means that regular network layer and control services such as call setup, virtual channel identifier/virtual path identifier (VCI/VPI) addressing, cell prioritization, and flow-control indication will continue to be used by mobile services. The baseline ATM network and signaling protocol are specified to particular mobility-related functions, such as address registration (roaming), broadcasting, handoff, and so forth.

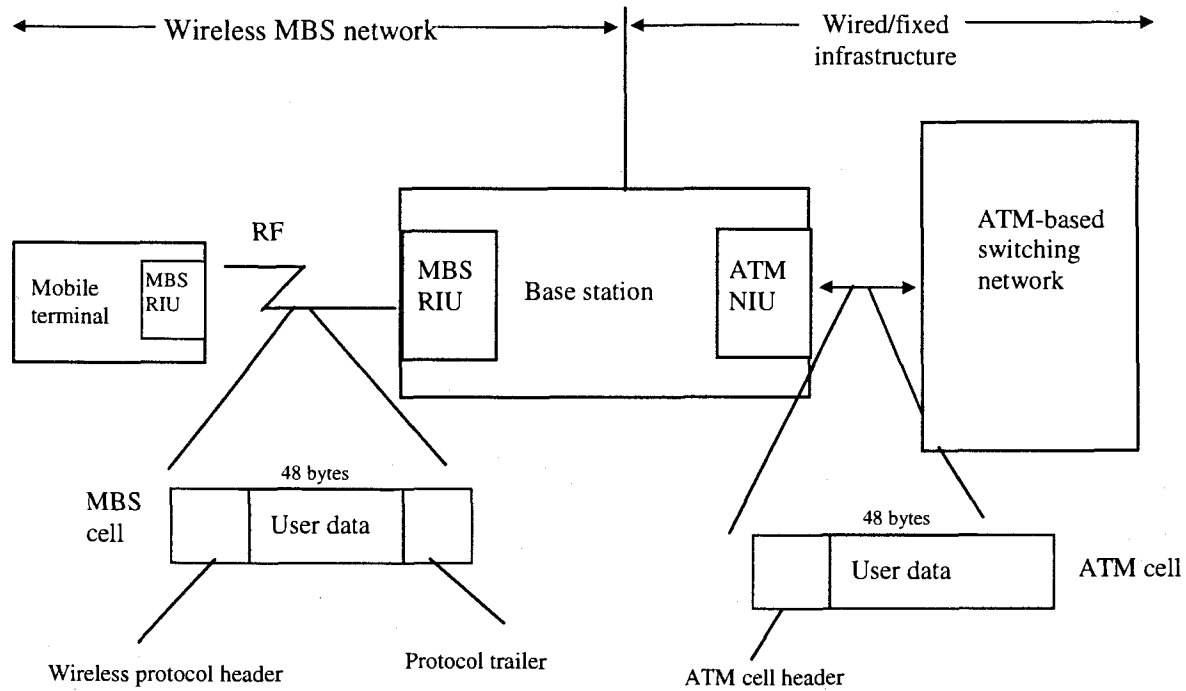


Figure 1.6 ATM-compatible MBS approach. Terms: radio interface unit (RIU); network interface unit (NIU).

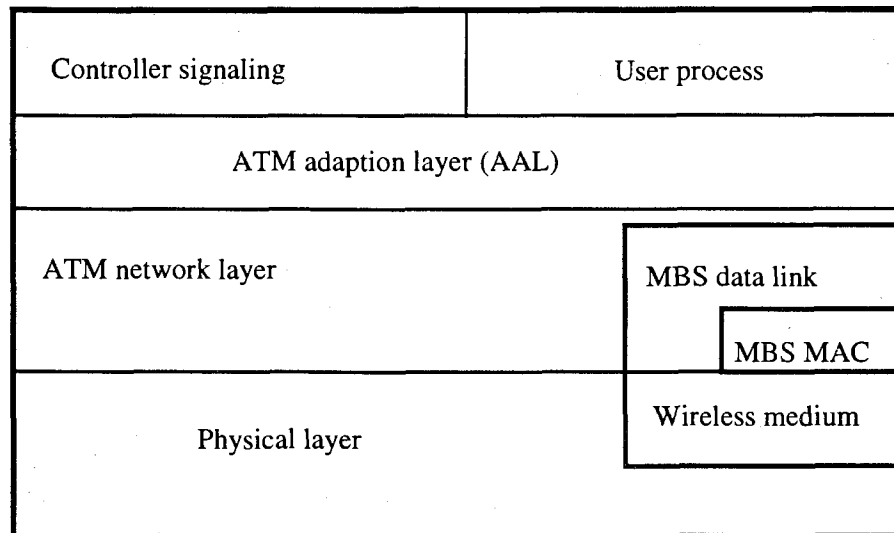


Figure 1.7 Relation of wireless network protocol layers.

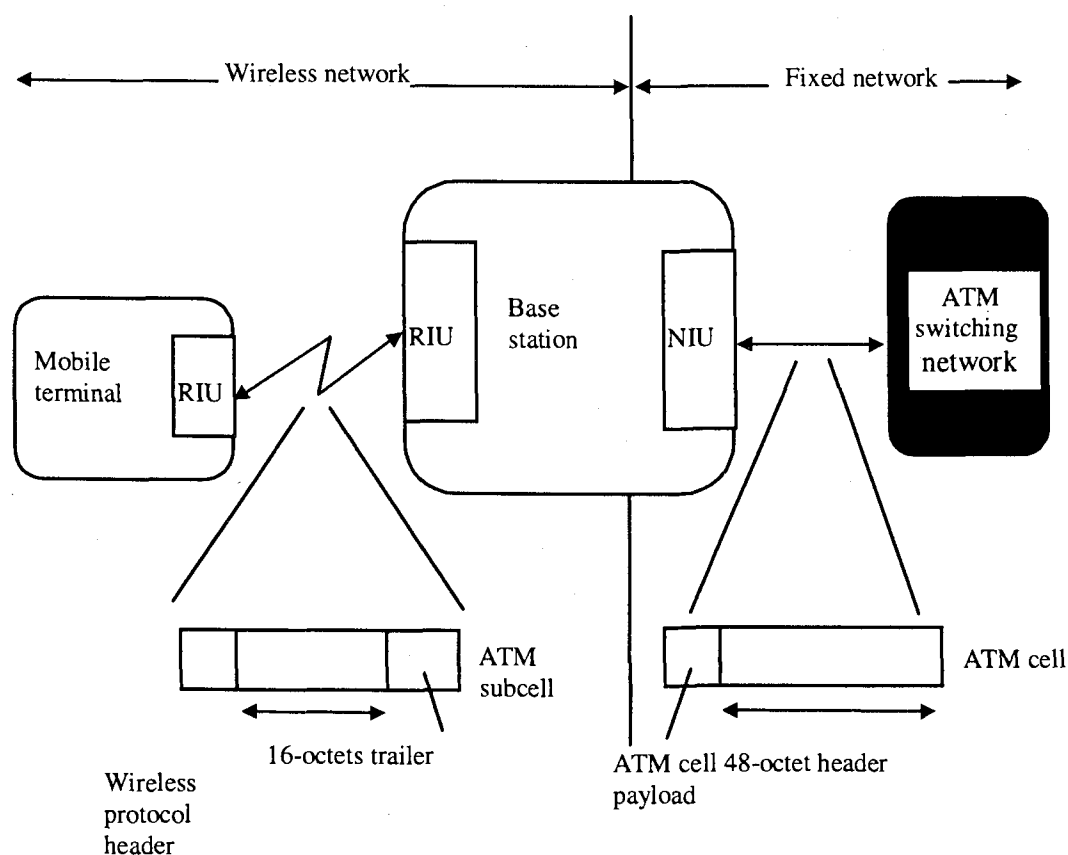


Figure 1.8 Conceptual view of an ATM-compatible air interface.

The payload of an ATM cell consists of 48 octets, meaning that without any segmentation, packet lengths of 384 bits would have to be transmitted over the mobile radio channel. Higher throughput levels over a fading mobile radio channel are achieved when using a packet of smaller lengths. So a suitable integer submultiple of a cell is chosen as the basic unit of data over the wireless radio medium. Based on the system parameters, a submultiple cell size of 16 octets or 128 bits is used as an appropriate value.

The air interface is terminated directly at the base station, as illustrated in Figure 1.8. Also shown is the segmentation of an ATM cell into its three subcells and the addition of an extra wireless ATM header.

1.3 MULTIPATH PROPAGATION

One of the basic reasons to use OFDM is the efficient way it can handle multipath propagation. To understand the effects of multipath fading, this section contains an overview of the most relevant parameters and models.

1.3.1 Multipath Channel Models

Fundamental work on modeling of the indoor radio channel is published in [45, 46]. One of the results of this work, which is also supported by many other measurements reported in the literature, is that the average received multipath power is an exponentially decaying function of the excess delay. Further, the amplitudes of individual multipath components are Rayleigh distributed. This observation has led to simplified channel models as used in [47, 48]. These models assume a fixed number of paths with equidistant delays. The path amplitudes are independent Rayleigh variables, while the path phases are uniformly distributed. Figure 1.9 shows an example of an average and an instantaneous power delay profile that were generated using this approach.

Compared to the more extensive models in [45, 46], the simplified model of [47, 48] may give somewhat optimistic results because the number of multipath components is fixed to the maximum possible amount. In the models of [45, 46], the number of paths is random. Paths arrive in clusters with Poisson distributed arrival times. Within a cluster, the path amplitudes are independent Rayleigh variables. The average power delay profile, averaged over a large number of channels, is an exponentially decaying function, just as for the models in [47, 48]. Thus, the only difference between the models is that the instantaneous power delay profiles have a slightly different shape, and channels generated by the method of [47, 48] generally show more multipath components than channels generated according to [45, 46]. This may give a somewhat optimistic diversity effect, because diversity is proportional to the number of paths. It probably does not make a difference when the models are used to determine the delay spread tolerance of a particular transmission system, however, because that is not depending on the number of paths, but rather on the amount of power in paths exceeding a certain excess delay. So, the channel models of [47, 48] seem a good basis to determine the delay spread tolerance of different modulation schemes. An additional advantage is that the simulation complexity is much lower than that of the models of [45, 46].

One of the key parameters in the design of a transmission system is the maximum delay spread value that it has to tolerate. For an idea of what typical delay spread figures are, the next section presents some measurement results obtained from the literature [49- 63].

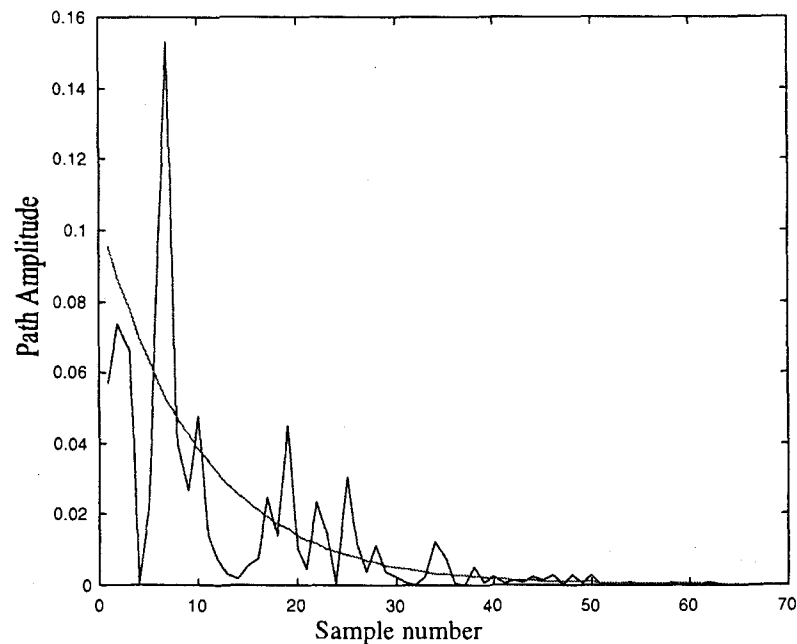


Figure 1.9 Example of generated average and instantaneous power delay profiles for a delay spread of 10 sampling intervals.

1.3.2 Delay Spread Values

Tables 1.3 to 1.5 summarize some delay spread results obtained from literature for frequencies from 800 MHz to 6 GHz. Two delay spread values are given; the *median* delay spread is the 50% value, meaning that 50% of all channels has a delay spread that is lower than the median value. Clearly, the median value is not so interesting for designing a wireless link, because there you want to guarantee that the link works for at least 90% or 99% of all channels. Therefore, the second column gives the measured *maximum* delay spread values. The reason to use maximum delay spread instead of a 90% or 99% value is that many papers only mention the maximum value. From the papers that do present cumulative distribution functions of their measured delay spreads, we can deduce that the 99% value is only a few percent smaller than the maximum measured delay spread.

Table 1.3
Measured delay spreads in frequency range of 800 MHz to 1.5 GHz.

Median delay spread [ns]	Maximum delay spread [ns]	Reference	Remarks
25	50	[46]	Office building
30	56	[58]	Office building
27	43	[59]	Office building
11	58	[60]	Office building
35	80	[61]	Office building
40	90		Shopping center
80	120		Airport
120	180		Factory
50	129	[62]	Warehouse
120	300		Factory

Table 1.4
Measured delay spreads in frequency range of 1.8 to 2.4 GHz

Median delay spread [ns]	Maximum delay spread [ns]	Reference	Remarks
40	120	[49]	Large building (New York stock exchange)
40	95	[50]	Office building
40	150	[51]	Office building
60	200	[54]	Shopping center
106	270		Laboratory
19	30	[55]	Office building: single room only
20	65	[56]	Office building
30	75		Cafeteria
105	170		Shopping center
30	56	[58]	Office building
25	30	[63]	Office building: single room only

Table 1.5
Measured delay spreads in frequency range of 4 to 6 GHz

Median delay spread [ns]	Maximum delay spread [ns]	Reference	Remarks
40	120	[49]	Large building (e.g., Stock Exchange)
50 35 10	60 55 35	[52]	Office building Meeting room (5m x 5m) with metal walls Single room with stone walls
40	130	[51]	Office building
40 65 25	120 125 65	[53]	Indoor sports arena Factory Office building
20	30	[63]	Office building: single room only

Interesting results that can be derived from the reported measurements are:

- Measurements done simultaneously on different frequencies show that there is no significant difference in delay spread in the frequency range of 800 MHz to 6 GHz.
- The delay spread is related to the building size; largest delay spreads (up to 270 ns) were measured in large buildings like shopping centers and factories. The reason for this phenomenon is that reflections can have larger delays if the distances between transmitter and reflectors (walls or other objects) are larger.
- For most office buildings, the maximum delay spread is in the range of 40 to 70 ns. Smaller delay spreads around 30 ns occur when both transmitter and receiver are within the same room. Delay spreads of 100 ns or more are seen only in office buildings with large rooms that are some tens of meters in diameter.
- Even small rooms (5m by 5m) can give significant delay spreads around 50 ns when there are metal walls [52]. The reason for this is that reflections from a metal wall only experience a small attenuation, so multiple reflections with significant delays still have considerable power, which increases the delay spread.

1.4 TIME VARIATION OF THE CHANNEL

To classify the time characteristics of the channel [1], the coherence time and Doppler spread are important parameters. The coherence time is the duration over which the channel characteristics do not change significantly. The time variations of the channel are evidenced as a Doppler spread in the frequency domain, which is determined as the width of the spectrum when a single sinusoid (constant envelope) is transmitted. Both

the time correlation function $\varphi_c(\Delta t)$ and the Doppler power spectrum $S_c(f)$ can be related to each other by applying the Fourier transform.

The range of values of the frequency f over which $S_c(f)$ is essentially nonzero is called the Doppler spread B_d of the channel. Because $S_c(f)$ is related to $\varphi_c(\Delta t)$ by the Fourier transform, the reciprocal of B_d is a measure of the coherence time $(\Delta t)_c$ of the channel; that is, $1/B_d$.

The coherence time $(\Delta t)_c$ is a measure of the width of the time correlation function. Clearly, a slow-changing channel has a large coherence time, or equivalently, a small Doppler spread. The rapidity of the fading can now be determined either from the correlation function $\varphi_c(\Delta t)$ or from the Doppler power spectrum $S_c(f)$. This implies that either the channel parameters $(\Delta t)_c$ or B_d can be used to characterize the rapidity of the fading. If the bit time T_b is large compared with the coherence time, then the channel is subject to fast fading. When selecting a bit duration that is smaller than the coherence time of the channel, the channel attenuation and phase shift are essentially fixed for the duration of at least one signaling interval. In this case, the channel is slowly fading or quasistatic. Like coherence bandwidth, there is no exact relationship between coherence time and Doppler spread. If the coherence time $(\Delta t)_c$ is defined as the time over which the time correlation function is above 0.5, $(\Delta t)_c$ is approximately given by $9/(16\pi B_d)$ [79, 80].

Doppler spread is caused by the differences in Doppler shifts of different components of the received signal, if either the transmitter or receiver is in motion. The frequency shift is related to the spatial angle between the direction of arrival of that component and the direction of vehicular motion. If a vehicle is moving at a constant speed V along the X axis, the Doppler shift f_m of the m th plane-wave component is given by $f_m = (V/\lambda)\cos(\alpha_m)$ [81], where α_m is the arrival angle of the m th plane-wave component relative to the direction of movement of the vehicle. It is worth noting here that waves arriving from ahead of the vehicle experience a positive Doppler shift, while those arriving from behind the vehicle have a negative shift. The maximum Doppler shift occurs at $\alpha_m = 0$, assuming $T_b \gg (\Delta t)_c$ for fast-fading channel and $T_b \ll (\Delta t)_c$ for slow-fading channel.

Indoor measurements [82] show that in any fixed location, temporal variations in the received signal envelope caused by movement of personnel and machinery are slow, having a maximum Doppler spread of about 6 Hz.

1.5 HISTORY OF OFDM

OFDM is a special case of multicarrier transmission, where a single datastream is transmitted over a number of lower rate subcarriers. It is worth mentioning here that OFDM can be seen as either a modulation technique or a multiplexing technique. One

of the main reasons to use OFDM is to increase the robustness against frequency selective fading or narrowband interference. In a single carrier system, a single fade or interferer can cause the entire link to fail, but in a multicarrier system, only a small percentage of the subcarriers will be affected. Error correction coding can then be used to correct for the few erroneous subcarriers. The concept of using parallel data transmission and frequency division multiplexing was published in the mid-1960s [64, 65]. Some early development is traced back to the 1950s [66]. A U.S. patent was filed and issued in January, 1970 [67].

In a classical parallel data system, the total signal frequency band is divided into N nonoverlapping frequency subchannels. Each subchannel is modulated with a separate symbol and then the N subchannels are frequency-multiplexed. It seems good to avoid spectral overlap of channels to eliminate interchannel interference. However, this leads to inefficient use of the available spectrum. To cope with the inefficiency, the ideas proposed from the mid-1960s were to use parallel data and FDM with overlapping subchannels, in which each carrying a signaling rate b is spaced b apart in frequency to avoid the use of high-speed equalization and to combat impulsive noise and multipath distortion, as well as to fully use the available bandwidth.

Figure 1.10 illustrates the difference between the conventional nonoverlapping multicarrier technique and the overlapping multicarrier modulation technique. As shown in Figure 1.10, by using the overlapping multicarrier modulation technique, we save almost 50% of bandwidth. To realize the overlapping multicarrier technique, however we need to reduce crosstalk between subcarriers, which means that we want orthogonality between the different modulated carriers.

The word orthogonal indicates that there is a precise mathematical relationship between the frequencies of the carriers in the system. In a normal frequency-division multiplex system, many carriers are spaced apart in such a way that the signals can be received using conventional filters and demodulators. In such receivers, guard bands are introduced between the different carriers and in the frequency domain which results in a lowering of spectrum efficiency.

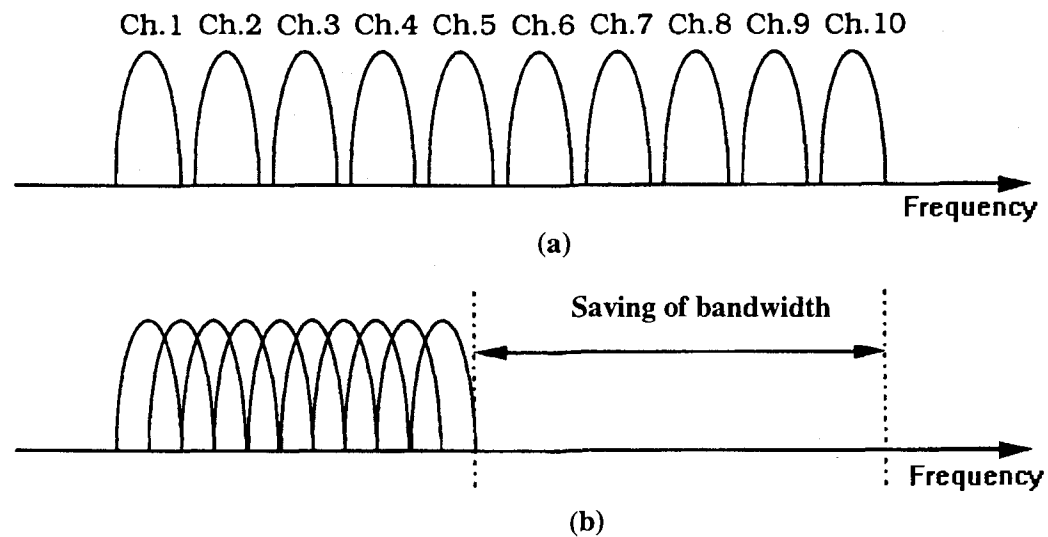


Figure 1.10 Concept of OFDM signal: (a) Conventional multicarrier technique, and (b) orthogonal multicarrier modulation technique.

It is possible, however, to arrange the carriers in an OFDM signal so that the sidebands of the individual carriers overlap and the signals are still received without adjacent carrier interference. To do this the carriers must be mathematically orthogonal. The receiver acts as a bank of demodulators, translating each carrier down to DC, with the resulting signal integrated over a symbol period to recover the raw data. If the other carriers all beat down the frequencies that, in the time domain, have a whole number of cycles in the symbol period T , then the integration process results in zero contribution from all these other carriers. Thus, the carriers are linearly independent (i.e., orthogonal) if the carrier spacing is a multiple of $1/T$. Chapter 2 presents in detail the basic principle of OFDM.

Much of the research focuses on the high efficient multicarrier transmission scheme based on “orthogonal frequency” carriers. In 1971, Weinstein and Ebert [68] applied the discrete Fourier transform (DFT) to parallel data transmission systems as part of the modulation and demodulation process. Figure 1.11 (a) shows the spectrum of the individual data of the subchannel. The OFDM signal, multiplexed in the individual spectra with a frequency spacing b equal to the transmission speed of each subcarrier, is shown in Figure 1.11(b). Figure 1.11 shows that at the center frequency of each subcarrier, there is no crosstalks from other channels. Therefore, if we use DFT at the receiver and calculate correlation values with the center of frequency of each subcarrier, we recover the transmitted data with no crosstalk. In addition, using the DFT-based multicarrier technique, frequency-division multiplex is achieved not by bandpass filtering but by baseband processing.

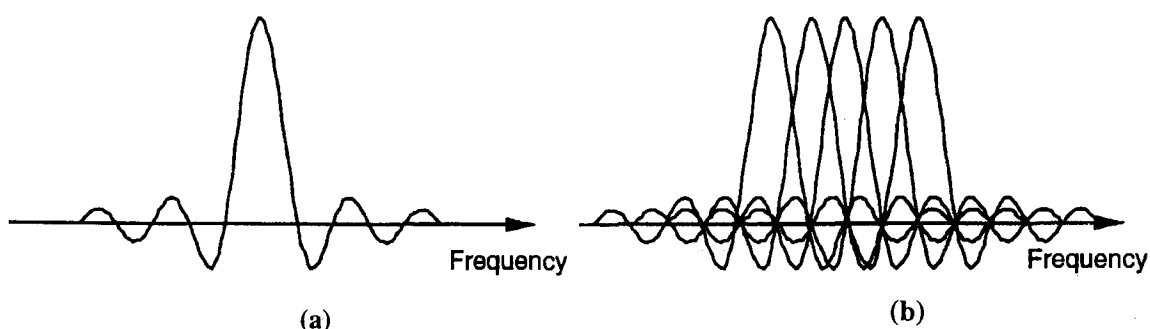


Figure 1.11 Spectra of (a) an OFDM subchannel and (b) an OFDM signal.

Moreover, to eliminate the banks of subcarrier oscillators and coherent demodulators required by frequency-division multiplex, completely digital implementations could be built around special-purpose hardware performing the fast Fourier transform (FFT), which is an efficient implementation of the DFT. Recent advances in very-large-scale integration (VLSI) technology make high-speed, large-size FFT chips commercially affordable. Using this method, both transmitter and receiver are implemented using efficient FFT techniques that reduce the number of operations from N^2 in DFT down to $M \log N$ [69].

In the 1960s, the OFDM technique was used in several high-frequency military systems such as KINEPLEX [66], ANDEFT [70], and KATHRYN [71]. For example, the variable-rate data modem in KATHRYN was built for the high-frequency band. It used up to 34 parallel low-rate phase-modulated channels with a spacing of 82 Hz.

In the 1980s, OFDM was studied for high-speed modems, digital mobile communications, and high-density recording. One of the systems realized the OFDM techniques for multiplexed QAM using DFT [72], and by using pilot tone, stabilizing carrier and clock frequency control and implementing trellis coding are also implemented [73]. Moreover, various-speed modems were developed for telephone networks [74].

In the 1990s, OFDM was exploited for wideband data communications over mobile radio FM channels, high-bit-rate digital subscriber lines (HDSL; 1.6 Mbps), asymmetric digital subscriber lines (ADSL; up to 6 Mbps), very-high-speed digital subscriber lines (VDSL; 100 Mbps), digital audio broadcasting (DAB), and high-definition television (HDTV) terrestrial broadcasting [75–80].

The OFDM transmission scheme has the following key advantages:

- OFDM is an efficient way to deal with multipath; for a given delay spread, the implementation complexity is significantly lower than that of a single carrier system with an equalizer.
- In relatively slow time-varying channels, it is possible to significantly enhance the capacity by adapting the data rate per subcarrier according to the signal-to-noise ratio of that particular subcarrier.

- OFDM is robust against narrowband interference, because such interference affects only a small percentage of the subcarriers.
- OFDM makes single-frequency networks possible, which is especially attractive for broadcasting applications.

On the other hand, OFDM also has some drawbacks compared with single-carrier modulation:

- OFDM is more sensitive to frequency offset and phase noise.
- OFDM has a relatively large peak-to-average power ratio, which tends to reduce the power efficiency of the RF amplifier.

1.6 PREVIEW OF THE BOOK

This book consists of 10 chapters. It covers all the necessary elements to achieve the OFDM-based WBMCS. In Chapter 2, the basics of OFDM are presented. It is explained how an OFDM signal is formed using the inverse fast Fourier transform, how the cyclic extension helps to mitigate the effects of multipath, and how windowing can limit the out-of-band radiation. Basic design rules are given how to choose the OFDM parameters, given a required bandwidth, multipath delay spread, and maximum Doppler spread.

In Chapter 3, we explain how coding and interleaving can be used to mitigate the effects of frequency-selective fading channels. *Quadrature amplitude modulation* is introduced as an appropriate modulation technique for the OFDM subcarriers.

Synchronization of the symbol clock and carrier frequency is the subject of Chapter 4. First, we discuss the sensitivity of OFDM to synchronization errors. Then, we describe different synchronization techniques. Special attention is given to packet transmission, which requires rapid synchronization at the beginning of each packet with a minimum of training overhead.

Chapter 5 describes channel estimation; that is, estimating the reference phases and amplitudes of all subcarriers. Various coherent and differential techniques are explained in conjunction with their relative merits on signal-to-noise ratio performance, overhead, and buffering delay.

The relatively large peak-to-average power (PAP) ratio of OFDM is the subject of Chapter 6. The distribution of the PAP ratio is shown, and various methods to reduce the PAP ratio are explained. This chapter demonstrates that for an arbitrary number of subcarriers, the PAP ratio can be reduced to about 5 dB without a significant loss in performance. This means that the required backoff—and hence the efficiency—of an RF power amplifier for an OFDM system is not much different from that for a single-carrier QPSK system.

In Chapter 7, we explain the basics of direct-sequence and frequency-hopping CDMA, which is especially helpful in understanding the following chapters on combinations of OFDM and CDMA.

Chapter 8 describes multicarrier CDMA. Different techniques with their transmitter and receiver architectures are introduced. Advantages and disadvantages compared with other CDMA techniques are discussed.

Orthogonal FDMA and frequency-hopping CDMA are the subjects of Chapter 9. It shows how OFDM and frequency hopping can be combined to get a multiple-access system with similar advantages as direct-sequence CDMA.

Finally, some applications of OFDM systems are described in Chapter 10: digital audio broadcasting, digital video broadcasting, wireless ATM in the Magic WAND project, and the new IEEE 802.11 and ETSI BRAN OFDM standards.

REFERENCES

- [1] Prasad, R., *Universal Wireless Personal Communications*, Norwood, MA: Artech House, 1998.
- [2] Prasad, R., "Wireless Broadband Communication Systems," *IEEE Comm. Mag.*, Vol. 35, p. 18, Jan. 1997.
- [3] Honcharenko, W., J. P. Kruys, D. Y. Lee, and N.J. Shah, "Broadband Wireless Access," *IEEE Comm. Mag.*, Vol. 35, pp. 20–26, Jan. 1997.
- [4] Correia, L. M., and R. Prasad, "An Overview of Wireless Broadband Communications," *IEEE Comm. Mag.*, Vol. 35, pp. 28–33, Jan. 1997.
- [5] Morinaga, M., M. Nakagawa, and R. Kohno, "New Concepts and Technologies for achieving Highly Reliable and High Capacity Multimedia Wireless Communications System," *IEEE Comm. Mag.* Vol. 35, pp. 34–40, Jan. 1997.
- [6] Da Silva, J. S., B. Arroyo-Fernandez, B. Barani, J. Pereira, and D. Ikonou, "Mobile and Personal Communications: ACTS and Beyond," *Proc. PIMRC'97*, Helsinki, Finland, Sep. 1997.
- [7] Prisoli, F. D., and R. Velt, "Design of Medium Access Control and Logical Link Control Functions for ATM Support in the MEDIAN System," *Proc. ACTS Mobile Comm. Summit'97*, pp. 734–744, Aalborg, Denmark, Oct. 1997.
- [8] Rheinschmitt, R., A. de Haz, and M. Umehinc, "AWACS MAC and LLC Functionality," *Proc. ACTS Mobile Comm. Summit'97*, pp. 745–750, Aalborg, Denmark, Oct. 1997.

-
- [9] van Nee, R., "An OFDM Modem for Wireless ATM," *Proceedings of IEEE 4th Symposium on Communications and Vehicular Technology in the Benelux*, Gent, Belgium, pp. 36-41, Oct. 7-8, 1996.
 - [10] Aldis, J., E. Busking, T. Kleijne, R. Kopmeiners, and R. van Nee, "Magic Into Reality, Building the WAND Modem," *Proc. ACTS Mobile Comm. Summit'97*, pp. 734-744, Aalborg, Denmark, Oct. 1997.
 - [11] Mikkonen, J., C. Corrado, C. Erci, and M. Proglar, "Emerging Wireless Broadband Networks," *IEEE Comm. Mag.*, Feb. 1988.
 - [12] Wu, G., Y. Hase, K. Taira, and K. Iwasak, "Emerging Wireless ATM Oriented MAC Protocol for High-Speed Wireless LAN," *Proc. PIMRC'97*, pp. 198-203, Helsinki, Finland, Sep. 1997.
 - [13] Prasad, R., and L. M. Correia, "Wireless Broadband Multimedia Communications," *International Wireless and Telecommunications Symposium*, Shah Alam, Malaysia, Vol. 2, pp. 55-70 May 14-16, 1997.
 - [14] Prasad, R., and L. M. Correia, "An Overview of Wireless Broadband Multimedia Communications," *Proc. MoMuC'97*, Seoul, Korea, pp. 17-31, Sep.-Oct. 1997.
 - [15] Chelouche, M., S. Hethuin, and L. Ramel, "Digital Wireless Broadband Corporate and Private Networks: RNET Concepts and Applications," *IEEE Comm. Mag.*, Vol. 35, pp. 42-51, Jan. 1997.
 - [16] IEEE 802.11, *IEEE Standard for Wireless LAN Medium Access Control and Physical Layer Specifications*, Nov. 1997.
 - [17] Fernandes, L., "R2067 MBS - Mobile Broadband System," in *Proc. ICUPC'93 — 2nd IEEE International Conference on Universal Personal Communications*, Ottawa, Canada, Oct., 1993.
 - [18] IEEE 802.11 Web URL: <http://grouper.ieee.org/groups/802/11/>.
 - [19] ETSI home page: <http://www.etsi.org/>.
 - [20] Kruys, J., "Standardization of Wireless High Speed Premises Data Networks," *Wireless ATM Workshop*, Espoo, Finland, Sep. 1996.
 - [21] van Nee, R., G. Awater, M. Morikura, H. Takanashi, M. Webster, and K. Halford, "New High Rate Wireless LAN Standards," *IEEE Communications Magazine*, Dec. 1999.
 - [22] IEEE, "Supplement to Standard for Telecommunications and Information Exchange Between Systems—LAN/MAN Specific Requirements—Part 11: Wireless MAC and PHY Specifications: Higher Speed Physical Layer Extension in the 2.4-GHz Band," P802.11b/D7.0, July 1999.
 - [23] WECA home page: <http://www.wirelessethernet.com>.

-
- [24] IEEE, "Supplement to Standard for Telecommunications and Information Exchange Between Systems—LAN/MAN Specific Requirements—Part 11: Wireless MAC and PHY Specifications: High Speed Physical Layer in the 5-GHz Band," P802.11a/D7.0, July 1999.
 - [25] WaveLAN home page: <http://www.wavelan.com>.
 - [26] Prasad, R., "Research Challenges in Future Wireless Personal Communications: Microwave Perspective," *Proc. 25th European Microwave Conference* (Keynote opening address), Bologna, Italy, pp. 4–11, Sept. 4–7, 1995.
 - [27] Prasad, R., "Overview of Wireless Personal Communications: Microwave Perspectives," *IEEE Comm. Mag.*, Vol. 35, pp. 104–108, April 1997.
 - [28] Smulders, P. F. M., "Broadband Wireless LANs: a feasibility study," *Ph.D. Thesis*, Eindhoven Univ. of Technology, Eindhoven, The Netherlands, Dec. 1995.
 - [29] Correia, L. M., and P. O. Frances, "A Propagation Model for the Estimation of the Average Received Power in an Outdoor Environment at the Millimeter Wave Band," *Proc. VTC'94 — IEEE VTS 44th Vehicular Technology Conference*, Stockholm, Sweden, pp. 1785–1788, July 1994.
 - [30] Lovnes, G., J. J. Reis, and R. H. Raekken, "Channel Sounding Measurements at 59 GHz in City Streets," *Proc. PIMRC'94 — 5th IEEE International Symposium on Personal, Indoor, and Mobile Radio Communications*, The Hague, The Netherlands, pp. 496–500, Sep. 1994.
 - [31] Fernandes, J. J., P. A. Watson, and J. C. Neves, "Wireless LANs: Physical Properties of Infrared Systems versus mmWave Systems," *IEEE Comm. Mag.*, Vol. 32, No.8, pp. 68–73, Aug. 1994.
 - [32] European Commission, "Communications for Society Visionary Research," European Commission, DG XIII/B, Brussels, Belgium, Feb. 1997.
 - [33] Rokitansky, C. –H., and M. Scheibenbogen (eds.), "Updated Version of System Description Document," *RACE Deliverable R2067/UA/WP215/DS/P/068.b1*, RACE Central Office, European Commission, Brussels, Belgium, Dec. 1995.
 - [34] Prasad, A. R., "Asynchronous Transfer Mode Based Mobile Broadband System," *Proc. IEEE 3rd Symposium on Comm. & Vech. Technology in Benelux*, Eindhoven, The Netherlands, pp. 143–148, Oct. 1995.
 - [35] Prasad, R., and L. Vandendorpe, "An Overview of Millimeter Wave Indoor Wireless Communication System," *Proc. 2nd Int. Conf. on Universal Personal Communications*, pp. 885–889, Ottawa, Canada, 1993.
 - [36] Prasad, R., and L. Vandendorpe, "Cost 231 Project: Performance Evaluation of a Millimetric-Wave Indoor Wireless Communications System," *RACE Mobile Telecommunications Workshop*, Metz, France, pp. 137–144, June 16–18, 1993.

-
- [37] Zauner, K., "On the ATM Road to Broadband," *Telecom Report International*, No.3, pp. 26–29, 1993.
 - [38] Tubtiang, H.I. Kwon and O. Pujolle, "A Simple ATM Switching Architecture for Broadband-ISDN and Its Performance," *Modeling and Performance Evaluation of ATM Technology (C-I5)*, pp. 361–367, IFIP 1993.
 - [39] Stallings, W., *Advances in ISDN and Broadband ISDN*, IEEE Computer Society Press, 1992.
 - [40] Leslie, I. M., D. R. McAuley, and D. L. Tennenhouse, "ATM Everywhere?" *IEEE Network*, pp. 40–46, March 1993.
 - [41] McTiffin, M. J., A. P. Hulbert, T. J. Ketseoglou, W. Heimsch, and O. Crisp, "Mobile access to an ATM Network Using A CDMA Air Interface," *IEEE J. Selected Areas in Comm.*, Vol. 12, No. 5, pp. 900–908, June 1994.
 - [42] Raychaudhri, D., "ATM-based Transport Architecture for Multiservices Wireless Personal Communication Networks," *IEEE J. Selected Areas in Comm.*, Vol.12, No. 8, pp. 1401–1414, Oct. 1994.
 - [43] Geij, R. R., "Mobile Multimedia Scenario using ATM and Microcellular Technologies," *Vehicular Technology*, Vol. 43, No. 3, pp. 699–703, Aug. 1994.
 - [44] Bakker, J. D., and R. Prasad, "Wireless Multimedia Communications Using a CDMA-based ATM Air Interface," *Proc. IEEE ISSSTA'96*, Mainz, Germany, pp. 1128–1132, Sept. 1996.
 - [45] Hashemi, H., "The Indoor Radio Propagation Channel," *Proceedings of the IEEE*, Vol. 81, no. 7, pp. 943–968, July 1993.
 - [46] Saleh, A. A. M., and R. A. Valenzuela, "A Statistical Model for Indoor Multipath Propagation," *IEEE Journal on Selected Areas in Communications*, vol. SAC-5, no. 2, pp. 128–137, Feb. 1987.
 - [47] Halls, G., "HIPERLAN Radio Channel Models and Simulation Results," RES10TTG 93/58.
 - [48] Chayat, N., "Tentative Criteria for Comparison of Modulation Methods," IEEE P802.11-97/96.
 - [49] Devasirvatham, D. M. J., "Multi-Frequency Propagation Measurements and Models in a Large Metropolitan Commercial Building for Personal Communications," *IEEE PIMRC '91*, pp. 98–103, London, UK, Sept. 23–25, 1991.
 - [50] Devasirvatham, D. M. J., "Time Delay Spread Measurements at 850 MHz and 1.7 GHz inside a Metropolitan Office Building," *Electronics Letters*, pp. 194–196, Feb. 2, 1989.

-
- [51] Devasirvatham, D. M. J., M. J. Krain and D. A. Rappaport, "Radio Propagation Measurements at 850 MHz, 1.7 GHz and 4 GHz Inside Two Dissimilar Office buildings," *Electronics Letters*, Vol. 26, No. 7, pp. 445-447, March 29, 1990.
 - [52] Hafesi, P., D. Wedge, M. Beach, M. Lawton, "Propagation Measurements at 5.2 GHz in Commercial and Domestic Environments," *IEEE PIMRC '97*, Helsinki, pp. 509-513, Sept. 1-4, 1997.
 - [53] Hawbaker, D. A., and T. S. Rappaport, "Indoor Wideband Radiowave Propagation Measurements at 1.3 GHz and 4.0 GHz," *Electronics Letters*, vol. 26, no. 21, pp. 1800-1802, Oct. 11, 1990.
 - [54] Johnson, I. T., and E. Gurdenelli, "Measurements of Wideband Channel Characteristics in Cells Within Man Made Structures of Area Less Than 0.2 km²," COST 231 TD(90)083.
 - [55] Lahteenmaki, J., "Indoor Measurements and Simulation of Propagation at 1.7 GHz," COST 231 TD(90)084.
 - [56] Anderson, P. C., O. J. M. Houen, K. Kladakis, K. T. Peterson, H. Fredskild and I. Zarnoczay, "Delay Spread Measurements at 2 GHz," COST 231 TD(91)029.
 - [57] Bultitude, R. J. C., et al., "The Dependence of Indoor Radio Channel Multipath Characteristics on Transmit/Receive Ranges," *IEEE Journal on Selected Areas in Communications*, Vol. 11, No. 7, pp. 979 - 990, Sep. 1993.
 - [58] Bultitude, R. J. C., S. A. Mahmoud and W. A. Sullivan, "A Comparison of Indoor Radio Propagation Characteristics at 910 MHz and 1.75 GHz," *IEEE Journal on Selected Areas in Communications*, Vol. 7, No. 1, pp. 20-30, Jan. 1989.
 - [59] Pahlavan, K., and S. J. Howard, "Frequency Domain Measurements of Indoor Radio Channels," *Electronics Letters*, vol. 25, no. 24, pp. 1645 - 1647, Nov. 23, 1989.
 - [60] Davies, R., and J. P. McGeehan, "Propagation Measurements at 1.7 GHz for Microcellular Urban Communications," *Electronics Letters*, vol. 26, no. 14, pp. 1053-1055, July 5, 1990.
 - [61] Zollinger, E., and A. Radovic, "Measured Time Variant Characteristics of Radio Channels in the Indoor Environment," COST 231 TD(91)089.
 - [62] Rappaport, T. S., and C. D. McGillem, "Characterization of UHF Multipath Radio Channels in Factory Buildings," *IEEE Transactions on Antennas and Propagation*, Vol. 37, No. 8, pp. 1058-1069, Aug. 1989.
 - [63] Nobles, P., and F. Halsall, "Delay Spread and Received Power Measurements Within a Building at 2 GHz, 5 GHz, and 17 GHz", *IEE Tenth International Conference on Antennas and Propagation*, Edinburgh, UK, April 14-17, 1997.

- [64] R. W. Chang, "Synthesis of Band Limited Orthogonal Signals for Multichannel Data Transmission," *Bell Syst. Tech. J.*, Vol. 45, pp. 1775–1796, Dec. 1996.
- [65] Salzberg, B. R., "Performance of an efficient parallel data transmission system," *IEEE Trans. Comm.*, Vol. COM-15, pp. 805 – 813, Dec. 1967.
- [66] Mosier, R. R., and R.G. Clabaugh, "Kineplex, a Bandwidth Efficient Binary Transmission System," *AIEE Trans.*, Vol. 76, pp. 723 – 728, Jan. 1958.
- [67] "Orthogonal Frequency Division Multiplexing," U.S. Patent No. 3, 488,4555, filed November 14, 1966, issued Jan. 6, 1970.
- [68] Weinstein, S. B., and P .M. Ebert, "Data Transmission by Frequency Division Multiplexing Using the Discrete Fourier Transform," *IEEE Trans. Comm.*, Vol. COM-19, pp. 628 – 634, Oct. 1971.
- [69] Zou, W. Y., and Y. Wu, "COFDM: an overview," *IEEE Trans. Broadc.*, Vol. 41, No. 1, pp. 1 – 8, March 1995.
- [70] Porter, G. C., "Error Distribution and Diversity Performance of a Frequency Differential PSK HF modem," *IEEE Trans. Comm.*, Vol., COM-16, pp. 567–575, Aug. 1968.
- [71] Zimmerman, M. S., and A. L. Kirsch, "The AN/GSC-10 (KATHRYN) variable rate data modem for HF radio," *IEEE Trans. Comm.*, Vol., COM-15, pp. 197 – 205, April 1967.
- [72] Hirosaki, B., "An Orthogonally Multiplexed QAM system Using the Discrete Fourier Transform," *IEEE Trans. Comm.*, Vol., COM-29, pp. 982 – 989, July 1981.
- [73] Hirosaki, B., "A 19.2 kbits Voice Band Data Modem Based on Orthogonality Multiplexed QAM Techniques," *Proc. of IEEE ICC'85*, pp. 21.1.1 – 5, 1985.
- [74] Keasler, W. E., and D. L. Bitzer, "High speed modem suitable for operating with a switched network," U.S. Patent No. 4,206,320, June 1980.
- [75] Chow, P. S., J. C. Tu and J. M. Cioffi, "Performance Evaluation of a Multichannel Transceiver System for ADSL and VHDSL services," *IEEE J. Selected Area*, Vol., SAC-9, No. 6, pp. 909 – 919, Aug. 1991.
- [76] Chow, P. S., J. C. Tu, and J. M. Cioffi, "A Discrete Multitone Transceiver System for HDSL Applications," *IEEE J. Selected Areas in Comm.*, Vol. SAC-9, No. 6, pp. 909 – 919, Aug. 1991.
- [77] Paiement, R. V., "Evaluation of Single Carrier and Multicarrier Modulation Techniques for Digital ATV Terrestrial Broadcasting," *CRC Report*, No. CRC-RP-004, Ottawa, Canada, Dec. 1994.

-
- [78] Sari, H., G. Karma, and I. Jeanclaude, "Transmission Techniques for Digital Terrestrial TV Broadcasting," *IEEE Comm. Mag.*, Vol.33, pp. 100–109, Feb. 1995.
 - [79] Oppenheim, A.V., and R.W. Schaffer, *Discrete-time Signal Processing*, Prentice-Hall International, ISBN 0-13-216771-9, 1989.
 - [80] Hara, S., M. Mouri, M. Okada, and N. Morinaga, "Transmission Performance Analysis of Multi-Carrier Modulation in Frequency Selective Fast Rayleigh Fading Channel," in *Wireless Personal Communications*, Kluwer Academic Publishers, Vol.2, pp. 335 – 356, 1996.
 - [79] Rappaport, T. S., *Wireless Communication Principles & Practice*, Prentice-Hall PTR, New Jersey, 1996.
 - [80] Steel, R., (ed.), *Mobile Radio Communications*, IEEE Press, 1994.
 - [81] Macrario, R. C. V., (ed.), "Personal & Mobile Communications," Peter Peregrinus Ltd., 1991.
 - [82] Howard, S. J., and K. Rappaport, "Performance of a DFE Modem Evaluted From Measured Indoor Radio Multipath Profiles," *Proc. ICC'90*, Vol. 4, pp. 335.2.1 – 335.2.5, April 1990.

Chapter 2

OFDM Basics

2.1 INTRODUCTION

The basic principle of OFDM is to split a high-rate datastream into a number of lower rate streams that are transmitted simultaneously over a number of subcarriers. Because the symbol duration increases for the lower rate parallel subcarriers, the relative amount of dispersion in time caused by multipath delay spread is decreased. Intersymbol interference is eliminated almost completely by introducing a guard time in every OFDM symbol. In the guard time, the OFDM symbol is cyclically extended to avoid intercarrier interference. This whole process of generating an OFDM signal and the reasoning behind it are described in detail in sections 2.2 to 2.4.

In OFDM system design, a number of parameters are up for consideration, such as the number of subcarriers, guard time, symbol duration, subcarrier spacing, modulation type per subcarrier, and the type of forward error correction coding. The choice of parameters is influenced by system requirements such as available bandwidth, required bit rate, tolerable delay spread, and Doppler values. Some requirements are conflicting. For instance, to get a good delay spread tolerance, a large number of subcarriers with a small subcarrier spacing is desirable, but the opposite is true for a good tolerance against Doppler spread and phase noise. These design issues are discussed in Section 2.5. Section 2.6 gives an overview of OFDM signal processing functions, while Section 2. ends this chapter with a complexity comparison of OFDM versus single-carrier systems.

2.2 GENERATION OF SUBCARRIERS USING THE IFFT

An OFDM signal consists of a sum of subcarriers that are modulated by using *phase shift keying (PSK)* or *quadrature amplitude modulation (QAM)*. If d_i are the complex

QAM symbols, N_s is the number of subcarriers, T the symbol duration, and f_c the carrier frequency, then one OFDM symbol starting at $t = t_s$ can be written as

$$s(t) = \text{Re} \left\{ \sum_{i=-\frac{N_s}{2}}^{\frac{N_s}{2}-1} d_{i+N_s/2} \exp(j2\pi(f_c - \frac{i+0.5}{T})(t-t_s)) \right\}, \quad t_s \leq t \leq t_s + T \quad (2.1)$$

$$s(t) = 0, \quad t < t_s \wedge t > t_s + T$$

In the literature, often the equivalent complex baseband notation is used, which is given by (2.2). In this representation, the real and imaginary parts correspond to the in-phase and quadrature parts of the OFDM signal, which have to be multiplied by a cosine and sine of the desired carrier frequency to produce the final OFDM signal. Figure 2.1 shows the operation of the OFDM modulator in a block diagram.

$$s(t) = \sum_{i=-\frac{N_s}{2}}^{\frac{N_s}{2}-1} d_{i+N_s/2} \exp(j2\pi \frac{i}{T}(t-t_s)) \quad , \quad t_s \leq t \leq t_s + T \quad (2.2)$$

$$s(t) = 0, \quad t < t_s \wedge t > t_s + T$$

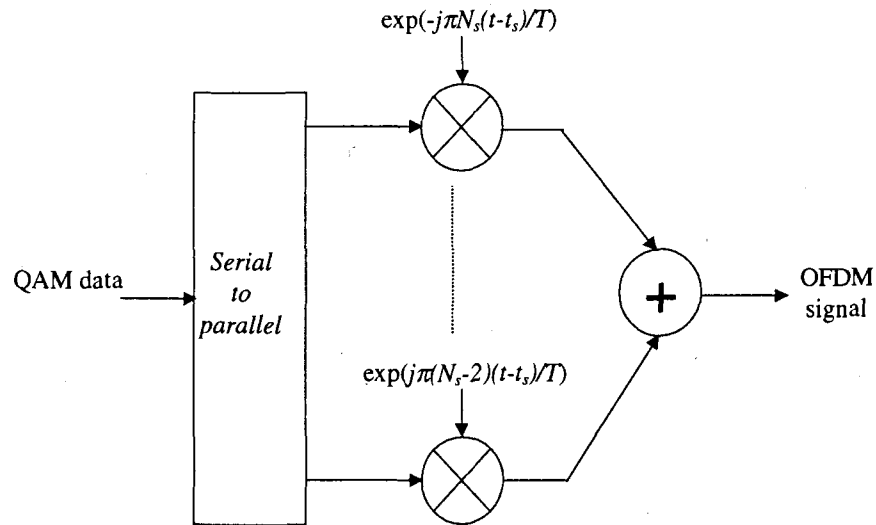


Figure 2.1 OFDM modulator.

As an example, Figure 2.2 shows four subcarriers from one OFDM signal. In this example, all subcarriers have the same phase and amplitude, but in practice the amplitudes and phases may be modulated differently for each subcarrier. Note that each subcarrier has exactly an integer number of cycles in the interval T , and the number of cycles between adjacent subcarriers differs by exactly one. This property accounts for

the orthogonality between the subcarriers. For instance, if the j th subcarrier from (2.2) is demodulated by downconverting the signal with a frequency of j/T and then integrating the signal over T seconds, the result is as written in (2.3). By looking at the intermediate result, it can be seen that a complex carrier is integrated over T seconds. For the demodulated subcarrier j , this integration gives the desired output $d_{j+N/2}$ (multiplied by a constant factor T), which is the QAM value for that particular subcarrier. For all other subcarriers, the integration is zero, because the frequency difference $(i-j)/T$ produces an integer number of cycles within the integration interval T , such that the integration result is always zero.

$$\begin{aligned}
 & \int_{t_s}^{t_s+T} \exp(-j2\pi \frac{j}{T}(t-t_s)) \sum_{i=-\frac{N_s}{2}}^{\frac{N_s}{2}-1} d_{i+N_s/2} \exp(j2\pi \frac{i}{T}(t-t_s)) dt \\
 &= \sum_{i=-\frac{N_s}{2}}^{\frac{N_s}{2}-1} d_{i+N_s/2} \int_{t_s}^{t_s+T} \exp(j2\pi \frac{i-j}{T}(t-t_s)) dt = d_{j+N_s/2} T
 \end{aligned} \tag{2.3}$$

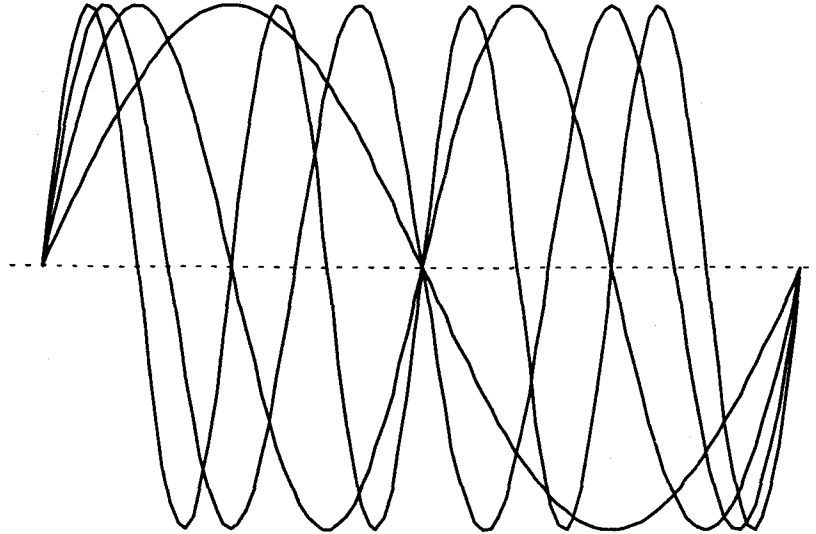


Figure 2.2 Example of four subcarriers within one OFDM symbol.

The orthogonality of the different OFDM subcarriers can also be demonstrated in another way. According to (2.1), each OFDM symbol contains subcarriers that are nonzero over a T -second interval. Hence, the spectrum of a single symbol is a convolution of a group of Dirac pulses located at the subcarrier frequencies with the spectrum of a square pulse that is one for a T -second period and zero otherwise. The amplitude spectrum of the square pulse is equal to $\text{sinc}(\pi f T)$, which has zeros for all frequencies f that are an integer multiple of $1/T$. This effect is shown in Figure 2.2, which shows the overlapping sinc spectra of individual subcarriers. At the maximum of each subcarrier spectrum, all other subcarrier spectra are zero. Because an OFDM

receiver essentially calculates the spectrum values at those points that correspond to the maxima of individual subcarriers, it can demodulate each subcarrier free from any interference from the other subcarriers. Basically, Figure 2.3 shows that the OFDM spectrum fulfills Nyquist's criterium for an intersymbol interference free pulse shape. Notice that the pulse shape is present in the frequency domain and not in the time domain, for which the Nyquist criterium usually is applied. Therefore, instead of intersymbol interference (ISI), it is intercarrier interference (ICI) that is avoided by having the maximum of one subcarrier spectrum correspond to zero crossings of all the others.

The complex baseband OFDM signal as defined by (2.2) is in fact nothing more than the inverse Fourier transform of N_s QAM input symbols. The time discrete equivalent is the inverse discrete Fourier transform (IDFT), which is given by (2.4), where the time t is replaced by a sample number n . In practice, this transform can be implemented very efficiently by the inverse fast Fourier transform (IFFT). An N point IDFT requires a total of N^2 complex multiplications—which are actually only phase rotations. Of course, there are also additions necessary to do an IDFT, but since the hardware complexity of an adder is significantly lower than that of a multiplier or phase rotator, only the multiplications are used here for comparison. The IFFT drastically reduces the amount of calculations by exploiting the regularity of the operations in the IDFT. Using the radix-2 algorithm, an N -point IFFT requires only $(N/2) \cdot \log_2(N)$ complex multiplications [1]. For a 16-point transform, for instance, the difference is 256 multiplications for the IDFT versus 32 for the IFFT—a reduction by a factor of 8! This difference grows for larger numbers of subcarriers, as the IDFT complexity grows quadratically with N , while the IFFT complexity only grows slightly faster than linear.

$$s(n) = \sum_{i=0}^{N_s-1} d_i \exp(j2\pi \frac{in}{N}) \quad (2.4)$$

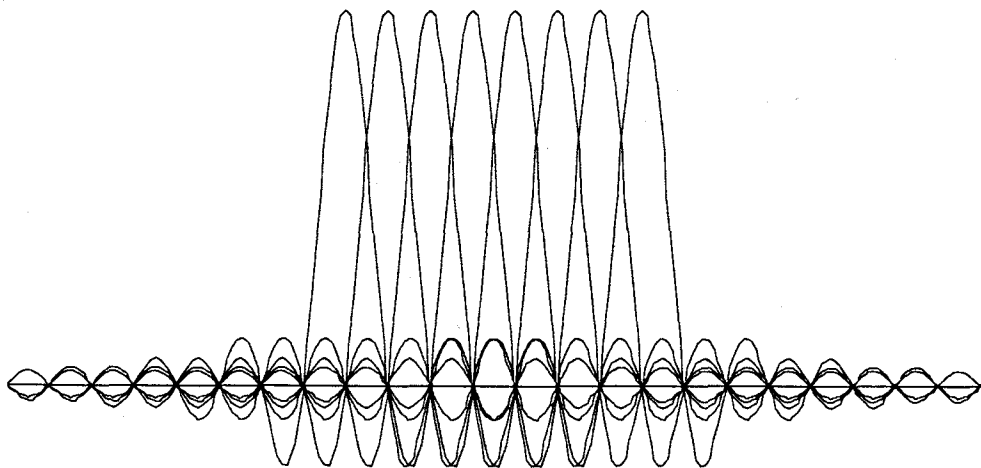


Figure 2.3 Spectra of individual subcarriers.

The number of multiplications in the IFFT can be reduced even further by using a radix-4 algorithm. This technique makes use of the fact that in a four-point IFFT, there are only multiplications by $\{1, -1, j, -j\}$, which actually do not need to be implemented by a full multiplier, but rather by a simple add or subtract and a switch of real and imaginary parts in the case of multiplications by j or $-j$. In the radix-4 algorithm, the transform is split into a number of these trivial four-point transforms, and non-trivial multiplications only have to be performed between stages of these four-point transforms. In this way, an N -point FFT using the radix-4 algorithm requires only $(3/8)N(\log_2 N - 2)$ complex multiplications or phase rotations and $N \log_2 N$ complex additions [1]. For a 64-point FFT, for example, this means 96 rotations and 384 additions, or 1.5 and 6 rotations and additions per sample, respectively.

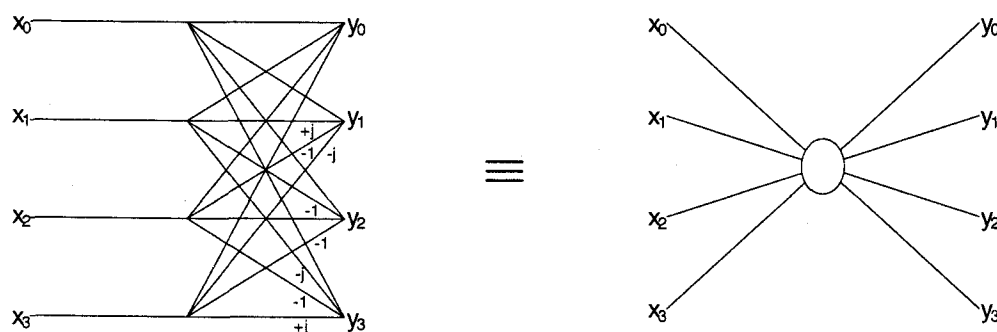


Figure 2.4 The radix-4 butterfly.

Figure 2.4 shows the four-point IFFT, which is known as the *radix-4 butterfly* that forms the basis for constructing larger IFFT sizes [1]. Four input values x_0 to x_3 are transformed into output values y_0 to y_3 by simple additions and trivial phase rotations. For instance, y_1 is given by $x_0 + jx_1 - x_2 - jx_3$, which can be calculated by doing four additions plus a few additional I/Q swappings and inversions to account for the multiplications by j and -1 .

The radix-4 butterfly can be used to efficiently build an IFFT with a larger size. For instance, a 16-point IFFT is depicted in Figure 2.5. The 16-point IFFT contains two stages with four radix-4 butterflies, separated by an intermediate stage where the 16 intermediate results are phase rotated by the twiddle factor ω^i , which is defined as $\exp(j2\pi i/N)$. Notice that for $N=16$, rotation by the twiddle factor ω^i reduces to a trivial operation for $i=0, 4, 8$ and 12 , where ω^i is $1, j, -1$ and $-j$, respectively. Taking this into account, the 16-point IFFT actually contains only eight non-trivial phase rotations, which is a factor of 32 smaller than the amount of phase rotations for the IDFT. These non-trivial phase rotations largely determine the implementation complexity, because the complexity of a phase rotation or complex multiplication is an order of magnitude larger than the complexity of an addition.

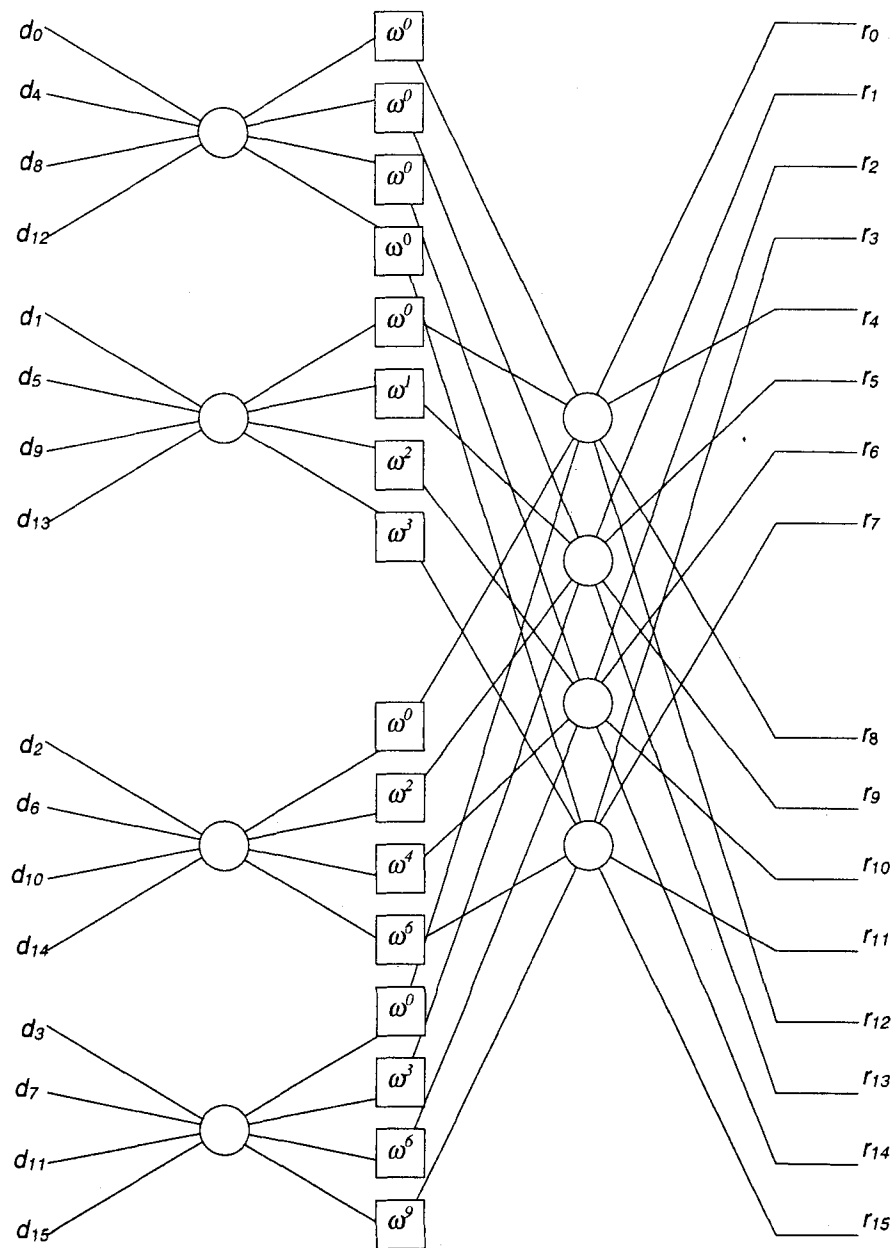


Figure 2.5 16-point IFFT using the radix-4 algorithm.

As an example of how to generate an OFDM symbol, let us assume that we want to transmit eight binary values $\{1 \ 1 \ 1 \ -1 \ 1 \ 1 \ -1 \ 1\}$ on eight subcarriers. The IDFT or IFFT then has to calculate:

$$\frac{1}{8} \begin{bmatrix} 1 & 1 & 1 & 1 & 1 & 1 & 1 & 1 \\ 1 & \frac{1}{2}\sqrt{2}(1+j) & j & \frac{1}{2}\sqrt{2}(-1+j) & -1 & \frac{1}{2}\sqrt{2}(-1-j) & -j & \frac{1}{2}\sqrt{2}(1-j) \\ 1 & j & -1 & -j & 1 & j & -1 & -j \\ 1 & \frac{1}{2}\sqrt{2}(-1+j) & -j & \frac{1}{2}\sqrt{2}(1+j) & -1 & \frac{1}{2}\sqrt{2}(1-j) & j & \frac{1}{2}\sqrt{2}(-1-j) \\ 1 & -1 & 1 & -1 & 1 & -1 & 1 & -1 \\ 1 & \frac{1}{2}\sqrt{2}(-1-j) & j & \frac{1}{2}\sqrt{2}(1-j) & -1 & \frac{1}{2}\sqrt{2}(1+j) & -j & \frac{1}{2}\sqrt{2}(-1+j) \\ 1 & -j & -1 & j & 1 & -j & -1 & j \\ 1 & \frac{1}{2}\sqrt{2}(1-j) & -j & \frac{1}{2}\sqrt{2}(-1-j) & -1 & \frac{1}{2}\sqrt{2}(-1+j) & j & \frac{1}{2}\sqrt{2}(1+j) \end{bmatrix} \begin{bmatrix} 1 \\ 1 \\ 1 \\ -1 \\ 1 \\ 1 \\ -1 \\ 1 \end{bmatrix} = \frac{1}{8} \begin{bmatrix} 4 \\ \sqrt{2}(1+j(\sqrt{2}-1)) \\ 2+2j \\ -\sqrt{2}(1+j(\sqrt{2}+1)) \\ 0 \\ -\sqrt{2}(1-j(\sqrt{2}+1)) \\ 2-2j \\ \sqrt{2}(1-j(\sqrt{2}-1)) \end{bmatrix} \quad (2.5)$$

The left-hand side of (2.5) contains the IDFT matrix, where every column corresponds to a complex subcarrier with a normalized frequency ranging from -4 to +3. The right-hand side of (2.5) gives the eight IFFT output samples that form one OFDM symbol. In practice, however, these samples are not enough to make a real OFDM signal. The reason is that there is no oversampling present, which would introduce intolerable aliasing if one would pass these samples through a digital-to-analog converter. To introduce oversampling, a number of zeros can be added to the input data. For instance, eight zeros could be added to the eight input samples of the previous example, after which a 16-point IFFT can be performed to get 16 output samples of a twice-oversampled OFDM signal. Notice that in the complex IFFT as in (2.5), the first half of the rows correspond to positive frequencies while the last half correspond to negative frequencies. Hence, if oversampling is used, the zeros should be added in the middle of the data vector rather than appending them at the end. This ensures the zero data values are mapped onto frequencies close to plus and minus half the sampling rate, while the nonzero data values are mapped onto the subcarriers around 0 Hz. For the data of the previous example, the oversampled input vector would become $\{1 \ 1 \ 1 \ -1 \ 0 \ 0 \ 0 \ 0 \ 0 \ 0 \ 0 \ 0 \ 1 \ 1 \ -1 \ 1\}$.

2.3 GUARD TIME AND CYCLIC EXTENSION

One of the most important reasons to do OFDM is the efficient way it deals with multipath delay spread. By dividing the input datastream in N_s subcarriers, the symbol duration is made N_s times smaller, which also reduces the relative multipath delay spread, relative to the symbol time, by the same factor. To eliminate intersymbol interference almost completely, a guard time is introduced for each OFDM symbol. The guard time is chosen larger than the expected delay spread, such that multipath components from one symbol cannot interfere with the next symbol. The guard time could consist of no signal at all. In that case, however, the problem of intercarrier interference (ICI) would arise. ICI is crosstalk between different subcarriers, which means they are no longer orthogonal. This effect is illustrated in Figure 2.6. In this example, a subcarrier 1 and a delayed subcarrier 2 are shown. When an OFDM receiver

tries to demodulate the first subcarrier, it will encounter some interference from the second subcarrier, because within the FFT interval, there is no integer number of cycles difference between subcarrier 1 and 2. At the same time, there will be crosstalk from the first to the second subcarrier for the same reason.

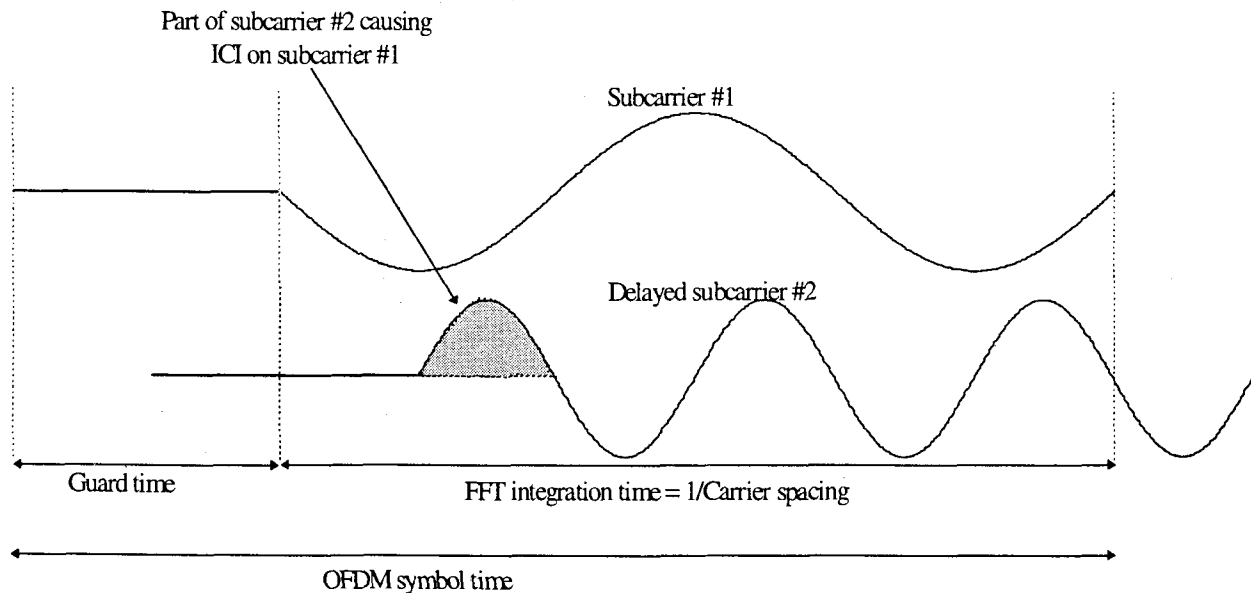


Figure 2.6 Effect of multipath with zero signal in the guard time; the delayed subcarrier 2 causes ICI on subcarrier 1 and vice versa.

To eliminate ICI, the OFDM symbol is cyclically extended in the guard time, as shown in Figure 2.7. This ensures that delayed replicas of the OFDM symbol always have an integer number of cycles within the FFT interval, as long as the delay is smaller than the guard time. As a result, multipath signals with delays smaller than the guard time cannot cause ICI.

As an example of how multipath affects OFDM, Figure 2.8 shows received signals for a two-ray channel, where the dotted curve is a delayed replica of the solid curve. Three separate subcarriers are shown during three symbol intervals. In reality, an OFDM receiver only sees the sum of all these signals, but showing the separate components makes it more clear what the effect of multipath is. From the figure, we can see that the OFDM subcarriers are BPSK modulated, which means that there can be 180-degree phase jumps at the symbol boundaries. For the dotted curve, these phase jumps occur at a certain delay after the first path. In this particular example, this multipath delay is smaller than the guard time, which means there are no phase transitions during the FFT interval. Hence, an OFDM receiver “sees” the sum of pure sine waves with some phase offsets. This summation does not destroy the orthogonality between the subcarriers, it only introduces a different phase shift for each subcarrier. The orthogonality does become lost if the multipath delay becomes larger than the

guard time. In that case, the phase transitions of the delayed path fall within the FFT interval of the receiver. The summation of the sine waves of the first path with the phase modulated waves of the delayed path no longer gives a set of orthogonal pure sine waves, resulting in a certain level of interference.

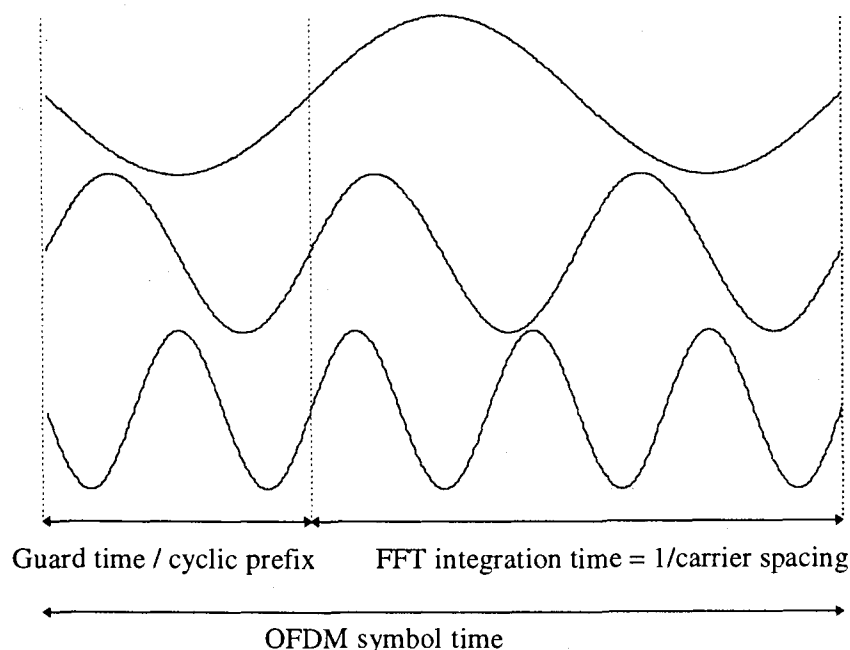


Figure 2.7 OFDM symbol with cyclic extension.

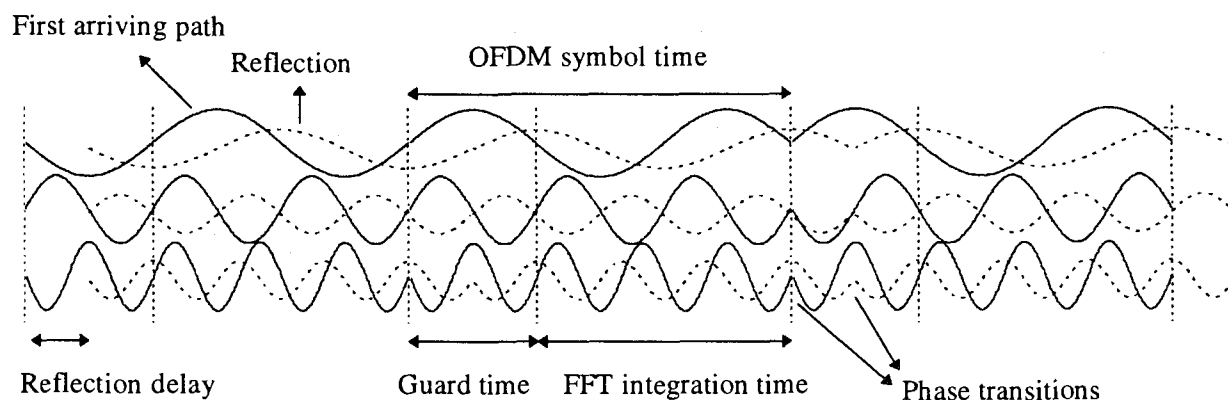


Figure 2.8 Example of an OFDM signal with three subcarriers in a two-ray multipath channel. The dashed line represents a delayed multipath component.

To get an idea what level of interference is introduced when the multipath delay exceeds the guard time, Figure 2.9 depicts three constellation diagrams that were derived from a simulation of an OFDM link with 48 subcarriers, each modulated by using 16-QAM. Figure 2.9(a) shows the undistorted 16-QAM constellation, which is observed whenever the multipath delay is below the guard time. In Figure 2.9(b), the multipath delay exceeds the guard time by a small 3% fraction of the FFT interval.

Hence, the subcarriers are not orthogonal anymore, but the interference is still small enough to get a reasonable received constellation. In Figure 2.9(c), the multipath delay exceeds the guard time by 10% of the FFT interval. The interference is now so large that the constellation is seriously blurred, causing an unacceptable error rate.

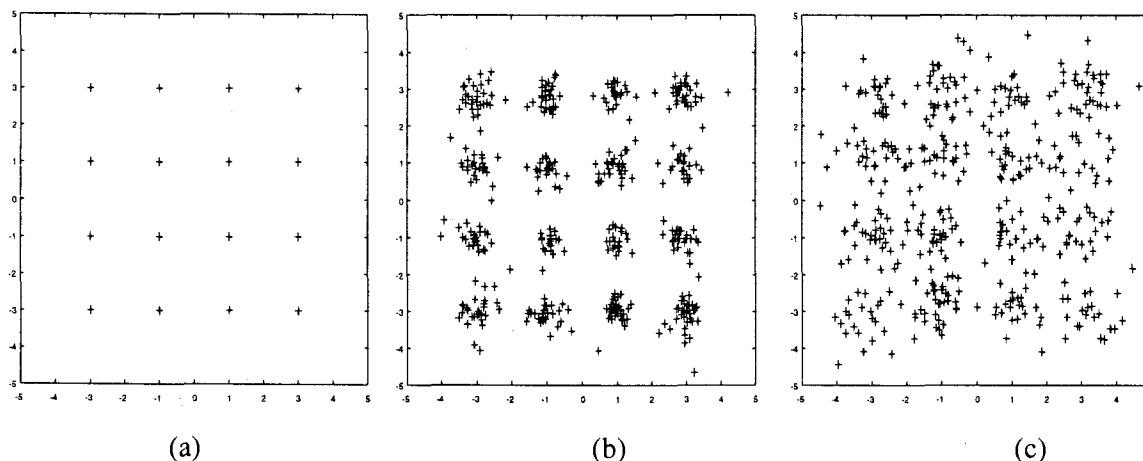


Figure 2.9 16-QAM constellation for a 48-subcarrier OFDM link with a two-ray multipath channel, the second ray being 6 dB lower than the first one. (a) delay < guard time; (b) delay exceeds guard time by 3% of the FFT interval; (c) delay exceeds guard time by 10% of the FFT interval.

2.4 WINDOWING

In the previous sections, it was explained how an OFDM symbol is formed by performing an IFFT and adding a cyclic extension. Looking at an example OFDM signal like in Figure 2.8, sharp phase transitions caused by the modulation can be seen at the symbol boundaries. Essentially, an OFDM signal like the one depicted in Figure 2.8 consists of a number of unfiltered QAM subcarriers. As a result, the out-of-band spectrum decreases rather slowly, according to a sinc function. As an example of this, the spectra for 16, 64, and 256 subcarriers are plotted in Figure 2.10. For larger number of subcarriers, the spectrum goes down more rapidly in the beginning, which is caused by the fact that the sidelobes are closer together. However, even the spectrum for 256 subcarriers has a relatively large -40 -dB bandwidth that is almost four times the -3 -dB bandwidth.

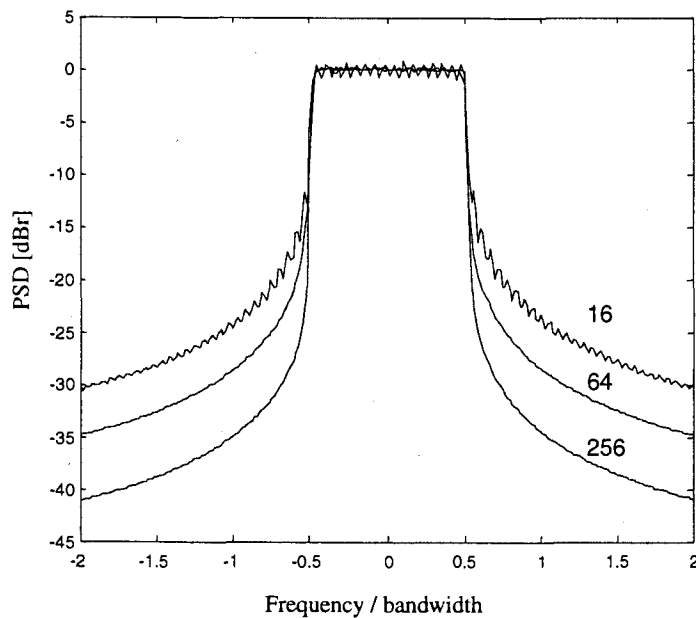


Figure 2.10 Power spectral density (PSD) without windowing for 16, 64, and 256 subcarriers.

To make the spectrum go down more rapidly, windowing can be applied to the individual OFDM symbols. Windowing an OFDM symbol makes the amplitude go smoothly to zero at the symbol boundaries. A commonly used window type is the raised cosine window, which is defined as

$$w(t) = \begin{cases} 0.5 + 0.5 \cos(\pi + t\pi / (\beta T_s)) & 0 \leq t \leq \beta T_s \\ 1.0 & \beta T_s \leq t \leq T_s \\ 0.5 + 0.5 \cos((t - T_s)\pi / (\beta T_s)) & T_s \leq t \leq (1 + \beta)T_s \end{cases} \quad (2.6)$$

Here, T_s is the symbol interval, which is shorter than the total symbol duration because we allow adjacent symbols to partially overlap in the roll-off region. The time structure of the OFDM signal now looks like Figure 2.11.

In equation form, an OFDM symbol starting at time $t = t_s = kT_s$ is defined as

$$s_k(t) = \text{Re} \left\{ w(t - t_s) \sum_{i=-\frac{N_s}{2}}^{\frac{N_s}{2}-1} d_{i+N_s(k+1/2)} \exp(j2\pi(f_c - \frac{i+0.5}{T})(t - t_s - T_{\text{prefix}})) \right\}, \quad t_s \leq t \leq t_s + T_s(1 + \beta)$$

$$s_k(t) = 0, \quad t < t_s \wedge t > t_s + T_s(1 + \beta) \quad (2.7)$$

In practice, the OFDM signal is generated as follows: first, N_c input QAM values are padded with zeros to get N input samples that are used to calculate an IFFT. Then, the last T_{prefix} samples of the IFFT output are inserted at the start of the OFDM symbol, and the first $T_{postfix}$ samples are appended at the end. The OFDM symbol is then multiplied by a raised cosine window $w(t)$ to more quickly reduce the power of out-of-band subcarriers. The OFDM symbol is then added to the output of the previous OFDM symbol with a delay of T_s , such that there is an overlap region of βT_s , where β is the rolloff factor of the raised cosine window.

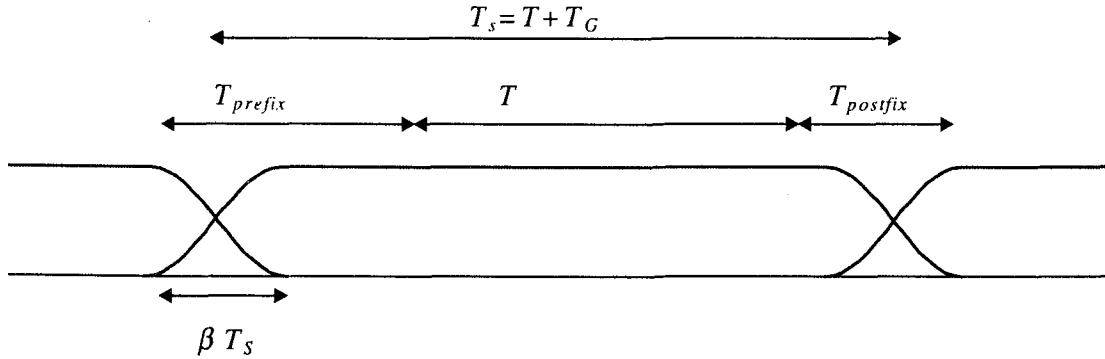


Figure 2.11 OFDM cyclic extension and windowing. T_s is the symbol time, T the FFT interval, T_G the guard time, T_{prefix} the preguard interval, $T_{postfix}$ the postguard interval, and β is the rolloff factor.

Figure 2.12 shows spectra for 64 subcarriers and different values of the rolloff factor β . It can be seen that a rolloff factor of 0.025—so the rolloff region is only 2.5% of the symbol interval—already makes a large improvement in the out-of-band spectrum. For instance, the -40 -dB bandwidth is more than halved to about twice the -3 -dB bandwidth. Larger rolloff factors improve the spectrum further, at the cost, however, of a decreased delay spread tolerance. The latter effect is demonstrated in Figure 2.13, which shows the signal structure of an OFDM signal for a two-ray multipath channel. The receiver demodulates the subcarriers by taking an FFT over the T -second interval between the dotted lines. Although the relative delay between the two multipath signals is smaller than the guard time, ICI and ISI are introduced because of the amplitude modulation in the gray part of the delayed OFDM symbol. The orthogonality between subcarriers as proved by (2.3) only holds when amplitude and phase of the subcarriers are constant during the entire T -second interval. Hence, a rolloff factor of β reduces the effective guard time by βT_s .

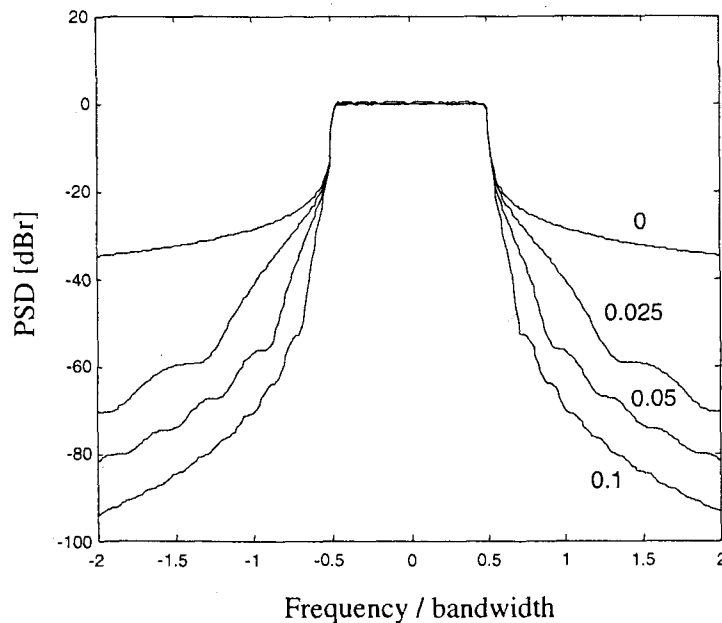


Figure 2.12 Spectra for raised cosine windowing with rolloff factors of 0 (rectangular window), 0.025, 0.05, and 0.1.

Instead of windowing, it is also possible to use conventional filtering techniques to reduce the out-of-band spectrum. Windowing and filtering are dual techniques; multiplying an OFDM symbol by a window means the spectrum is going to be a convolution of the spectrum of the window function with a set of impulses at the subcarrier frequencies. When filtering is applied, a convolution is done in the time domain and the OFDM spectrum is multiplied by the frequency response of the filter. When using filters, care has to be taken not to introduce rippling effects on the envelope of the OFDM symbols over a timespan that is larger than the rolloff region of the windowing approach. Too much rippling means the undistorted part of the OFDM envelope is smaller, and this directly translates into less delay spread tolerance. Notice that digital filtering techniques are more complex to implement than windowing. A digital filter requires at least a few multiplications per sample, while windowing only requires a few multiplications per symbol, for those samples which fall into the rolloff region. Hence, because only a few percent of the samples are in the rolloff region, windowing is an order of magnitude less complex than digital filtering.

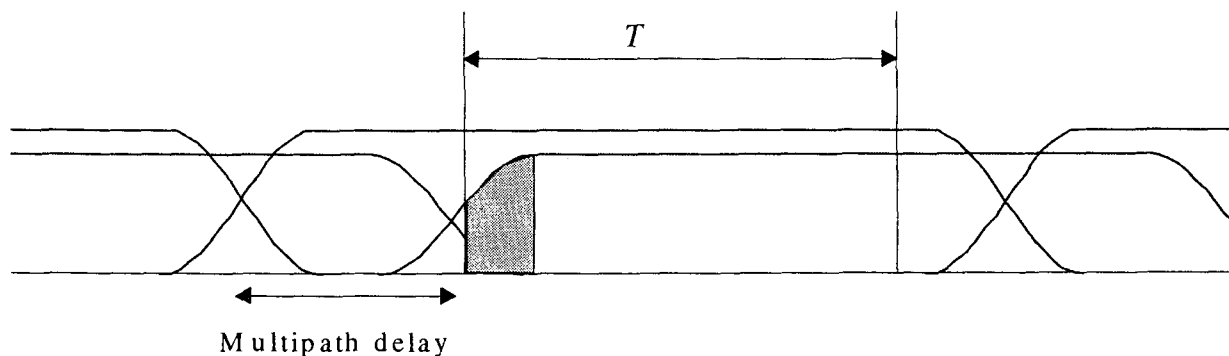


Figure 2.13 OFDM symbol windows for a two-ray multipath channel, showing ICI and ISI, because in the gray part, the amplitude of the delayed subcarriers is not constant.

2.5 CHOICE OF OFDM PARAMETERS

The choice of various OFDM parameters is a tradeoff between various, often conflicting requirements. Usually, there are three main requirements to start with: bandwidth, bit rate, and delay spread. The delay spread directly dictates the guard time. As a rule, the guard time should be about two to four times the root-mean-squared delay spread. This value depends on the type of coding and QAM modulation. Higher order QAM (like 64-QAM) is more sensitive to ICI and ISI than QPSK; while heavier coding obviously reduces the sensitivity to such interference.

Now that the guard time has been set, the symbol duration can be fixed. To minimize the signal-to-noise ratio (SNR) loss caused by the guard time, it is desirable to have the symbol duration much larger than the guard time. It cannot be arbitrarily large, however, because a larger symbol duration means more subcarriers with a smaller subcarrier spacing, a larger implementation complexity, and more sensitivity to phase noise and frequency offset [2], as well as an increased peak-to-average power ratio [3, 4]. Hence, a practical design choice is to make the symbol duration at least five times the guard time, which implies a 1-dB SNR loss because of the guard time.

After the symbol duration and guard time are fixed, the number of subcarriers follows directly as the required -3 -dB bandwidth divided by the subcarrier spacing, which is the inverse of the symbol duration less the guard time. Alternatively, the number of subcarriers may be determined by the required bit rate divided by the bit rate per subcarrier. The bit rate per subcarrier is defined by the modulation type (e.g., 16-QAM), coding rate, and symbol rate.

As an example, suppose we want to design a system with the following requirements:

- Bit rate: 20 Mbps
- Tolerable delay spread: 200 ns
- Bandwidth: < 15 MHz

The delay-spread requirement of 200 ns suggests that 800 ns is a safe value for the guard time. By choosing the OFDM symbol duration 6 times the guard time ($4.8 \mu\text{s}$), the guard time loss is made smaller than 1 dB. The subcarrier spacing is now the inverse of $4.8 - 0.8 = 4 \mu\text{s}$, which gives 250 kHz. To determine the number of subcarriers needed, we can look at the ratio of the required bit rate and the OFDM symbol rate. To achieve 20 Mbps, each OFDM symbol has to carry 96 bits of information ($96/4.8 \mu\text{s} = 20 \text{ Mbps}$). To do this, there are several options. One is to use 16-QAM together with rate $\frac{1}{2}$ coding to get 2 bits per symbol per subcarrier. In this case, 48 subcarriers are needed to get the required 96 bits per symbol. Another option is to use QPSK with rate $\frac{3}{4}$ coding, which gives 1.5 bits per symbol per subcarrier. In this case, 64 subcarriers are needed to reach the 96 bits per symbol. However, 64 subcarriers means a bandwidth of $64 \cdot 250 \text{ kHz} = 16 \text{ MHz}$, which is larger than the target bandwidth. To achieve a bandwidth smaller than 15 MHz, the number of subcarriers needs to be smaller than 60. Hence, the first option with 48 subcarriers and 16-QAM fulfills all the requirements. It has the additional advantage that an efficient 64-point radix-4 FFT/IFFT can be used, leaving 16 zero subcarriers to provide oversampling necessary to avoid aliasing.

An additional requirement that can affect the chosen parameters is the demand for an integer number of samples both within the FFT/IFFT interval and in the symbol interval. For instance, in the above example we want to have exactly 64 samples in the FFT/IFFT interval to preserve orthogonality among the subcarriers. This can be achieved by making the sampling rate $64/4 \mu\text{s} = 16 \text{ MHz}$. However, for that particular sampling rate, there is no integer number of samples with the symbol interval of $4.8 \mu\text{s}$. The only solution to this problem is to change one of the parameters slightly to meet the integer constraint. For instance, the number of samples per symbol can be set to 78, which gives a sampling rate of $78/4.8 \mu\text{s} = 16.25 \text{ MHz}$. Now, the FFT interval becomes $64/16.25 \text{ MHz} = 3.9385 \mu\text{s}$, so both guard time and subcarrier spacing are slightly larger than in the case of the original FFT interval of $4 \mu\text{s}$.

2.6 OFDM SIGNAL PROCESSING

The previous sections described how the basic OFDM signal is formed using the IFFT, adding a cyclic extension and performing windowing to get a steeper spectral rolloff. However, there is more to it to build a complete OFDM modem. Figure 2.14 shows the block diagram of an OFDM modem, where the upper path is the transmitter chain and the lower path corresponds to the receiver chain. In the center we see the IFFT, which modulates a block of input QAM values onto a number of subcarriers. In the receiver, the subcarriers are demodulated by an FFT, which performs the reverse operation of an IFFT. An interesting feature of the FFT/IFFT is that the FFT is almost identical to an IFFT. In fact, an IFFT can be made using an FFT by conjugating input and output of the FFT and dividing the output by the FFT size. This makes it possible to use the same hardware for both transmitter and receiver. Of course, this saving in complexity is only possible when the modem does not have to transmit and receive simultaneously.

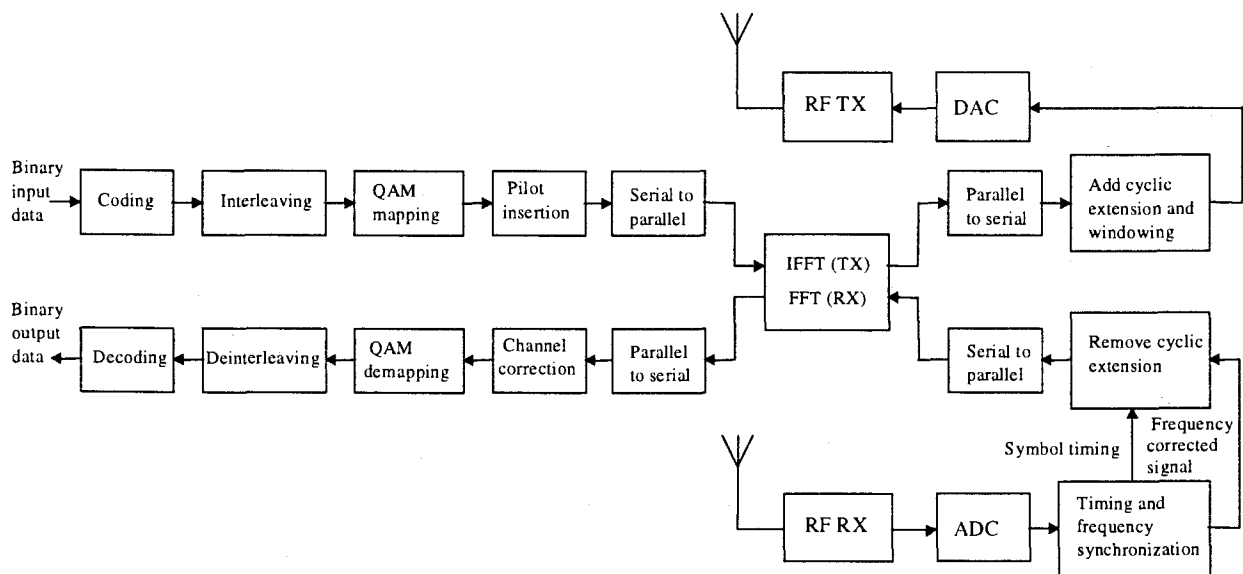


Figure 2.14 Block diagram of an OFDM transceiver.

The functions before the IFFT have not been discussed till now. Binary input data is first encoded by a forward error correction code. The encoded data is then interleaved and mapped onto QAM values. These functions are discussed in more detail in the next chapter.

In the receiver path, after passing the RF part and the analog-to-digital conversion, the digital signal processing starts with a training phase to determine symbol timing and frequency offset. An FFT is used to demodulate all subcarriers. The output of the FFT contains N_s QAM values, which are mapped onto binary values and decoded to produce binary output data. To successfully map the QAM values onto binary values, first the reference phases and amplitudes of all subcarriers have to be acquired. Alternatively, differential techniques can be applied. All of these receiver functions are highlighted in the following chapters.

2.7 IMPLEMENTATION COMPLEXITY OF OFDM VERSUS SINGLE-CARRIER MODULATION

One of the main reasons to use OFDM is its ability to deal with large delay spreads with a reasonable implementation complexity. In a single-carrier system, the implementation complexity is dominated by equalization, which is necessary when the delay spread is larger than about 10% of the symbol duration. OFDM does not require an equalizer. Instead, the complexity of an OFDM system is largely determined by the FFT, which is used to demodulate the various subcarriers. In the following example, it is demonstrated that the processing complexity of an OFDM modem can be significantly less than that of a single carrier modem, given the fact that both can deal with the same amount of delay spread. Notice that some papers mention the use of a

single-tap equalizer for OFDM, when they are referring to the phase correction in case of a coherent OFDM receiver. We will not use this somewhat confusing terminology, because the term equalization suggests that an attempt is made to invert the channel, while an OFDM receiver is doing the opposite; weak subcarriers are not being extra amplified to equalize the channel, but rather, they get a low weight in the decoding. In this way, OFDM avoids the problem of noise enhancement that is present in linear equalization techniques.

Figure 2.15 shows the block diagram of a decision feedback equalizer with symbol-spaced taps. Such an equalizer can be used to combat delay spread in single-carrier systems using quadrature amplitude modulation (QAM) or some form of constant amplitude modulation such as Gaussian Minimum Shift Keying (GMSK) or offset-QPSK. From references [5, 6], it can be learned that at least 8 feedforward and 8 feedback taps are required to handle a delay spread of 100 ns for a GMSK modem at a data rate of 24 Mbps. We can use this information to compare a single carrier system with the 24 Mbps mode of the new IEEE 802.11 OFDM standard, which can handle delay spreads up to 250 ns using a 64-point FFT. In order to increase the delay spread tolerance of a GMSK modem to the same level, the equalizer length has to be increased by a factor of 250/100, so it has 20 feedforward and feedback taps. Fortunately, for GMSK only the real outputs of the complex multiplications are used, so each multiplier has to perform two real multiplications per sample. Hence, the number of real multiplications per second becomes $2 \cdot 20 \cdot 24 \cdot 10^6 = 960 \cdot 10^6$. Notice we only count the feedforward taps here, since the feedback taps consist of trivial rotations, while the feedforward taps consist of full multiplications. For the OFDM system, a 64-point FFT has to be processed by every OFDM symbol duration which is 4 μ s, see chapter 10. With a radix-4 algorithm, this requires 96 complex multiplications [1], which gives a processing load of $96 \cdot 10^6$ real multiplications per second. So, in terms of multiplications per second, the equalizer of the single carrier system is 10 times more complex than the FFT of the OFDM system! This complexity difference grows with the bit rate, or rather with the bandwidth – delay spread product, which is a measure of the relative amount of inter-symbol interference. For instance, if we want to double the bit rate in the previous example by doubling the bandwidth, but the delay spread tolerance has to stay the same, then the number of subcarriers and the guard time has to be doubled for OFDM, while for the single-carrier system, both the number of equalizer taps and the sampling rate are doubled. The latter means that the number of multiplications per second is quadrupled, so the equalizer complexity grows quadratically with the bandwidth – delay spread product. For OFDM, a double-sized FFT has to be calculated in the same amount of time in order to double the rate. For the radix-2 algorithm, this means an increase in the number of multiplications of $M \log_2(2N) / (N/2) \log_2 N = 2(1 + 1/\log_2 N)$, where N is the FFT size for the half-rate system. The complexity of the FFT grows only slightly faster than linear with the bandwidth – delay spread product, which explains why OFDM is more attractive than a single carrier system with equalization for relatively large bandwidth – delay spread products (values around 1 or larger). It should be noted that the complexity difference between the FFT and the equalizer is less if the equalization is done in the frequency domain, as

described in [7]. In this case, equalization is twice as complex, because both an FFT and an IFFT have to be performed to do frequency domain equalization on a signal block.

Another complexity advantage of OFDM is the fact that the FFT does not really require full multiplications, but rather phase rotations, which can be efficiently implemented by the CORDIC algorithm [8]. Because phase rotations do not change the amplitude, they do not increase the dynamic range of the signals, which simplifies the fixed point design.

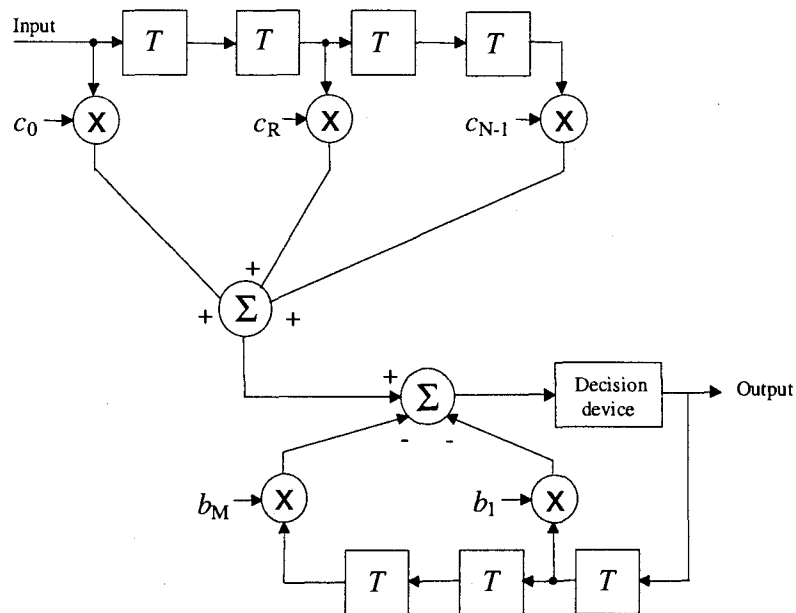


Figure 2.15 Decision-feedback equalizer.

Except for the difference in complexity, OFDM has another advantage over single carrier systems with equalizers. For the latter systems, the performance degrades abruptly if the delay spread exceeds the value for which the equalizer is designed. Because of error propagation, the raw bit error probability increases so quickly that introducing lower rate coding or a lower constellation size does not significantly improve the delay spread robustness. For OFDM, however, there are no such nonlinear effects as error propagation, and coding and lower constellation sizes can be employed to provide fallback rates that are significantly more robust against delay spread. This is an important consideration, as it enhances the coverage area and avoids the situation that users in bad spots cannot get any connection at all.

REFERENCES

- [1] Blahut, R. E., *Fast Algorithms for Digital Signal Processing*. Reading, MA: Addison-Wesley, 1985.
- [2] Pollet, T., M. van Bladel and M. Moeneclaey, "BER Sensitivity of OFDM Systems to Carrier Frequency Offset and Wiener Phase Noise," *IEEE Trans. on Comm.*, Vol. 43, No. 2/3/4, pp. 191–193, Feb.–Apr. 1995.
- [3] Pauli, M., and H. P. Kuchenbecker, "Minimization of the Intermodulation Distortion of a Nonlinearly Amplified OFDM Signal," *Wireless Personal Communications*, Vol. 4, No. 1, pp. 93–101, Jan. 1997.
- [4] Rapp, C., "Effects of HPA-Nonlinearity on a 4-DPSK/OFDM Signal for a Digital Sound Broadcasting System," *Proc. of the Second European Conference on Satellite Communications*, Liège, Belgium, pp.179–184, Oct. 22–24, 1991.
- [5] Tellado-Mourelo, J., E. K.Wesel, J. M.Cioffi, "Adaptive DFE for GMSK in Indoor Radio Channels," *IEEE Trans. on Sel. Areas in Comm.*, Vol. 14, No. 3, pp. 492–501, Apr. 1996.
- [6] Wales, S. W., "Modulation and Equalization Techniques for HIPERLAN," *Proc. of PIMRC/WCN*, The Hague, The Netherlands, Sept. 21–23, pp. 959–963, 1994.
- [7] Sari, H., G. Karam, I. Jeanclaude, "Transmission Techniques for Digital Terrestrial TV Broadcasting," *IEEE Communications Magazine*, Feb. 1995, pp. 100–109.
- [8] Parhi, K. K., and T. Nishitani, *Digital Signal Processing for Multimedia Systems*. New York: Marcel Dekker, Inc., 1999.

Chapter 3

Coding and Modulation

3.1 INTRODUCTION

We explained in the previous chapter how OFDM avoids the problem of intersymbol interference by transmitting a number of narrowband subcarriers together with using a guard time. This does give rise to another problem, however, which is the fact that in a multipath fading channel, all subcarriers will arrive at the receiver with different amplitudes. In fact, some subcarriers may be completely lost because of deep fades. Hence, even though most subcarriers may be detected without errors, the overall bit-error ratio (BER) will be largely dominated by a few subcarriers with the smallest amplitudes, for which the bit-error probability is close to 0.5. To avoid this domination by the weakest subcarriers, forward-error correction coding is essential. By using coding across the subcarriers, errors of weak subcarriers can be corrected up to a certain limit that depends on the code and the channel. A powerful coding means that the performance of an OFDM link is determined by the average received power, rather than by the power of the weakest subcarrier.

This chapter starts with a review of block codes and convolutional codes. Then, it introduces interleaving as a way to randomize error bursts that occur when adjacent subcarriers are lost in a deep fade. Section 3.4 describes QAM as the most commonly used modulation technique in OFDM, after which Section 3.5 shows the important relation between coding and modulation. Thus, this chapter presents a brief overview of coding and modulation [1–9].

3.2 FORWARD-ERROR CORRECTION CODING

3.2.1 Block Codes

A *block code* encodes a block of k input symbols into n coded symbols, with n being larger than k . The purpose of adding the redundant $n-k$ symbols is to increase the *minimum Hamming distance*, which is the minimum number of different symbols between any pair of code words. For a minimum Hamming distance of d_{\min} , the code can correct t errors where t is given by

$$t \leq \text{floor}\left(\frac{d_{\min} - 1}{2}\right) \quad (3.1)$$

Here, $\text{floor}(x)$ denotes the floor function that rounds x downward to the closest integer value. The minimum Hamming distance is upperbound by the number of redundant symbols $n-k$ as

$$d_{\min} \leq n - k + 1 \quad (3.2)$$

For binary codes, only repetition codes and single-parity check codes reach this upperbound. A class of nonbinary codes that does reach the above bound are the *Reed-Solomon codes*. Because of their good distance properties and the availability of efficient coding and decoding algorithms [6, 7], Reed-Solomon codes are the most popularly used block codes. Reed-Solomon codes are defined for blocks of symbols with m bits per symbol, where the code length n is related to m by

$$n = 2^m - 1 \quad (3.3)$$

The number of input symbols k is related to m and the required minimum Hamming distance d_{\min} as

$$k = 2^m - d_{\min} \quad (3.4)$$

There appears to be little flexibility in the available code lengths as indicated by (3.3). However, a Reed-Solomon code can easily be shortened to any arbitrary length

by leaving a number of input bits zero and deleting the same amount of output bits. It is also possible to extend the code length to a power of 2 by adding an extra parity symbol.

According to (3.1) and (3.2), a Reed-Solomon code can correct up to $\text{floor}((n-k)/2)$ erroneous symbols. Each symbol contains m bits, so a maximum amount of $m \cdot \text{floor}((n-k)/2)$ erroneous bits may be corrected. The latter is only true, however, if all bit errors occur within the maximum amount of correctable symbol errors. So if a Reed-Solomon is designed to correct up to two symbol errors containing 8 bits per symbol, it cannot correct an arbitrary combination of three bit errors, as these errors may occur in three different symbols. This characteristic makes Reed-Solomon codes particularly useful for correcting bursty channels. One example of such a channel is an OFDM link in the presence of multipath fading, which causes the errors to be concentrated in a few subcarriers that are hit by deep fades.

3.2.2 Convolutional Codes

A convolutional code maps each k bits of a continuous input stream on n output bits, where the mapping is performed by convolving the input bits with a binary impulse response. The convolutional encoding can be implemented by simple shift registers and modulo-2 adders. As an example, Figure 3.1 shows the encoder for a rate 1/2 code which is actually one of the most frequently applied convolutional codes. This encoder has a single data input and two outputs A_i and B_i , which are interleaved to form the coded output sequence $\{A_1B_1A_2B_2 \dots\}$. Each pair of output bits $\{A_i, B_i\}$ depends on seven input bits, being the current input bit plus six previous input bits that are stored in the length 6 shift register. This value of 7—or in general the shift register length plus 1—is called the *constraint length*. The shift register taps are often specified by the corresponding generator polynomials or generator vectors. For the example of Figure 3.1, the generator vectors are $\{1011011, 1111001\}$ or $\{133, 171\}$ octal. The ones in the generator vectors correspond with taps on the shift register.

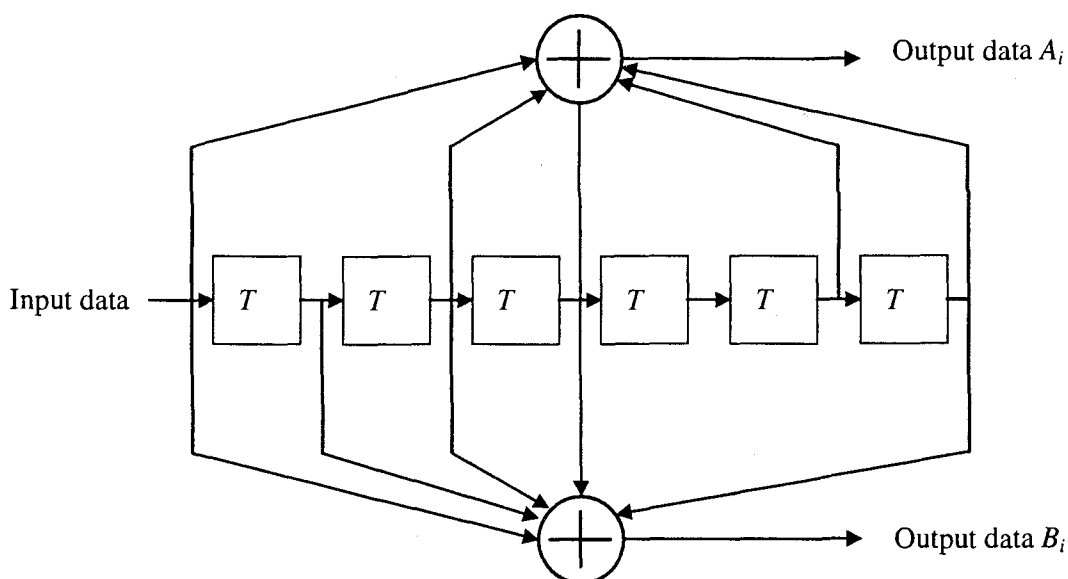


Figure 3.1 Block diagram of a constraint length 7 convolutional encoder.

Decoding of convolutional codes is most often performed by *soft decision Viterbi decoding*, which is an efficient way to obtain the optimal maximum likelihood estimate of the encoded sequence. A description of this decoding technique can be found in [8]. The complexity of Viterbi decoding grows exponentially with the constraint length. Hence, practical implementations do not go further than a constraint length of about 10. Decoding of convolutional codes with larger constraint length is possible by using suboptimal decoding techniques like sequential decoding [8].

Because convolutional codes do not have a fixed length, it is more difficult to specify their performance in terms of Hamming distance and a number of correctable errors. One measure that is used is the *free distance*, which is the minimum Hamming distance between arbitrarily long different code sequences that begin and end with the same state of the encoder, where the state is defined by the contents of the shift registers of the encoder. For example, the code of Figure 3.1 has a free distance of 10. When hard decision decoding is used, this code can correct up to $\text{floor}((10-1)/2) = 4$ bit errors within each group of encoded bits with a length of about 3 to 5 times the constraint length. When soft decision decoding is used, however, the number of correctable errors does not really give a useful measure anymore. A better performance measure is the *coding gain*, which is defined as the gain in the bit energy-to-noise density ratio E_b/N_o relative to an uncoded system to achieve a certain bit error ratio. The E_b/N_o gain is equivalent to the gain in input signal-to-noise ratio (SNR) minus the rate loss in dB because of the redundant bits. As an example, Figure 3.2 shows the bit error ratio versus E_b/N_o for uncoded QPSK and for coded QPSK using the previously mentioned constraint length 7 code. It can be seen from the figure that for a bit-error ratio of 10^{-4} , the coded link needs about 5 dB less E_b/N_o compared with that of the uncoded link. For lower bit error ratios, this coding gain converges to a maximum value of about 5.5 dB.

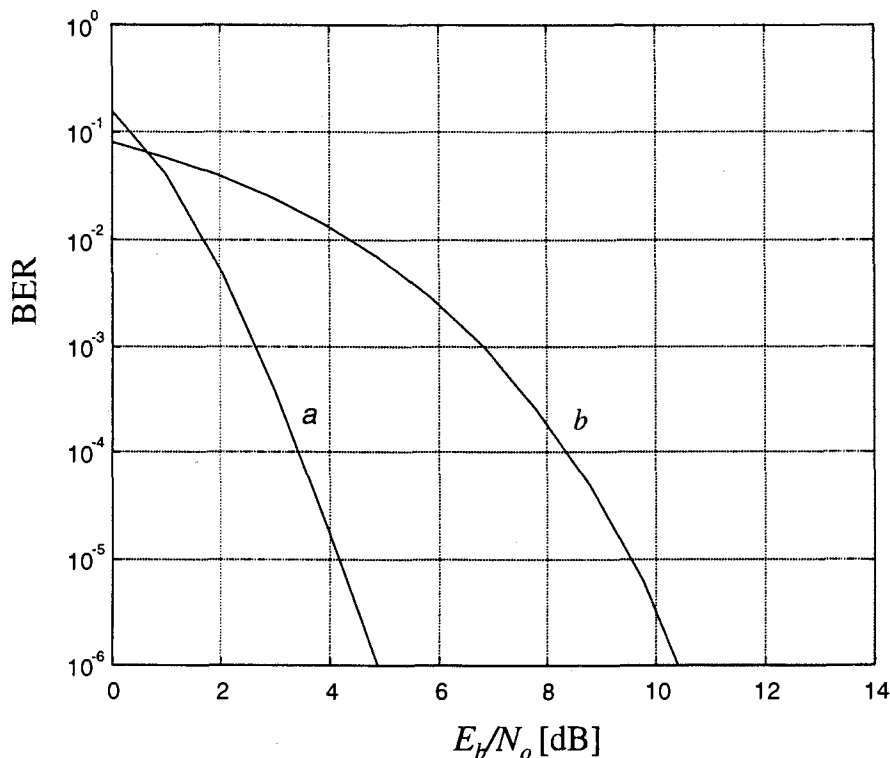


Figure 3.2 BER versus E_b/N_o for coded and uncoded QPSK in AWGN.

In the above curves, we have used the bit energy-to-noise density ratio E_b/N_o , which is equivalent to the ratio of the signal power P and the noise power in a bandwidth equal to the bit rate N_o/T_b , where T_b is the bit time. Some other useful SNR definitions are the input SNR and the symbol energy-to-noise density ratio E_s/N_o , which is equivalent to the ratio of the signal power and the noise power within a bandwidth equal to the symbol rate N_o/T_s , where T_s is the symbol duration. E_s/N_o is equivalent to the SNR for individual subcarriers, plus the guard time loss in dB. It is related to E_b/N_o as

$$\frac{E_s}{N_o} = \frac{E_b}{N_o} \frac{T_s}{T_b} \quad (3.5)$$

The input signal-to-noise ratio SNR_i is related to E_b/N_o as

$$SNR_i = \frac{E_b}{N_o} \frac{1}{BT_b} = \frac{E_b}{N_o} \frac{bN_s r}{BT_s} \quad (3.6)$$

Here, B is the input noise bandwidth, b is the number of coded bits per subcarrier, N_s the number of subcarriers, and r the coding rate. Basically, the SNR_i is equal to E_b/N_o multiplied by the ratio of bit rate and bandwidth. The latter ratio is equivalent to the spectral efficiency in bps/Hz. The spectral efficiency depends on the number of bits per subcarrier b , which is determined by the constellation size, the coding rate r , and the guard time, which appears indirectly in (3.6) as a part of the

symbol duration T_s . The number of subcarriers has no influence on the spectral efficiency, because the noise bandwidth increases linearly with the number of subcarriers.

A convolutional code can be punctured to increase the coding rate. For instance, increasing the rate of the above rate 1/2 code to 3/4 is done by deleting 2 of every 6 bits at the output of the encoder. The punctured output sequence for a rate 3/4 code is $\{A_1B_1A_2B_3A_4B_4A_5B_6A_7B_7 \dots\}$. For a rate 2/3 code, the punctured output sequence is $\{A_1B_1A_2A_3B_3A_4A_5B_5 \dots\}$. To decode the punctured sequence, the original rate 1/2 decoder can be used. Before decoding, erasures have to be inserted in the data at the locations of the punctured bits.

3.2.3 Concatenated Codes

Instead of using a single block code or convolutional code, it is also possible to combine or concatenate two codes. The main advantage of a concatenated code is that it can provide a large coding gain with less implementation complexity as a comparable single code. Figure 3.3 shows the block diagram of a concatenated coding scheme. The input bits are first coded and interleaved by an outer coder and interleaver. The coded bits are then again coded and interleaved by an inner coder and interleaver. Usually, the inner code is a convolutional code and the outer code a block code; for instance, a Reed-Solomon code. The motivation behind this is that the convolutional code with soft decision decoding performs better for relatively low-input SNRs. The hard decision block decoder then cleans up the relatively few remaining errors in the decoded output bits of the convolutional decoder. The task of the interleavers is to break up bursts of errors as much as possible. In case of an outer block code, the outer interleaver preferably separates symbols by more than the block length of the outer encoder. Compared with a single-code system, concatenated coding has more delay because of the extra interleaving, which can be a disadvantage for packet communications where the interleaving delay affects turnaround time and throughput. A good overview of achievable performance of concatenated coding is given in [3].

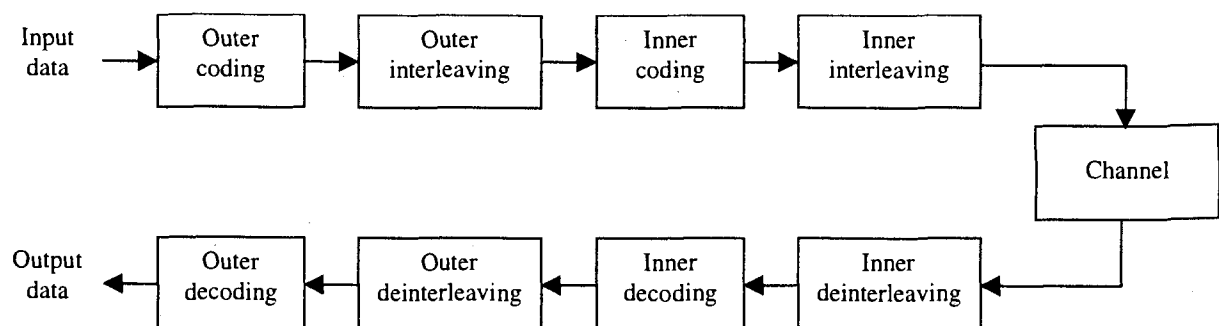


Figure 3.3 Concatenated coding/decoding.

3.3 INTERLEAVING

Because of the frequency selective fading of typical radio channels, the OFDM subcarriers generally have different amplitudes. Deep fades in the frequency spectrum may cause groups of subcarriers to be less reliable than others, thereby causing bit errors to occur in bursts rather than being randomly scattered. Most forward error-correction codes are not designed to deal with error bursts. Therefore, interleaving is applied to randomize the occurrence of bit errors prior to decoding. At the transmitter, the coded bits are permuted in a certain way, which makes sure that adjacent bits are separated by several bits after interleaving. At the receiver, the reverse permutation is performed before decoding. A commonly used interleaving scheme is the block interleaver, where input bits are written in a matrix column by column and read out row by row. As an example of such an interleaver, Figure 3.4 shows the bit numbers of a block interleaver operating on a block size of 48 bits. After writing the 48 bits in the matrix according to the order as depicted in the figure, the interleaved bits are read out row by row, so the output bit numbers are 0, 8, 16, 24, 32, 40, 1, 9, . . . , 47. Instead of bits, the operation can also be applied on symbols; for instance, the matrix can be filled with 48 16-QAM symbols containing 4 bits per symbol, so the interleaving changes the symbol order but not the bit order within each symbol. Interleaving on a symbol-basis is especially useful for Reed-Solomon codes, as these codes operate on symbols rather than bits. A Reed-Solomon code can correct up to a certain number of symbol errors per block length, so interleaving should be done over several block lengths, in order to spread bursts of symbol errors over a number of different Reed-Solomon blocks.

0	8	16	24	32	40
1	9	17	25	33	41
2	10	18	26	34	42
3	11	19	27	35	43
4	12	20	28	36	44
5	13	21	29	37	45
6	14	22	30	38	46
7	15	23	31	39	47

Figure 3.4 Interleaving scheme.

For a general block interleaver with a block size of N_B bits and d columns, the i th interleaved bit is equal to the k th encoded input bit, where k is given by

$$k = id - (N_B - 1) \text{floor}\left(\frac{id}{N_B}\right) \quad (3.7)$$

Instead of a block interleaver, it is also possible to use a convolutional interleaver. An example of this type of interleaver is shown in Figure 3.5. The interleaver cyclically writes each input symbol or bit into one of K shift registers that introduce a delay of 0 to $k-1$ symbol durations. The shift registers are read out cyclically to produce the interleaved symbols.

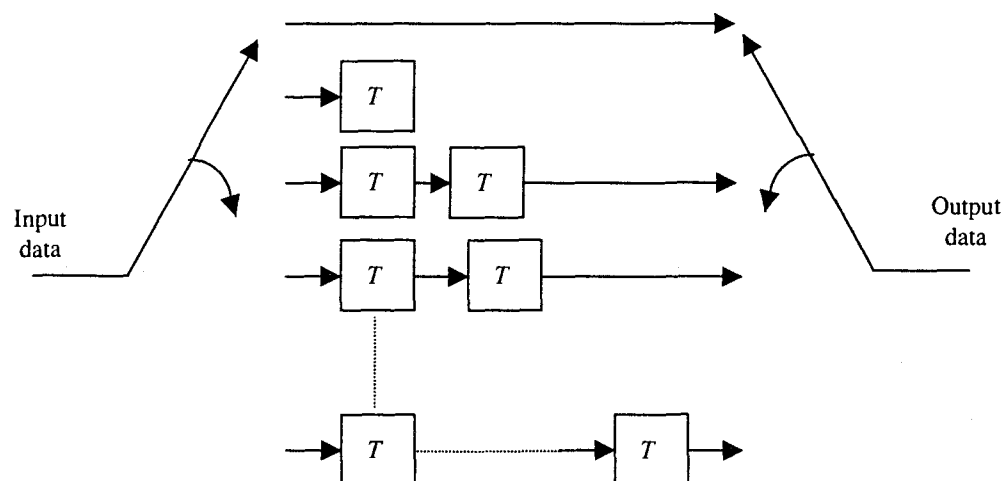


Figure 3.5 Convolutional interleaver.

3.4 QUADRATURE AMPLITUDE MODULATION

Quadrature amplitude modulation (QAM) is the most popular type of modulation in combination with OFDM. Especially rectangular constellations are easy to implement as they can be split into independent *Pulse amplitude modulated* (PAM) components for both the in-phase and the quadrature part. Figure 3.6 shows the rectangular constellations of Quadrature Phase Shift Keying (QPSK), 16-QAM, and 64-QAM. The constellations are not normalized; to normalize them to an average power of one—assuming that all constellation points are equally likely to occur—each constellation has to be multiplied by the normalization factor listed in Table 3.1. The table also mentions Binary Phase Shift Keying (BPSK), which uses two of the four QPSK constellation points ($1+j$, $-1-j$).

Table 3.1 also gives the loss in the minimum squared Euclidean distance between two constellation points, divided by the gain in data rate of that particular QAM type relative to BPSK. This value defines the maximum loss in E_b/N_o relative to BPSK that is needed to achieve a certain bit-error ratio in an uncoded QAM link. The BER curves in Figure 3.7 illustrate that the E_b/N_o loss values of Table 3.1 are quite accurate for BER values below 10^{-2} . The difference between QPSK and 16-QAM is about 4 dB. From 16-QAM to 64-QAM, almost 4.5 dB extra E_b/N_o is required. For larger constellation sizes, the E_b/N_o penalty of increasing the number of bits per symbol by 1 converges to 3 dB.

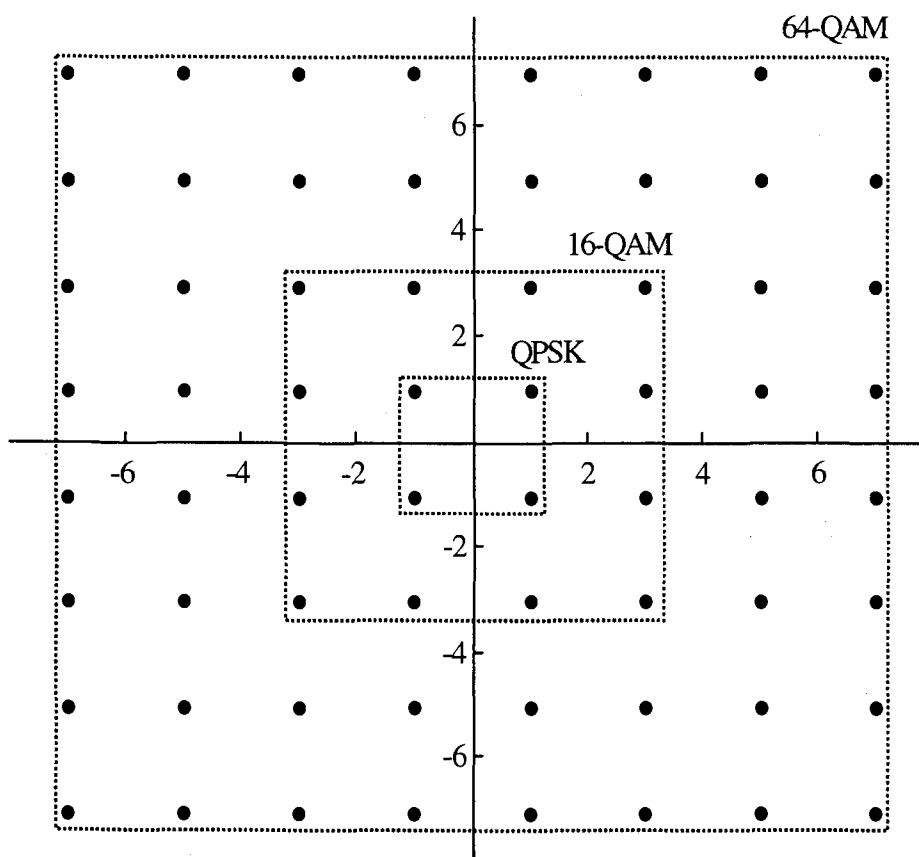


Figure 3.6 QPSK, 16-QAM, and 64-QAM constellations.

Table 3.1
QAM normalization factors and normalized Euclidean distance differences.

Modulation	Normalization factor	Maximum E_b/N_o loss relative to BPSK in dB
BPSK	$1/\sqrt{2}$	0
QPSK	$1/\sqrt{2}$	0
16-QAM	$1/\sqrt{10}$	3.98
64-QAM	$1/\sqrt{42}$	8.45

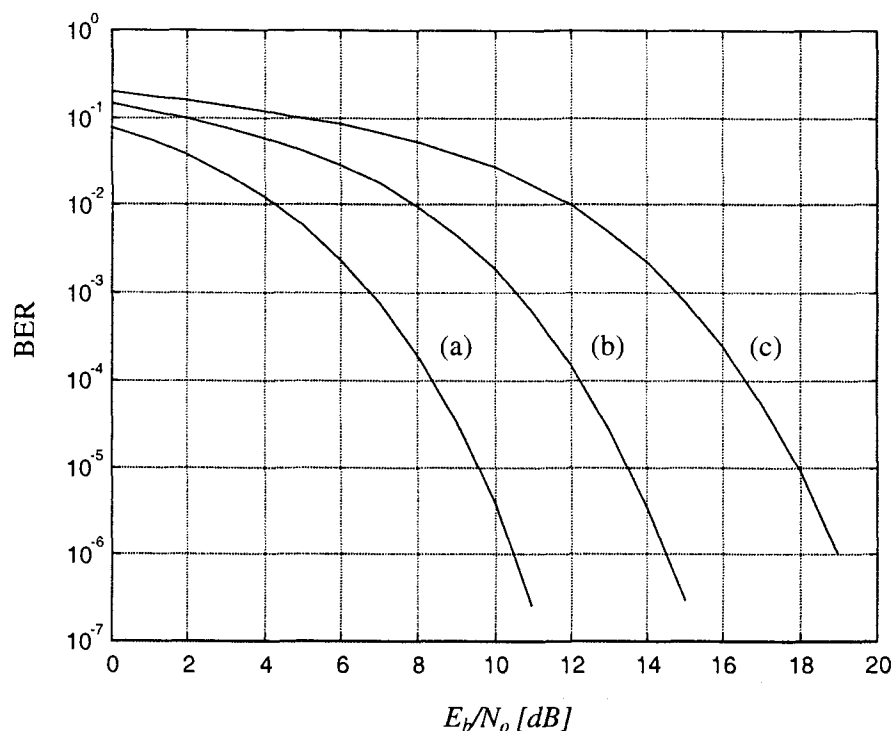


Figure 3.7 BER versus E_b/N_o for (a) BPSK/QPSK, (b) 16-QAM, (c) 64-QAM.

3.5 CODED MODULATION

When coding is applied to a QAM signal, it is important to consider the relation between coding and modulation to obtain the best result. In [9], Trellis coding was introduced as a way to attain coding gain without bandwidth expansion, meaning that all redundancy is obtained by increasing the constellation size. It was demonstrated in [9] that coding gains up to 6 dB can be obtained by going from uncoded QPSK to Trellis-coded 8-PSK using rate 2/3 coding. This technique is based on partitioning the PSK or QAM constellations into subsets with a high Euclidean distance within each subset. For instance, each 2 8-PSK constellation points with a relative phase difference of 180° define a subset with the same Euclidean distance as BPSK. The minimum Euclidean distance between different subsets is much smaller. Hence, coding is applied on the bits defining the subset number, such that the minimum Euclidean distance of the coded signal becomes equal to the distance within each subset.

A disadvantage of the above Trellis coding approach is that although the codes can have a large minimum Euclidean distance, the minimum Hamming distance is only 1, because bits within a subset are left uncoded. Hence, if one Trellis-coded symbol is lost, this immediately results in one or more bit errors. For OFDM this is a very undesirable property, as the data of several subcarriers may be lost by deep fades. This illustrates that the minimum Euclidean distance is not the only relevant parameter when selecting a good code for OFDM. For frequency selective channels, an additional criterion is that the Euclidean distance should be spread over as many symbols as possible, such that a few lost symbols have the smallest possible impact on the

probability of a decoding error [1]. As a consequence, in fading channels it is preferable to use high-order QAM constellations in combination with low-rate coding schemes. It is demonstrated in [1] that a specially designed rate 1/4 code with constraint length 7 together with a 16-QAM constellation can give good performance even on channels where more than half of the subcarriers are lost, with a degradation of less than 2 dB in the required signal-to-noise ratio relative to an ideal AWGN channel.

One of the disadvantages of special Trellis codes is that they are designed for specific constellations, such that you need a different encoder and decoder for different constellations. A practical approach to avoid this problem is to use standard binary codes together with Gray-encoded QAM. In [4], for instance, an efficient way is described to use a standard binary convolutional code together with 16-QAM. This scheme can easily be extended to an arbitrary rectangular QAM constellation. To do this, binary input data are converted into QAM symbols according to a Gray code mapping. For 16-QAM, for instance, the in-phase and quadrature parts are separately formed as 4 level PAM values, determined by two bits b_0 and b_1 , as shown in Figure 3.8. The vertical lines indicate the regions for which the bit values are 1.

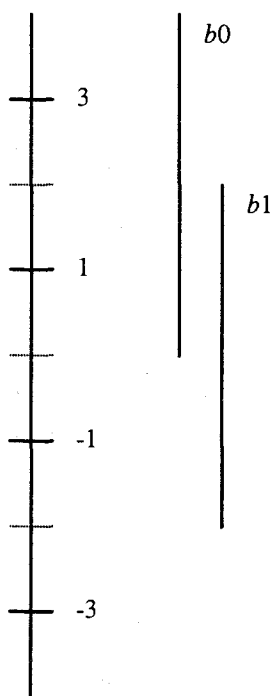


Figure 3.8 Gray mapping of two bits into 4 level PAM.

In the receiver, the incoming QAM symbols have to be demapped into one-dimensional values with corresponding metrics for the Viterbi decoder. For QPSK, the demapping is simply taking the in-phase and quadrature values as the two desired metrics. For the case of 16-QAM, the in-phase and quadrature values are treated as independent 4 level PAM signals, which are demapped into 2 metrics as shown in Figure 3.9. Here, the input values are normalized such that 2 corresponds to a decision

level, above which b_1 is zero. The scale of the output values depends on the required quantization level of the Viterbi decoder, which typically ranges from 3 to 8 bits. Notice that the metric for b_0 can be twice as large as for b_1 in case the in-phase or quadrature value is -3 or $+3$. This indicates the fact that the b_0 values are indeed more reliable in this case, as the minimum Euclidean distance from a $+3$ value to an erroneous b_0 value of -1 is 4, while the minimum distance between two different b_1 values is always 2. This difference in reliability of bits becomes even larger for higher order QAM. For instance, Figure 3.10 shows the demapping of 3-bit metrics for the case of 8 level PAM, which is used to make a 64-QAM constellation.

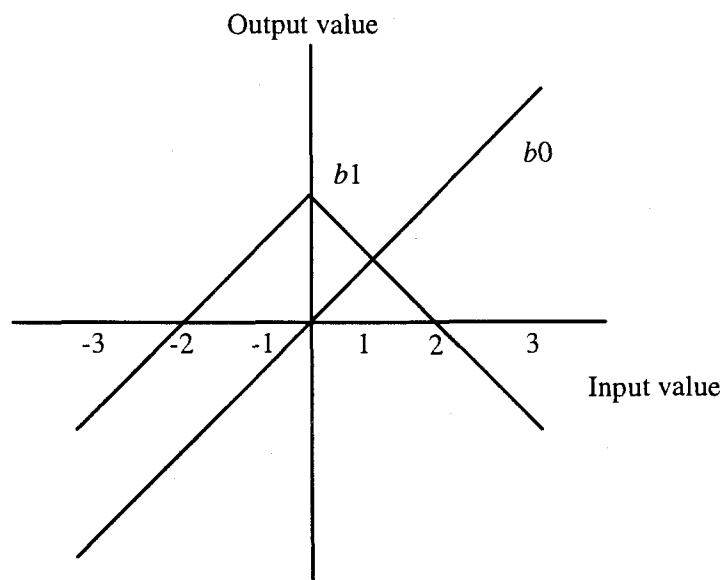


Figure 3.9 Demapping of 4 level PAM into 2 metrics.

Figure 3.11 shows the BERs versus E_b/N_o for several combinations of coding rates and QAM types in an AWGN channel. An interesting effect is that the coding gain relative to the uncoded QAM curves of Figure 3.7 becomes larger for larger QAM constellations. At a BER of 10^{-5} , for instance, the coding gains for a rate 1/2 code are approximately 5.5, 7, and 8.5 dB for QPSK, 16-QAM, and 64-QAM, respectively. This is explained by the fact that the uncoded error probability is determined mainly by the least significant bits in the Gray mapping; for instance, the b_3 values in Figure 3.10. When coding is used, then the error probability depends on an average over several coded bits; for instance, several b_1 , b_2 , and b_3 values in the case of 64-QAM. As a result of this averaging, the minimum squared Euclidean distance between different coded QAM sequences is larger than in the situation where only the least significant bits like b_3 in Figure 3.10 are transmitted. Therefore, the coding gain is larger than in the case of QPSK or BPSK, where all bits have the same weight.

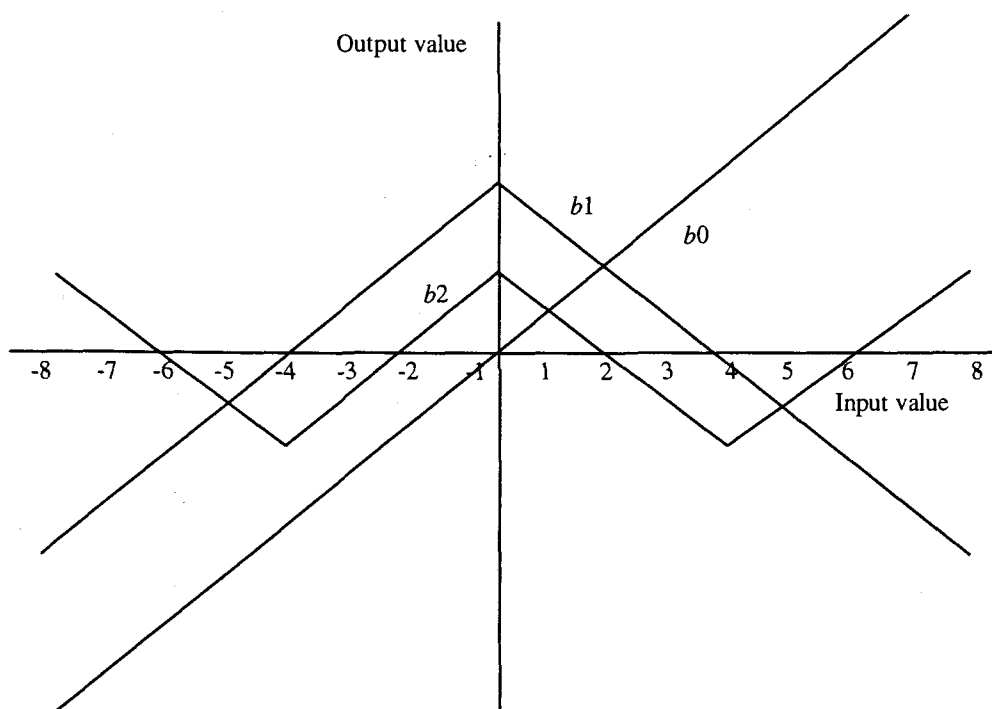


Figure 3.10 Demapping of 8 level PAM into 3 metrics.

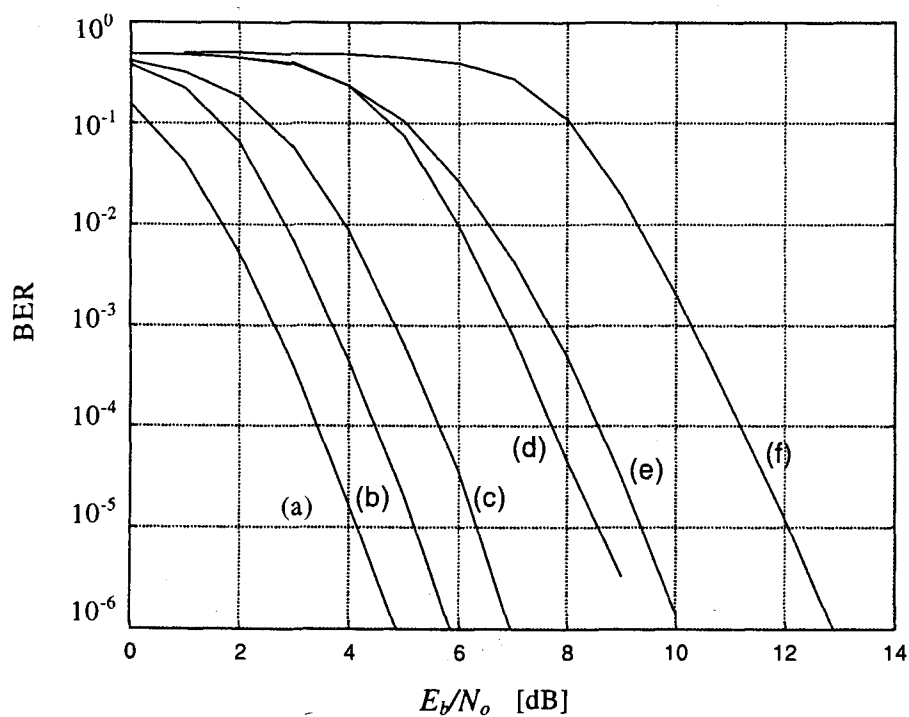


Figure 3.11 BERs versus E_b/N_o in AWGN for a constraint length 7 convolutional code with (a) QPSK, rate $1/2$; (b) QPSK, rate $3/4$; (c) 16-QAM, rate $1/2$; (d) 16-QAM, rate $3/4$; (e) 64-QAM, rate $1/2$; (f) 64-QAM, rate $3/4$.

Other interesting information that can be derived from Figure 3.11 is the coding gain of a particular coded modulation type when compared with the uncoded QAM constellation that gives the same net data rate or the same efficiency in bps/Hz. For instance, the curve for 16-QAM with rate 1/2 coding can be compared with the curve for uncoded QPSK in Figure 3.7, as both have the same efficiency of 2 bps/Hz. It can be seen from the figures that for a BER of 10^{-5} , coded 16-QAM gives a coding gain of about 3 dB, compared with that of uncoded QPSK.

Figure 3.12 shows simulated BERs versus mean E_b/N_o for a Rayleigh fading channel with an exponentially decaying power delay profile. This channel was introduced in Chapter 1. Curves are drawn for various normalized delay spreads $\tau_{rms}N_s/T$, which is the rms delay spread as defined in Chapter 1 multiplied by the bandwidth of the OFDM signal. The normalized delay spread makes it possible to generalize delay spread results, independent of the number of subcarriers or the absolute bandwidth value of an OFDM system. It is required though that the number of subcarriers be significantly larger (a factor of 4 is sufficient) than the constraint length of the convolutional code, such that the code is able to fully benefit from the frequency diversity of the channel. The fact that the performance of an OFDM link depends only on the normalized delay spread $\tau_{rms}N_s/T$ can be understood better by realizing that the rms delay spread is approximately equal to the inverse of the coherence bandwidth of the channel, which determines the characteristics of bandwidth and spacing of fades in the channel frequency response. A small normalized delay spread is equivalent to a small ratio of OFDM signal bandwidth and coherence bandwidth. In such a situation, the channel frequency response is relatively flat within the OFDM signal bandwidth, so if there is a deep fade, all the subcarriers are significantly attenuated. In the case of a large normalized delay spread, a fade only affects a few adjacent subcarriers. There can be several fades within the OFDM signal bandwidth, with relatively strong subcarriers between the fades. As a result, the average signal power is much more constant over several channels than in the case of small delay spreads. The coding benefits from this by using the stronger subcarriers to compensate for the attenuated subcarriers.

Except for the delay spread, the guard time T_G is also normalized in Figure 3.12 and all other figures in this chapter. The normalized guard time is defined here as T_GN_s/T ; the same normalization as for the guard time is applied to maintain a fixed ratio between delay spread and guard time, independent of the number of subcarriers N_s and the FFT interval T . Because the E_b/N_o loss caused by the guard time depends on the ratio T_G/T , rather than the normalization chosen here, the guard time loss is not included in the following figures. This makes it possible to see from Figure 3.12 for what ratio of guard time and delay spread the system breaks down because of ISI and ICI. In Figure 3.12, for instance, an error floor is starting to appear for a normalized delay spread of 4; the ratio of guard time and delay spread is 3 for this case. Hence, for QPSK with rate 3/4 coding, the guard time should be at least three times the delay spread to achieve an average BER less than 10^{-4} .

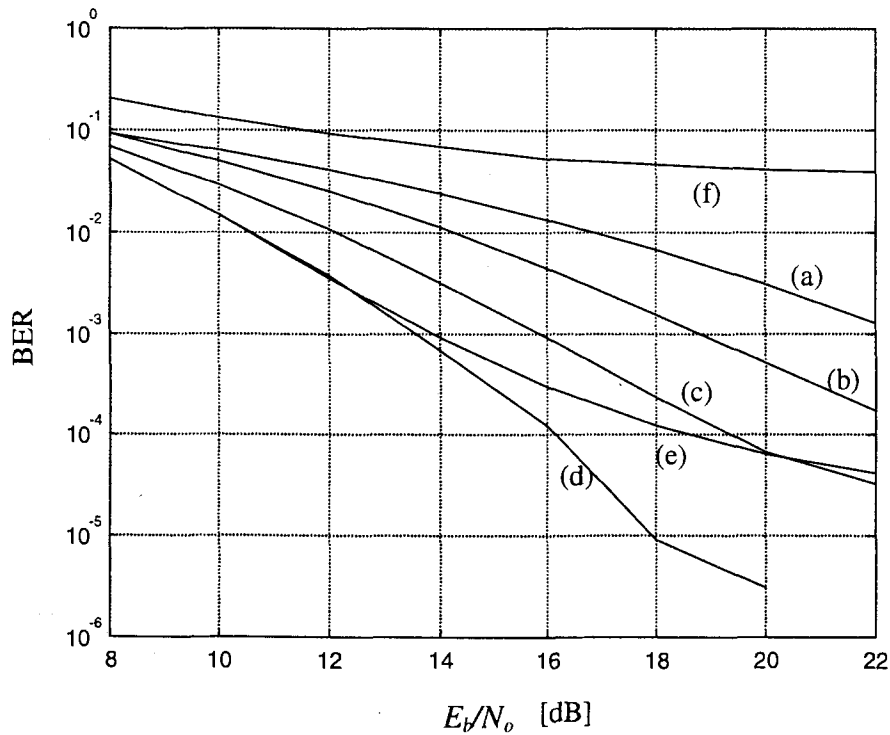


Figure 3.12 BERs versus mean E_b/N_o in a Rayleigh fading channel for QPSK, rate 3/4 convolutional coding, normalized guard time $T_G N_f/T = 12$, normalized delay spread $\tau_{rms} N_f/T =$ (a) 0.25, (b) 0.5, (c) 1, (d) 2, (e) 4, (f) 8.

Notice that Figure 3.12 uses the mean E_b/N_o , which is the average value over a large number of independent channels. The instantaneous E_b/N_o of an individual channel can be significantly smaller or larger than this mean value, especially for low delay spreads where the instantaneous signal power is determined by a single Rayleigh fading path. For larger delay spreads, the variation in the instantaneous signal power becomes much smaller because of the increased frequency diversity of the channel. Low instantaneous E_b/N_o values, which dominate the error ratio, occur much less frequently than at low delay spreads, hence the improved performance. The larger the delay spread, the smaller the E_b/N_o can be, until the delay spread becomes so large that ISI and ICI become limiting factors.

Figure 3.13 shows packet-error ratios (PERs) for 256-byte packets, simulated for the same conditions as Figure 3.12. For relatively slowly time-varying channels, as encountered for instance in indoor wireless LAN applications, the packet-error ratio averaged over a large number of fading channels is equivalent to the coverage outage probability, which is the probability of an unacceptably large packet-error ratio at a certain location within the coverage range. For instance, at an E_b/N_o value of 18 dB and a normalized delay spread between 0.5 and 4, a packet error ratio of 1% means that 1% of the channels generate most of the packet errors—caused by deep fades or ISI/ICI—while the remaining 99% of the channels have a much lower error ratio.

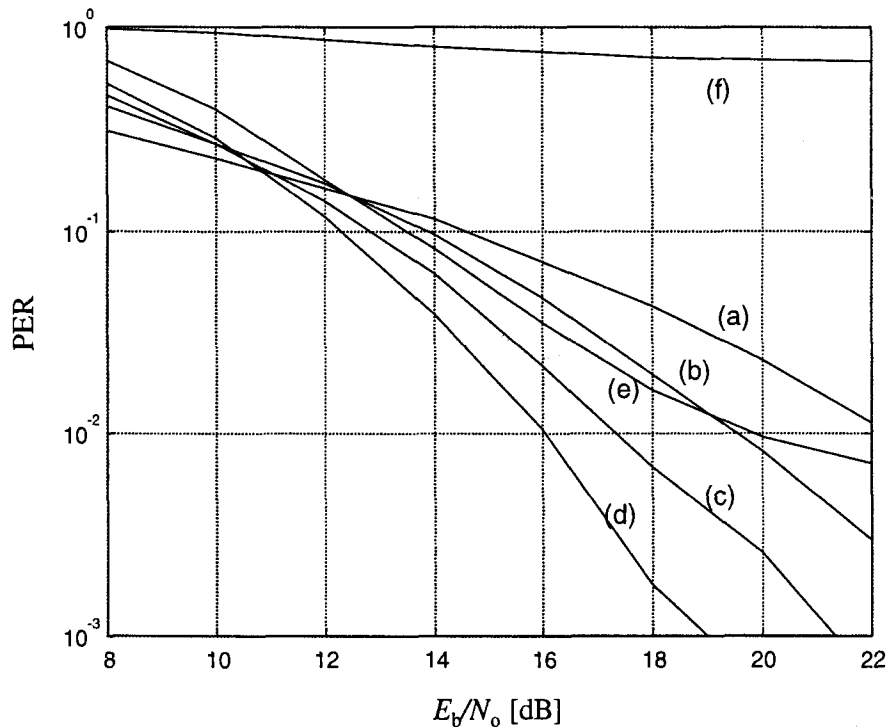


Figure 3.13 PERs versus mean E_b/N_o in a Rayleigh fading channel for QPSK, rate 3/4 convolutional coding, packet length = 256 bytes, normalized guard time $T_G N/T = 12$, normalized delay spread $\tau_{rms} N_s/T =$ (a) 0.25, (b) 0.5, (c) 1, (d) 2, (e) 4, (f) 8.

Figure 3.14 shows simulated BERs and PERs for 256-byte packets in a Rayleigh fading channel with an exponentially decaying power delay profile. Two different combinations of coding rate and QAM type are used. Curves (a) and (c) are based on 16-QAM with rate 1/2 coding, giving a spectral efficiency of 2 bps/Hz, while curves (b) and (d) use QPSK with rate 3/4 coding, giving an efficiency of 1.5 bps/Hz. This example leads to the surprising result that in a fading channel, a higher order QAM system with a better spectral efficiency can be actually better in terms of E_b/N_o performance than a system with a lower spectral efficiency based on a lower order QAM, while the opposite is true in AWGN as demonstrated by Figure 3.11. The explanation for this effect is that in a frequency selective channel where a certain percentage of the subcarriers can be completely lost in deep fades, the ability to correct for those lost subcarriers by having a large Hamming distance is more important than a large minimum Euclidean distance for each individual subcarrier. In the example of Figure 3.11, the rate 1/2 code combined with 16-QAM can tolerate more weak subcarriers than the rate 3/4 code with QPSK, resulting in an E_b/N_o gain that is larger than the loss in Euclidean distance of 16-QAM versus QPSK.

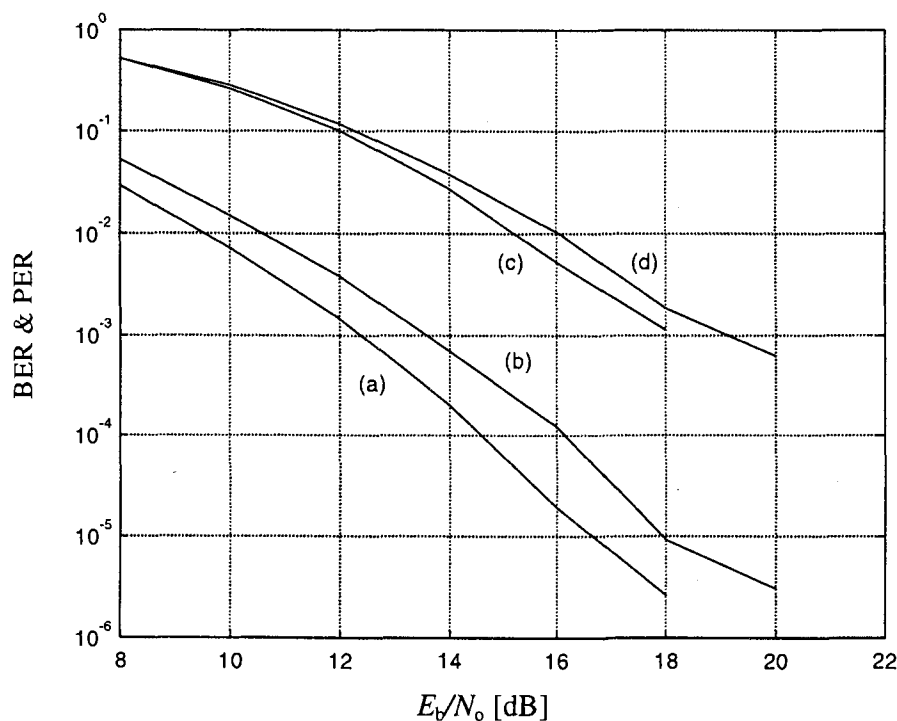


Figure 3.14 PER and BER versus mean E_b/N_0 in a Rayleigh fading channel for a packet length of 256 bytes and a normalized delay spread $\tau_{rms}N_s/T = 2$. (a) BER of 16-QAM, rate 1/2 coding; (b) BER of QPSK, rate 3/4 coding; (c) PER of 16-QAM, rate 1/2 coding; (d) PER of QPSK, rate 3/4 coding.

As mentioned before, when the delay spread increases, the performance of an OFDM link increases until a limit is reached where ISI and ICI cause an unacceptably high error floor. This error floor depends on the type of modulation and coding rate. Figure 3.15 illustrates this with simulation curves of the packet error floor versus the normalized delay spread τ_{rms}/T_G . No noise was present in the simulations, so all errors are purely caused by ISI and ICI. As expected, more delay spread can be tolerated for smaller QAM constellations. There is little difference, however, in the robustness of, for instance QPSK with rate 3/4 coding and 16-QAM with rate 1/2 coding, thanks to the fact that the latter is able to tolerate more erroneous subcarriers, which partly compensates the smaller distance between constellation points.

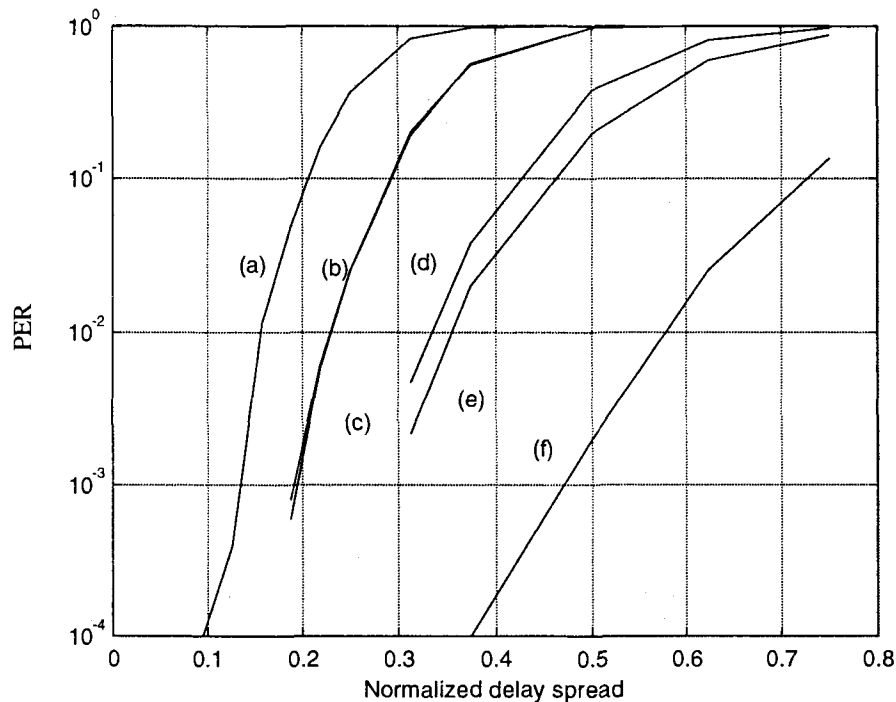


Figure 3.15 Irreducible packet error ratios versus normalized delay spread τ_{rms}/T_G for 256 byte packets and (a) 64-QAM, rate $\frac{3}{4}$; (b) 64-QAM, rate $\frac{1}{2}$; (c) 16-QAM, rate $\frac{3}{4}$; (d) 16-QAM, rate $\frac{1}{2}$; (e) QPSK, rate $\frac{3}{4}$; (f) QPSK, rate $\frac{1}{2}$.

When an OFDM system has to be designed, Figure 3.15 can be used to derive a minimum requirement on the guard time, based on the maximum delay spread for which the system should work. For instance, for a tolerable packet-error floor of 1%, the guard time has to be about twice the delay spread for QPSK with rate 1/2 coding, but it has to be six times the delay spread for 64-QAM with rate 3/4 coding.

REFERENCES

- [1] Wesel, R. D., "Joint Interleaver and Trellis Code Design," *Proceedings of IEEE Globecom*, 1997.
- [2] Le Floch, B., M. Alard, and C. Berrou, "Coded Orthogonal Frequency Division Multiplex," *Proceedings of the IEEE*, Vol. 83, no. 6, June 1995.
- [3] Alard, M., and R. Lasalle, "Principles of Modulation and Channel Coding for Digital Broadcasting for Mobile Receivers," *EBU Technical Review*, No. 224, pp. 168 - 190.
- [4] Wang, Q., and L. Y. Onotera, "Coded QAM Using a Binary Convolutional Code," *IEEE Transactions on Communications*, Vol. 43, No. 6, June 1995.
- [5] Wesel, R. D., and J. M. Cioffi, "Fundamentals of Coding for Broadcast OFDM," *Proceedings of IEEE ASILOMAR-29*, 1996.
- [6] Massey, J. L., "Shift-Register Synthesis and BCH Decoding," *IEEE Transactions on Information Theory*, IT-15, pp. 122 - 127, Jan. 1979.

- [7] Berlekamp, E. R., "The Technology of Error Correcting Codes," *Proceedings of the IEEE*, Vol.68, No.5, pp.564 – 593, May 1980.
- [8] Charles Lee, L. H., "*Convolutional Coding: Fundamentals and Applications*," London: Artech House, 1997.
- [9] Ungerboeck, G., "Channel Coding with Multilevel/Phase Signals," *IEEE Transactions on Information Theory*, Vol. IT-28, No.1, pp.55-67, Jan. 1982.



CHAPTER 9

Orthogonal Frequency Division Multiple Access

9.1 INTRODUCTION

The previous chapter described some ways in which OFDM could be used both as a modulation scheme and as part of the multiple access technique, by applying a spreading code in the frequency domain. In this chapter, a variation on this theme is described, namely orthogonal frequency division multiple access (OFDMA). In OFDMA, multiple access is realized by providing each user with a fraction of the available number of subcarriers. In this way, it is equal to ordinary frequency division multiple access (FDMA); however, OFDMA avoids the relatively large guard bands that are necessary in FDMA to separate different users. An example of an OFDMA time-frequency grid is shown in Figure 9.1, where seven users *a* to *g* each use a certain fraction—which may be different for each user—of the available subcarriers. This particular example in fact is a mixture of OFDMA and Time Division Multiple Access (TDMA), because each user only transmits in one out of every four timeslots, which may contain one or several OFDM symbols.

9.2 FREQUENCY-HOPPING OFDMA

In the previous example of OFDMA, every user had a fixed set of subcarriers. It is a relatively easy change to allow hopping of the subcarriers per timeslot, as depicted in Figure 9.2. Allowing hopping with different hopping patterns for each user actually transforms the OFDMA system in a frequency-hopping CDMA system. This has the benefit of an increased frequency diversity, because each user uses all of the available bandwidth, as well as the interference averaging benefit that is common for all CDMA variants. By using forward-error correction coding over multiple hops, the system can correct for subcarriers in deep fades or subcarriers that are interfered by other users. Because the interference and fading characteristics change for every hop, the system

performance depends on the average received signal power and interference, rather than on the worst case fading and interference power.

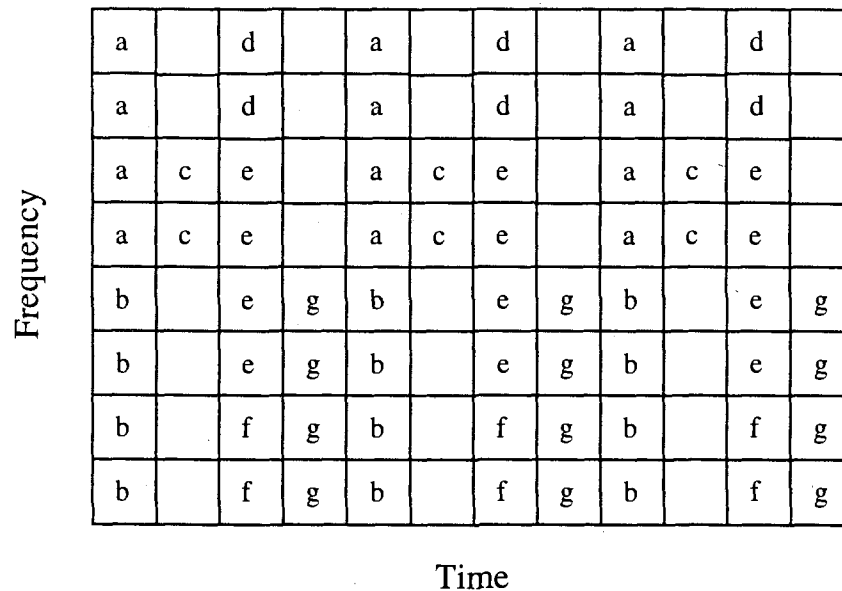


Figure 9.1 Example of the time-frequency grid with seven OFDMA users, a to g, which all have a fixed set of subcarriers every four timeslots.

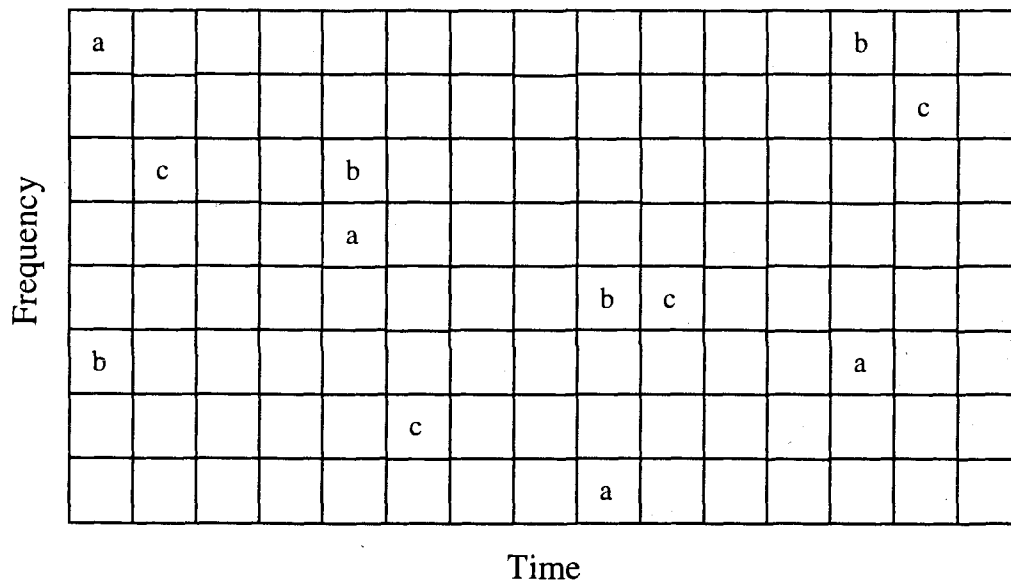


Figure 9.2 Example of the time-frequency grid with three hopping users, a, b and c, which all have one hop every four time slots.

A major advantage of frequency-hopping CDMA systems over direct-sequence or multicarrier CDMA systems is that it is relatively easy to eliminate intracell interference by using orthogonal hopping patterns within a cell. An example of such an orthogonal hopping set is depicted in Figure 9.3. For N subcarriers, it is always possible to construct N orthogonal-hopping patterns. Some useful construction rules for generating hopping patterns can be found in [1].

Frequency	a	f	e	d	c	b
	b	a	f	e	d	c
	c	b	a	f	e	d
	d	c	b	a	f	e
	e	d	c	b	a	f
	f	e	d	c	b	a
Time						

Figure 9.3 Example of six orthogonal hopping patterns with six different hopping frequencies.

9.3 DIFFERENCES BETWEEN OFDMA AND MC-CDMA

The main differences between OFDMA and the MC-CDMA techniques discussed in Chapter 8 is that users within the same cell use a distinct set of subcarriers, while in MC-CDMA, all users use all subcarriers simultaneously. To distinguish different users, orthogonal or near-orthogonal spreading codes are used in MC-CDMA. Because of code distortion by multipath fading channels, however, MC-CDMA loses its orthogonality in the uplink even for a single cell. This makes rather complicated equalization techniques necessary, which introduce a loss in SNR performance and diminish the complexity advantage of OFDM over single-carrier techniques. OFDMA does not have this disadvantage, because in a single cell, all users have different subcarriers, thereby eliminating the possibility of intersymbol or intercarrier interference. Hence, OFDMA does not suffer from intracell interference, provided that the effects of frequency and timing offsets between users are kept at a sufficiently low level. This is a major advantage of OFDMA compared with MC-CDMA and DS-CDMA, because in those systems, intracell interference is the main source of interference. A typical ratio of intracell and intercell interference is 0.55 [2]. Because the system capacity is inversely proportional to the total amount of interference power, a capacity gain of 2.8 can be achieved by eliminating all intracell interference, so that is the maximum capacity gain of OFDMA over DS-CDMA and MC-CDMA networks.

The main advantages of using CDMA in general or MC-CDMA in particular is interference averaging. In CDMA, the interference consists of a much larger number of interfering signals than the interference in a non-CDMA system. Each interfering signal is subject to independent fading, caused by shadowing and multipath effects. For both the CDMA and the non-CDMA system, an outage occurs when the total interference power (after despreading for the CDMA system) exceeds some maximum value. In a non-CDMA system, the interference usually consists of a single or a few cochannel interferers. Because of fading, the interference power is fluctuating over a large range,

so a large fading margin has to be taken into account, which reduces system capacity. In a CDMA system, the interference is a sum of a large number of interfering signals. Because all these signals fade independently, the fluctuation in the total interference power is much less than the power fluctuation of a single interfering signal. Hence, in a CDMA system the fading margin can be significantly smaller than the margin for a non-CDMA system. This improvement in margin largely determines the capacity gain of a CDMA system.

In OFDMA, interference averaging is obtained by having different hopping patterns within each cell. The hopping sequences are constructed in such a way that two users in different cells interfere with each other only during a small fraction of all hops. In a heavily loaded system, many hops will interfere, but the interference will be different for each hop. Hence, by forward-error correction across several hops, the OFDMA performance will be limited by the average amount of interference rather than the worst case interference. An additional advantage of OFDMA over DS-CDMA and MC-CDMA is that there are some relatively simple ways to reduce the amount of intercell interference. For instance, the receiver can estimate the signal quality of each hop and use this information to give heavily interfered hops a lower weight in the decoding process.

Another important feature of CDMA is the possibility to perform soft handover by transmitting two signals from different base stations simultaneously on the same channel to one mobile terminal. Combining the signals from different base stations gives a diversity gain that significantly reduces the fading margin, because the probability that two base stations are in a fade is much smaller than the probability that one base station is in a fade. Less fading means that less power has to be transmitted, and hence less interference is generated, which gives an improvement in the capacity of the system. A nice feature of CDMA soft handover is that it has no impact on the complexity of the mobile terminal; as far as the mobile terminal is concerned, the overlapping signals of different base stations have the same effect as overlapping signals caused by multipath propagation.

For OFDMA systems, two basic soft handover methods exist, applicable to both the uplink and the downlink. (base station-to-mobile, mobile-to-base station). A requirement for both methods is that the transmissions from and to the base stations are synchronized such that the delay differences at the two base stations are well within the guard time of the OFDM symbols.

The first technique is to use the same set of subcarriers and the same hopping sequence in two cells to connect to two base stations. Hence, in the downlink the mobile receives a sum of two signals with identical data content. The mobile is not able to distinguish between the two base stations; the effect of soft handover is similar to that of adding extra multipath components, increasing the diversity gain. This type of soft handover is similar to soft handover in DS-CDMA networks.

The second way for soft handoff is to use different sets of subcarriers in two cells. In contrast to the first method, in the downlink the mobile has to distinguish now

between the two base stations. It has to demodulate the signals from the two base stations separately, after which they can be combined, preferably by using maximal ratio combining. This type of soft handover is similar to the one that could be used in a non-CDMA network.

Advantages of the second method over the first—in the downlink—are an increased SNR gain because of receiver diversity, and more freedom for the base stations to allocate available subcarriers. In the first method, base stations are forced to use the same subcarriers. A main advantage of the first method is its simpler implementation; no additional hardware is needed, only some extra protocol features to connect to two base stations simultaneously. The second method does require extra hardware, because it has to demodulate an extra set of subcarriers. Further, it has to perform extra processing for the maximal ratio combining of the signals from the different base stations.

9.4 OFDMA SYSTEM DESCRIPTION

As an example of an OFDMA system, this section gives a description of a system that was proposed for the European UMTS [3, 4]. Table 9.1 summarizes the parameters and key technical characteristics of this OFDMA air interface.

Table 9.1
Parameters of the Proposed OFDMA system

No.	Parameter	Value
1	Subcarrier spacing	4.1666 kHz
2	Symbol time	288.46 μ s
3	Number of subcarriers per bandslot of 100 kHz	24
4	Pre-guard time	38 μ s
5	Post-guard time	8 μ s
6	Modulation unit	1 bandslot and 1 time slot (= 1 symbol)
7	Modulation block	4 time slots and 1 bandslot

Figure 9.4 illustrates the time-frequency grid of the OFDMA system. The resources (time and frequency) are allocated based on the type of services and operational environment. The number of timeslots and bandslots per user is variable to realize variable data rates. The smallest data rate is obtained for one bandslot of 24 subcarriers per timeslot of 288.46 μ s.

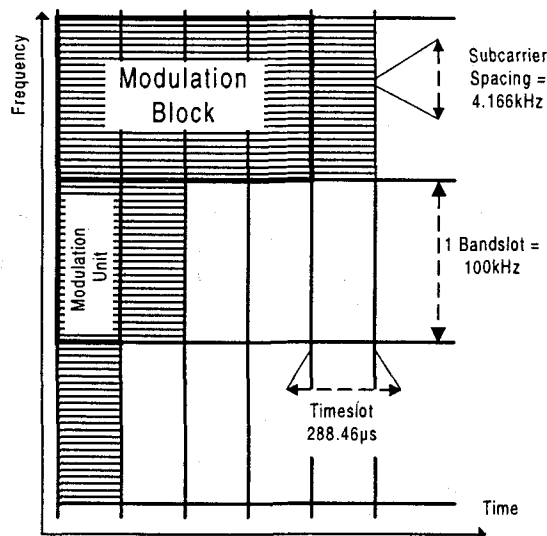


Figure 9.4 Time-frequency grid.

The following summary shows some advantages of the proposed OFDMA system:

- Use of frequency-hopping OFDMA for interference averaging and frequency diversity;
- Time-division duplex MAC with dynamic channel allocation used for unpaired spectrum allocations, asymmetrical services, and unlicensed usage;
- Straightforward and efficient high bit rate support by allocating more subcarriers and/or timeslots;
- Small guard band requirements at approximately 100 kHz;
- No frequency planning option available; effective re-use factor of 1;
- GSM backwards compatibility; and
- Minimum bandwidth requirements for system deployment only 1.6 MHz (or less) and deployment possible in steps of 100kHz.

Figure 9.5 shows the TDMA frame structure. Each frame is of length 4.615 ms, which is divided into 4 subframes of length 1.1534 ms. A sub-frame contains 4 time-slots of duration 288.46 μ s. The timeslot contains a guard period, power control information and data. Every OFDM symbol is mapped onto one time-slot. The structure of an OFDMA symbol is depicted in Figure 9.6.

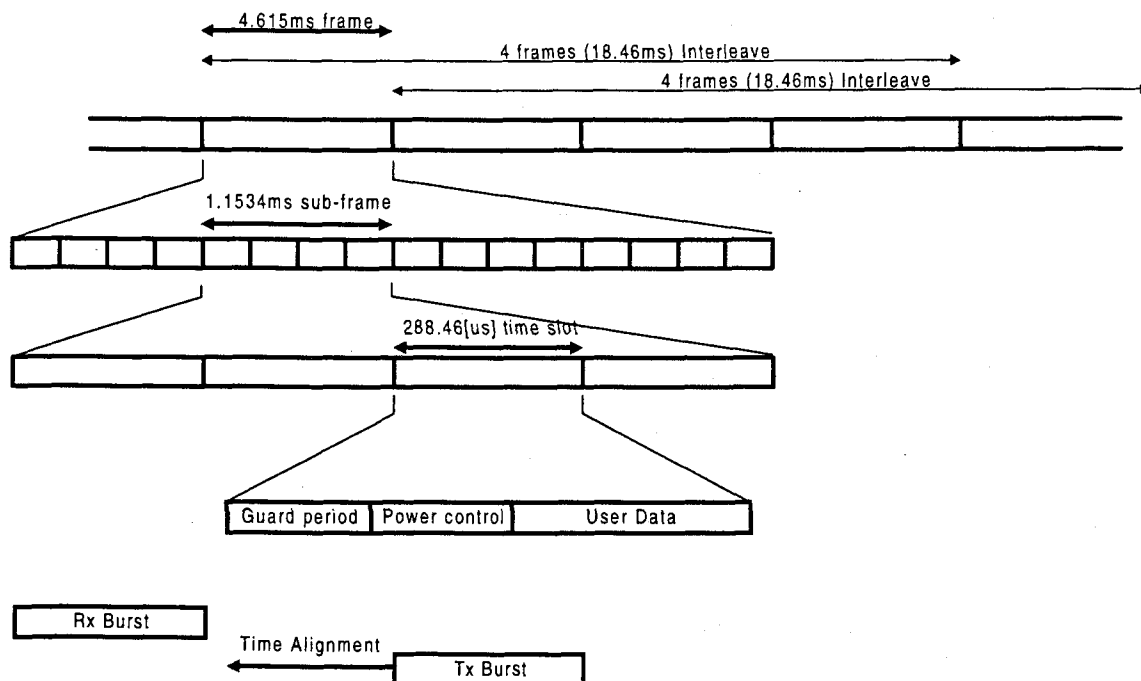


Figure 9.5 Frame (TDMA) Structure.

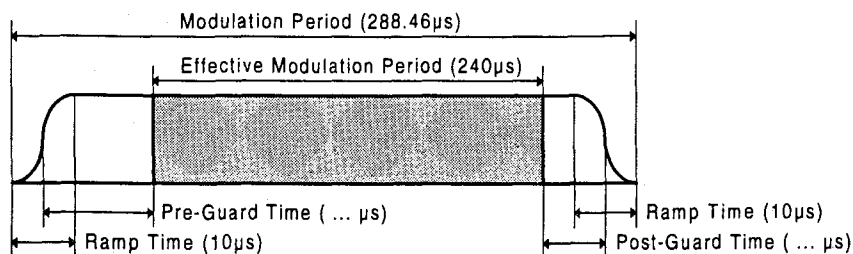


Figure 9.6 OFDM modulation burst.

The whole system frequency band is divided into small blocks (bandslots) with a fixed number of subcarriers. To maintain compatibility with GSM, a 100-kHz bandslot is chosen that consists of 24 subcarriers. Therefore, the subcarrier spacing is $100/24 = 4.167$ kHz. Figure 9.7 shows the OFDMA frequency structure.

In each bandslot, the two subcarriers at the edge of the bandslot are left unmodulated to relax receiver blocking requirements. In addition, the interference of two adjacent blocks of subcarriers is reduced, which may occur when their orthogonality is compromised because of nonlinear PA effects. Adjacent bandslots can be concatenated to allow transmission of wideband services.

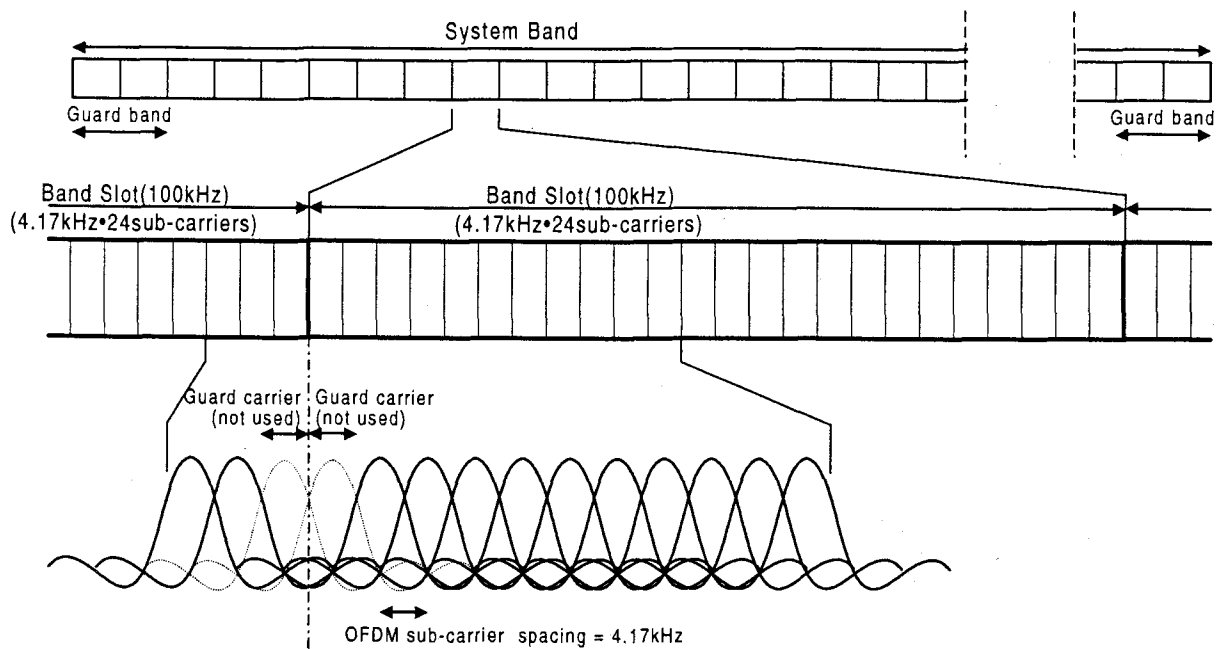


Figure 9.7 OFDMA frequency structure.

9.4.1 Channel Coding

Convolutional encoding and soft-decision Viterbi decoding is used for the basic data transmission. The objective of this coding is to achieve good quality in the tough mobile radio channel. A constraint length of seven is used together with variable coderates in the range of $1/4$ to $3/4$. To achieve very low bit-error rates (e.g. 10^{-6}) for video encoding or data transmission, a concatenated coding scheme is used with an inner convolutional code and an outer Reed-Solomon code.

9.4.2 Modulation

The modulation schemes of the OFDMA proposal are QPSK and 8-PSK with differential encoding in the frequency domain. An optional coherent mode with 16-QAM is available, which uses pilot subcarriers to obtain a channel estimate at the receiver. For differential encoding, each bandslot contains one known reference subcarrier value, as depicted in Figure 9.8.

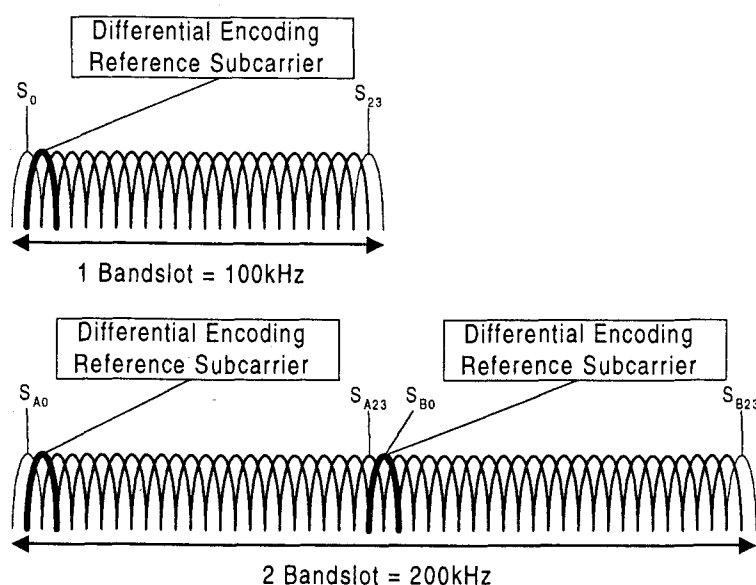


Figure 9.8 Reference subcarrier allocation.

9.4.3 Time and Frequency Synchronization

Synchronization is an essential issue for the OFDMA system. The following aspects are considered for uplink and downlink: initial modulation timing synchronization, modulation timing tracking, initial frequency offset synchronization, and frequency tracking.

9.4.4 Initial Modulation Timing Synchronization

Initial timing synchronization is required to adjust the mobile station's internal timing to the base station's timeframe. After switching on, the mobile station monitors the initial acquisition channel (IACH) and the broadcast channel (BCCH).

After the mobile has detected the base station's timing, it sends a random access channel (RACH) packet to the base station. The base station measures the time offset for the received RACH packet and sends back the necessary timing advance to the mobile (similar to GSM). In the frame structure of the OFDMA system, reserved slots for reception of RACH packets exist.

Because of the time and frequency structure of the OFDMA system, the timing tracking is less critical compared with other OFDM systems where users are interleaved in the frequency domain. The base station can measure the position of the received OFDM burst within the allocated slot for each mobile station individually and send the according timing alignment information back to the mobile station. In addition, timing information can be refined and tracked after the transformation in the subcarrier domain, where a time shift is observed as a phase rotation.

In the mobile station, the timing information is obtained and adjusted by the above-mentioned correlation algorithm. Accurate timing information is required to determine the position of the useful data samples within each burst so the FFT window can be placed correctly. The guard samples relax the requirement for accurate timing because the position of the FFT window can be shifted within the guard time without performance degradation. Additional timing offset correction can be performed to cope with the FFT window misplacements.

9.4.5 Initial Frequency Offset Synchronization

After initial timing synchronization of the mobile station, the frequency offset can be measured by phase comparison of the (ideally) equal time samples within each burst. Equal samples are placed in the guard interval of the OFDM burst. A phase rotation indicates a frequency offset. Using this technique, a frequency error up to half the subcarrier spacing can be detected. The initial offset, however, can be larger, so it has to be detected using the specially designed symbols in the IACH channel.

9.4.6 Synchronization Accuracy

The proposed synchronization, acquisition, and tracking algorithm is independent of the modulation scheme (coherent or noncoherent). For coherent 16-QAM reception, further processing in the frequency (subcarrier domain) is possible to improve the performance. Frequency domain time tracking (or combined time-domain/frequency-domain tracking algorithms) can be based on observing phase shifts of the known pilots within the time-frequency grid on the subcarrier domain.

In the downlink, only an IACH is multiplexed to allow fast and precise initial timing and frequency synchronization. In the actual communication mode, timing and frequency tracking can be performed using a correlation-based synchronization algorithm. In the uplink, the rough timing offset is detected by the base station by measuring the arrival time of the RACH burst. This gives an initial time-advance value that is reported back to the mobile. During communication, the arrival time of the burst is detected by the base station using the proposed tracking algorithm (same as in the downlink) or a tracking algorithm in the frequency (subcarrier) domain, based on the detected constellation rotation.

Both algorithms can also be combined. The alignment values are calculated regularly and reported to the mobile station. Accuracy requirements are relaxed because the design of the burst allows some overlapping arrival (another advancing feature of the raised cosine pulse-shaping besides the reduction of out-of-band emission). In addition, the guard time helps to compensate timing misalignments. The OFDMA burst design provides a guard interval at the front and an additional guard interval at the back

of the OFDM symbol—see Figure 9.9—which provides robustness against a timing inaccuracy of $\pm 10 \mu\text{s}$.

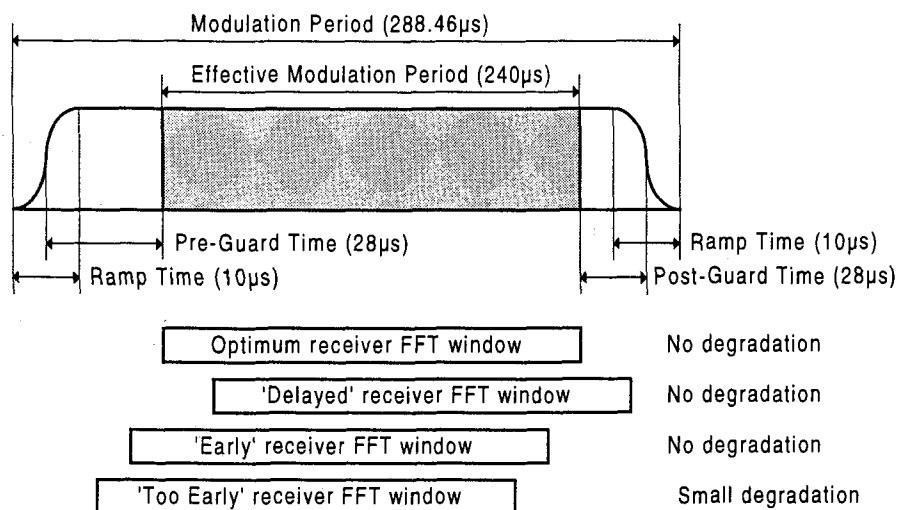


Figure 9.9 OFMDA burst and synchronization requirements.

9.4.7 Power Control

Power control in the uplink removes the unevenness of received signal strength at the base station side and decreases the total power to the minimum level required to support the specified quality of service (e.g. BER). The accuracy is less critical than CDMA because with OFDMA, orthogonality is always provided within one cell. A precise power control, however, not only improves the transmission performance but also minimizes the interference to other cells and therefore increases overall capacity.

The OFDMA concept uses both closed-loop and open-loop power control. Based on quality parameters, measured on a slot-by-slot basis, the power is adjusted in the mobile as well as in the base station transmitter. Each receiver measures the quality of the received burst (C/I ratio) and transmits in the next burst a request to the opposite transmitter to increase, keep, or decrease the power level in steps of 1 dB. For the fastest power control mode, one subcarrier is dedicated to carry power control information, and the power is then adjusted on a frame-by-frame basis (each 1.152 ms). Figure 9.10 depicts the power control operation.

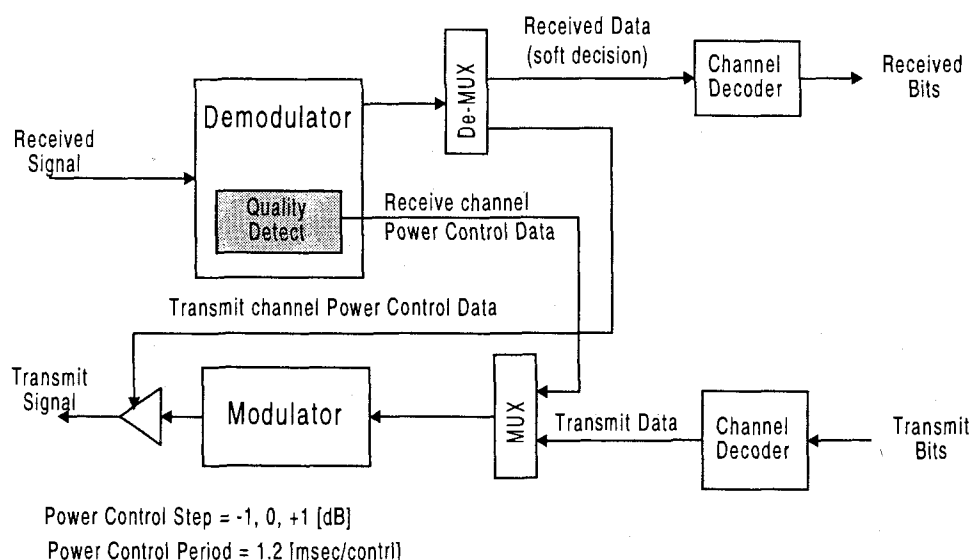


Figure 9.10 Operation of power control in a mobile station.

9.4.8 Random Frequency-Hopping Operation

Frequency hopping is very effective to achieve frequency diversity and interference diversity. Frequency diversity is useful to average the frequency-selective channel properties (fading dips). Interference diversity is one of the important techniques used in the OFDMA proposal and has been shown to improve capacity in slow frequency-hopping TDMA systems [8].

The random hopping pattern is designed to be orthogonal within one cell (no collisions in the time-frequency grid) and random between cells (this causes cochannel interference).

The frequency hopping pattern has to fulfill certain requirements:

- Orthogonality within one cell,
- Support of a variety of services by assigning different bandwidth (number of bandslots),
- Support of a variety of services by assigning timeslots (number of timeslots), and
- Support of a couple of timeslot structures (4-TDMA, 8-TDMA, 16-TDMA) within the pattern.

The hopping pattern is generated at the base station according to the expected service and traffic requirement and assigned to the cell. This assignment can be modified because of changes in the traffic characteristics. The base station can then support a set of services and a certain number of users for each service.

9.4.9 Dynamic Channel Allocation (Fast DCA)

Besides FH hopping mode, the system can also be operated in time division duplex (TDD) mode. Unlike the FH mode, the TDD mode does not separate the spectrum in an uplink and a downlink. Instead, it assigns bandslots individually to uplink or downlink connections. In TDD mode, a dynamic channel allocation algorithm is employed to avoid (rather than to average) excessive interference. The TDD mode is intended for pico-cellular, indoor use. The indoor environment is characterized by

- Short radio propagation delays (100m is traversed in 0.3 μ s, or 0.1% of the symbol duration),
- Greater demand for high rate services, reducing the interference averaging advantage of frequency-hopping mode,
- High-speed data traffic is often asymmetric, prompting flexible division of bandwidth between uplink and downlink, and
- Less severe propagation conditions than those outdoor; mobility-induced Doppler spread and delay spread are both lower.

In the TDD mode, the transmissions of mobile users are scheduled by the base station, which regularly transmits a frame map containing:

- Bandslot allocations for the next frame. Bandslots can be allocated to
 - The base station for downlink transmission to a single terminal,
 - The base station for downlink transmission to all terminals (broadcast),
 - A single terminal for an uplink transmission, and
 - All (or a group of) terminals for contention based access,
- Transmit power assignments for MTs,
- Acknowledgements for contention traffic received in the previous frame,
- Slots are allocated on a connection basis, so that connection-dependent QoS can be provisioned (a mobile can have one or more connections), and
- Control data and user data are transmitted on different connections.

Terminals can transmit requests for bandslots in contention slots designated by the base station in the FM. They can also piggyback requests onto uplink transmissions, which provides contention free access, particularly under heavy traffic conditions. The base station performs interference measurements in all bandslots, except at the timeslots in which it is transmitting. This information is used by the bandslot allocation algorithm to assign uplink transmissions to slots with minimal interference. Note that an uplink transmission in an interference free slot (as measured by the base station) may interfere with a simultaneous uplink transmission at a neighboring base station. No simultaneous uplink and downlink transmissions may be scheduled within a cell. Therefore, the inability of the base station to measure interference in slots in which it is transmitting, does not reduce capacity.

The frame layout is entirely decided by the DCA algorithm. Like the FH algorithm, the DCA algorithm is distributed and does not rely on communication by

way of the infrastructure. Also, as the FH algorithm, it is not part of the system specification, the algorithm may be vendor specific, allowing competitive positioning within a standardized system.

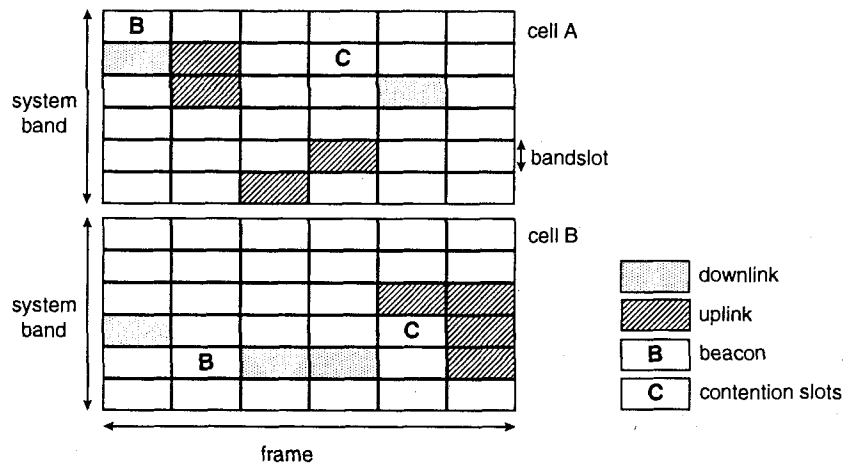


Figure 9.11 Example of frame layout.

An example of a frame layout is shown in Figure 9.11. The figure is purely illustrative. The frame duration and system bandwidth have unrealistically small values. Also, the packets, such as the frame map—that is transmitted in the beacon—and user data packets, occupy more than one bandslot in practice.

In general, the applied DCA algorithm must strive to reduce intracell and intercell interference. Constant bit-rate traffic causes long-term interference that is highly predictive of the interference in the next slot. If traffic is bursty, the predictive value of interference measurements is limited. Because a base station is not aware whether bandslots in neighboring cells are allocated to circuit mode or packet mode connections, base stations and mobiles average measurements over longer periods of time. As a rule, busy slots (high average interference level) are avoided for any transmission. Quiet slots (low average interference) are assigned to constant bit-rate connections, or to the guaranteed part of a variable bit-rate connection. Slots with medium average interference are assigned to connections with bursty traffic, which use contention mode access.

Initial association does not differ from the procedure in FH mode. When joining the base station, a mobile station first detects the location of the initial acquisition channel and the broadcast channel. The broadcast channel is used to convey the location of the frame map in the current frame to the mobile station. Once the frame map is located, it can be tracked because it advertises when it is moved to a different location.

9.4.10 Simple Dynamic Channel Allocation

Simple DCA assigns a fixed resource (bandslots and timeslots) to a communication during setup. This assignment is kept for the whole duration of the communication. This scheme is very simple but cannot react on varying interference or channel conditions compared with fast DCA where the “actual best” channel (= timeslot and bandslot combination) is used for transmission. This scheme has a lower performance than the fast DCA operation but can be used for simple (uncoordinated) applications like cordless telephony.

9.4.11 OFDMA Capacity

System-level simulations were conducted for various types of services and environments. The simulations were conducted in accordance with [7]. Table 9.2 lists the simulated capacities.

Table 9.2
Capacities for various services and environments.

	Environment	Cell capacity (#Users/MHz/Cell) (uplink/downlink)	Spectrum efficiency (kbps/MHz/Cell) (uplink/downlink)
Data 384 kbps	Outdoor to indoor and pedestrian A		440/465
Data 2048 kbps	Indoor		240/240
Speech 8 kbps	Indoor office A	33.0/31.0	132/124
Speech 8 kbps	Outdoor to indoor and pedestrian A	30.75/32.25	123/129
Speech 8 kbps	Vehicular A	27.0/30.5	108/122

9.5 CONCLUSIONS

OFDMA is a very flexible multiple access scheme. In combination with frequency hopping, it offers all the benefits of direct-sequence CDMA or multicarrier CDMA systems, with the following additional advantages:

- OFDMA can achieve a larger system capacity because it is not affected by intracell interference, which is the dominant source of interference in DS-CDMA and MC-CDMA.
- OFDMA is flexible in terms of the required bandwidth; it can easily be scaled to fit in a certain available piece of spectrum simply by changing the number of used subcarriers. DS-CDMA and MC-CDMA require a fixed and relatively large chunk of spectrum because of the fixed spread-spectrum chip rate.

- OFDMA seems more suited than DS-CDMA and MC-CDMA for support of large data rates. When the data rates per user become larger, the spreading gain becomes lower, so the performance of a CDMA system converges to that of a nonspread system. In that case, OFDMA with dynamic channel allocation instead of frequency hopping makes more sense than multicode DS-CDMA or MC-CDMA.

REFERENCES

- [1] Pottie, G. J., and A. R. Calderbank, "Channel Coding Strategies for Cellular Radio," *IEEE International Symposium on Information Theory*, San Antonio, TX, Jan. 1993.
- [2] Viterbi, A. J., "The Orthogonal-Random. Waveform Dichotomy for Digital Mobile Communication," *IEEE Personal Communications*, pp.18–24, First Quarter 1994.
- [3] OFDMA Evaluation Report, "The Multiple Access Scheme Proposal for the UMTS Terrestrial Radio Air Interface (UTRA) System, Part 1: System Description and Performance Evaluation," SMG2 Tdoc 362a/97, 1997.
- [4] Suzuki, M., R. Boehnke, and K. Sakoda, "BDMA - Band Division Multiple Access. new Air-Interface for 3rd Generation Mobile System, UMTS, in Europe," *Proceedings ACTS Mobile Communications Summit*, Aalborg, Denmark, pp. 482–488, Oct. 1997.
- [5] Rohling, H., and R. Grünheid, "Performance Comparison of Different Multiple Access Schemes for the Downlink of an OFDM Communication System," *Proceedings of IEEE VTC '97*, Phoenix, AZ, pp. 1365–1369, May 1997.
- [6] Chuang, J., "An OFDM Based System with Dynamic Packet Assignment and Interference Suppression for Advanced Internet Service," *Globecom '98*, Sydney, Australia, May 1998.
- [7] ETSI draft specification on the selection procedure for the choice of radio transmission technologies of the Universal Mobile Telecommunication System (UMTS), ETR/SMG-50402, Vers. 0.9.5.
- [8] Olofsson, H., J. Naslund, and J. Sköld, "Interference Diversity Gain in Frequency Hopping GSM," *Proceedings IEEE Vehicular Technology Conference*, Chicago, pp. 102–106, June 1995.

CHAPTER 10

Applications of OFDM

10.1 INTRODUCTION

This chapter describes four applications of OFDM in wireless systems. The first two are broadcasting applications for both audio and television. The Digital Audio Broadcasting (DAB) standard was in fact the first OFDM-based standard. The main reasons to choose OFDM for this system, which also applies to Digital Video Broadcasting (DVB), are the possibility to make a single frequency network and the efficient handling of multipath delay spread.

After DAB and DVB, two wireless LAN applications are described. The first one is an OFDM-based wireless ATM network, which was developed in the European Magic WAND project. The last section describes the OFDM-based IEEE, ETSI and MMAC wireless LAN standard for the 5-GHz band, providing data rates of 6 up to 54 Mbps. This new standard is the first to use OFDM in packet-based wireless communication, after projects like Magic WAND demonstrated the viability of OFDM for this type of application.

10.2 DIGITAL AUDIO BROADCASTING

DAB is the successor of current analog audio broadcasting based on AM and FM. DAB offers improved sound quality, comparable to that of a compact disc, new data services, and a higher spectrum efficiency. DAB was standardized in 1995 by the European Telecommunications Standards Institute (ETSI) as the first standard to use OFDM [1, 2]. The basis for this standard was the specification developed by the European Eureka 147 DAB project, which started in 1988.

DAB has four transmission modes using different sets of OFDM parameters, which are listed in Table 10.1. The parameters for modes I to III are optimized for use

in specific frequency bands, while mode IV was introduced to provide a better coverage range at the cost of an increased vulnerability to Doppler shift.

Table 10.1
DAB OFDM Parameters.

	Mode I	Mode II	Mode III	Mode IV
Number of subcarriers	1,536	384	192	768
Subcarrier spacing	1 kHz	4 kHz	8 kHz	2 kHz
Symbol time	1.246 ms	311.5 μ s	155.8 μ s	623 μ s
Guard time	246 μ s	61.5 μ s	30.8 μ s	123 μ s
Carrier frequency	<375 MHz	<1.5 GHz	<3 GHz	<1.5 GHz
Transmitter separation	<96 km	<24 km	<12 km	<48 km

One important reason to use OFDM for DAB is the possibility to use a single frequency network, which greatly enhances the spectrum efficiency. In a single-frequency network, a user receives the same signal from several transmitters simultaneously. Because of the propagation differences among transmitters, there is some delay between the arrival of the signals. This is illustrated in Figure 10.1, where two DAB signals arrive at the user with a delay difference that is equal to the distance difference ($d_1 - d_2$) divided by the speed of light. Basically, to the user this situation is equivalent to a two-ray multipath channel. Hence, as long as the propagation differences between the two signals are smaller than the guard time of the OFDM symbols, no ISI or ICI will occur. The addition of the two time-shifted signals creates a diversity advantage for the user; the probability that the sum of both signals has an unacceptably low power because of shadowing or flat fading is much lower than the probability that one of the individual signals is too weak.

The DAB transmitted data consists of a number of audio signals, sampled at 48 kHz with an input resolution up to 22 bits. The digital audio signal is compressed to a rate in the range of 32 to 384 kbps, depending on the desired quality. The signal is divided into frames of 24 ms. The start of a frame is indicated by a null symbol, which is a silence period that is slightly larger than the duration of a normal OFDM symbol. Then, a reference OFDM symbol is sent which serves as the starting point for the differential decoding of the QPSK-modulated subcarriers. Differential encoding is applied in the time domain, so in the receiver, the phase of each subcarrier is compared with the phase of the same subcarriers from the previous OFDM symbol.

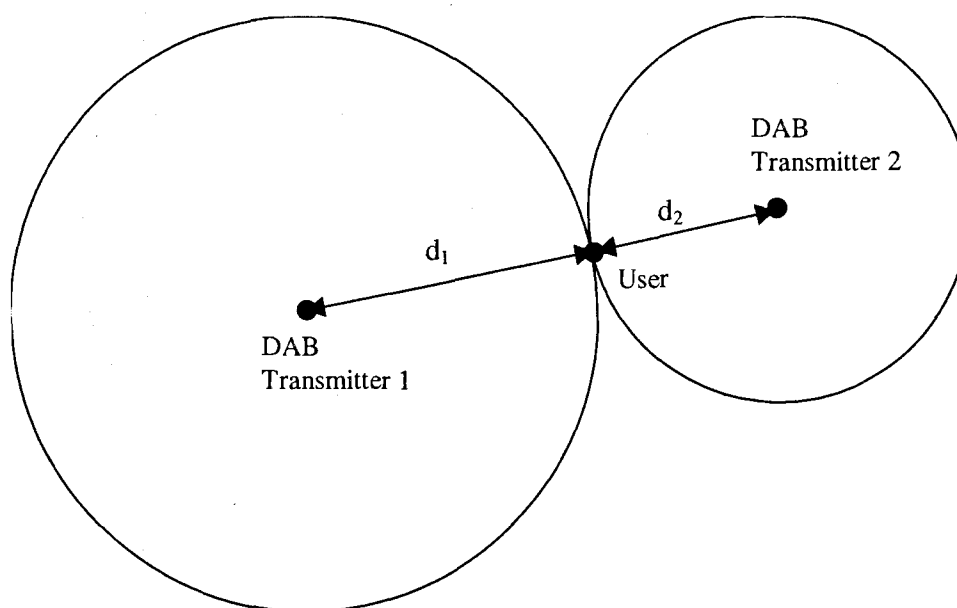


Figure 10.1 User receiving two DAB transmitters.

The digital input data is encoded by a rate $1/4$ convolutional code with constraint length 7 to provide protection against fading subcarriers. The coding rate can be increased up to $8/9$ by puncturing. This gives a maximum total data rate of $1,536 \times 2 \times 8/9 \times 1/1.246 \cdot 10^{-3}$, which is approximately 2.2 Mbps. The coded data are interleaved to separate coded bits in the frequency domain as much as possible, which avoids large error bursts in case of a deep fade affecting a group of subcarriers.

10.3 TERRESTRIAL DIGITAL VIDEO BROADCASTING

Research on a digital system for television broadcasting has been carried out since the late 1980s. In 1993, a pan-broadcasting-industry group started the Digital Video Broadcasting (DVB) project. Within this project, a set of specifications was developed for the delivery of digital television over satellites, cable, and through terrestrial transmitters. This section describes the terrestrial DVB system, which was standardized in 1997 [3, 4].

Terrestrial DVB uses OFDM with two possible modes, using 1,705 and 6,817 subcarriers, respectively. These modes are referred to as 2k and 8k modes, respectively, as these are the sizes of the FFT/IFFT needed to generate and demodulate all subcarriers. The main reason to have two modes were doubts about the implementability of the 8k subcarrier system. Basically, the 2k system is a simplified version which requires an FFT/IFFT that is only a quarter of the size that is needed for the 8k system. Because the guard time is also four times smaller, the 2k system can handle less delay spread and less propagation delay differences among transmitters within a single-frequency network. The FFT interval duration for the 8k system is 896

μs , while the guard time can have four different values from 28 to 224 μs . The corresponding values for the 2k system are four times smaller.

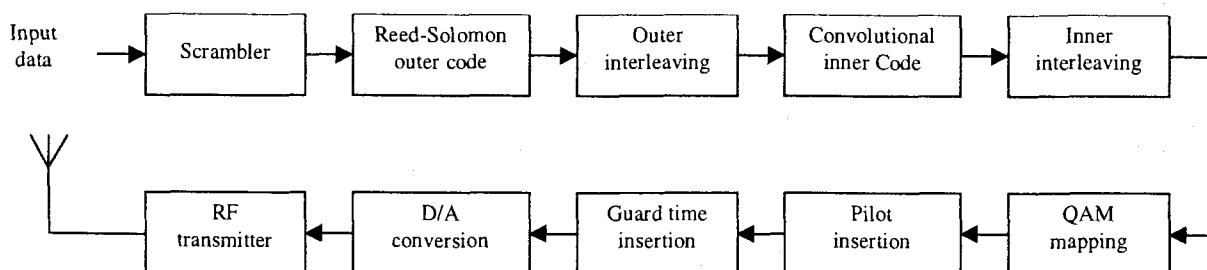


Figure 10.2 Block diagram of a DVB-T transmitter.

Figure 10.2 shows a block diagram of a DVB-T transmitter. The input data are divided into groups of 188 bytes, which are scrambled and coded by an outer shortened Reed-Solomon code (204,188, $t=8$). This code can correct up to eight erroneous bytes in a frame of 204 bytes. The coded bits are interleaved by a convolutional interleaver that interleaves byte-wise with a depth of 12 bytes and then again coded by a rate 1/2, constraint length 7 convolutional code with generator polynomials (171, 133 octal). The rate of this latter code can be increased by puncturing to 2/3, 3/4, 5/6, or 7/8. The convolutionally encoded bits are interleaved by an inner interleaver and then mapped onto QPSK, 16-QAM, or 64-QAM symbols.

For 16-QAM and 64-QAM, optional hierarchical coding can be applied. In this case, the constellation points are moved farther away from the origin so the quadrants can be detected more reliably than the position within each quadrant. This is illustrated in Figure 10.3 for a hierarchical 16-QAM constellation. For this constellation, the minimum distance between points from different quadrants is double the distance of a normal 16-QAM constellation, where the constellation points would have values of 1 and 3 instead of 2 and 4. Corrected for the increased power of the constellation, the detection of the quadrants has a 3-dB SNR advantage over the detection of points in a normal 16-QAM constellation. The advantage of this hierarchical coding is that users for which the SNR is just too low to decode all bits can at least decode the two most significant bits that determine the quadrant. These bits give them the same video signal, but at a lower resolution.

To obtain reference amplitudes and phases to perform coherent QAM demodulation, pilot subcarriers are transmitted. For the 8k mode, in each symbol there are 768 pilots, so 6,048 subcarriers remain for data. The 2k mode has 192 pilots and 1,512 data subcarriers. The position of the pilots varies from symbol to symbol with a pattern that repeats after four OFDM symbols. The pilots allow a receiver to estimate the channel both in frequency as well as in time, which is important as for mobile receivers there can be significant channel changes within a few OFDM symbols.

Techniques to do this type of two-dimensional channel estimation based on pilot subcarriers are described in Chapter 5.

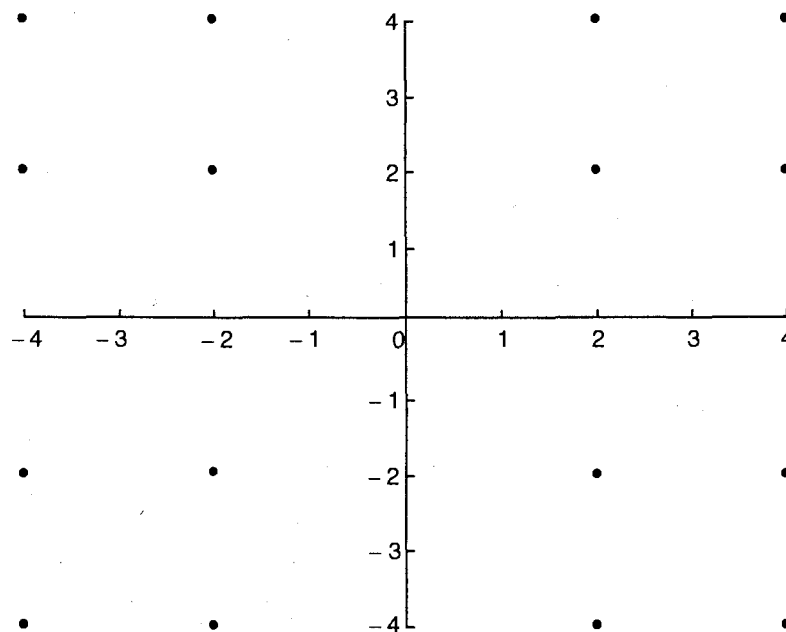


Figure 10.3 Hierarchical 16-QAM.

10.4 MAGIC WAND

The Magic WAND (Wireless ATM Network Demonstrator) project was part of the European ACTS (Advanced Communications Technology and Server) program [5]. The Magic WAND consortium members implemented a prototype wireless ATM network based on OFDM modulation. This prototype had a large impact on standardization activities in the 5-GHz band. First, by employing OFDM-based modems, Magic WAND helped to gain acceptance for OFDM as a viable modulation type for high-rate wireless communications. Second, the wireless ATM-based approach of Magic WAND forms the basis for the standardization of the HIPERLAN type 2 Data Link Layer.

Figure 10.4 shows one of the prototype Magic WAND 5-GHz modems demonstrating wireless video playback and Web browsing applications at the Demo '98 exhibition in Berlin [6].

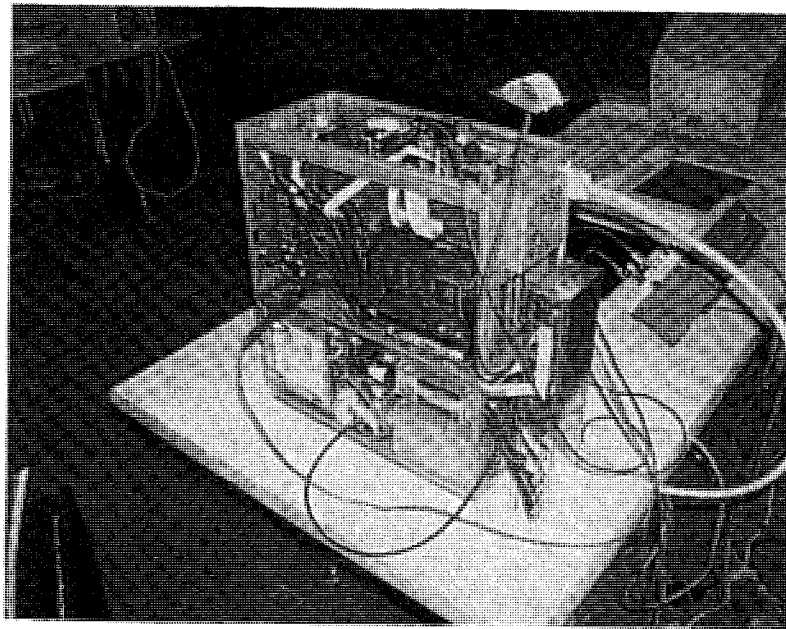


Figure 10.4 Magic WAND prototype 5-GHz modem.

10.4.1 Magic WAND Physical Layer

The main parameters of the WAND physical layer are listed in Table 10.2. OFDM with 16 subcarriers is used, the number of which was chosen to facilitate implementation. The 400-ns guard time provides a delay spread tolerance of about 50 ns. Because of a 240-ns rolloff time (see Chapter 2), the effective guard time is only 160 ns. While this is sufficient for most office buildings and the WAND trial site, a realistic product would require more delay spread robustness to also cover large office buildings and factory halls.

The OFDM subcarriers are 8-PSK modulated. At a symbol rate of 13.3 Msymbols/s, this gives a raw bit rate of 40 Mbps. The rate 1/2 complementary coding reduces the data rate to 20 Mbps. The subcarrier spacing is 1.25 MHz, which gives a total (3-dB) bandwidth of 20 MHz.

The packet preamble is 8.4 μ s in duration and consists of one OFDM symbol, repeated seven times. This preamble is used for packet detection, automatic gain control, frequency offset estimation, symbol timing, and channel estimation.

The PHY payload holds an odd number of half-slots. Each half-slot consists of 9 symbols or 27 bytes. This number was chosen so that a full slot, of 54 bytes, can hold an ATM cell (which is 52 bytes long), and is also a multiple of 3 bytes, which is imposed by the PHY's modulation scheme.

Table 10.2
Main parameters of the WAND OFDM modem.

Number of subcarriers	16
Modulation	8-PSK
Coding	Two interleaved length 8 complementary codes, rate $\frac{1}{2}$
Bit rate (after decoding)	20 Mbps (24 bits per symbol)
Symbol time	1.2 μ s
Guard time	0.4 μ s
Windowing	Raised cosine, rolloff factor = 0.2
Subcarrier spacing	1.25 MHz
Training length	7 symbols
Carrier frequency	5.2 GHz
Peak output power	1W

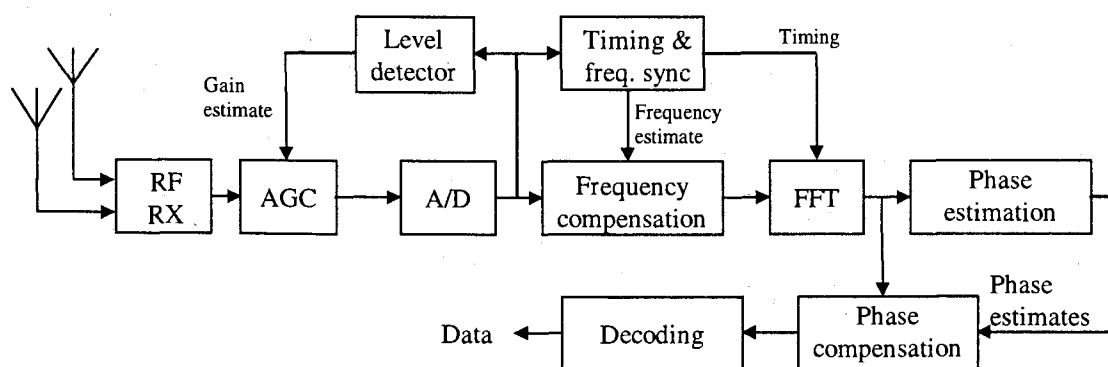


Figure 10.5 OFDM receiver.

Figure 10.5 shows a block diagram of the OFDM receiver. The RF receiver takes care of amplifying and down-converting the signal. The automatic gain control (AGC) is one of the most difficult parts in the receiver, since the gain has to settle within 3 μ s after start of reception. After the analog-to-digital (A/D) conversion, the frequency of the signal has to be estimated and corrected for, because OFDM is sensitive to frequency errors (see Chapter 4).

By taking the FFT of groups of samples at the right time instants, the receiver obtains amplitude and phase estimates of the 16 subchannels. From the initial training sequence, the receiver has to acquire and track the reference phases for all subchannels. After phase compensation, finally the 24 information bits can be decoded from the 16 complex subcarrier values.

10.4.2 Coding

The WAND modem uses complementary codes for both forward-error correction coding and peak-to-average power (PAP) reduction. Length 8 complementary codes are used, with four input 8-PSK phases generating eight complex code outputs as described in Chapter 6. By taking the IFFT of these complex values, an OFDM signal with a low PAP ratio is obtained. To encode all 16 subcarriers, two length 8 codes are interleaved, which maximizes the benefits of frequency diversity. It is also possible to use length 16 complementary codes, but for that length, only five phases can be encoded into 16 subcarriers, reducing the coding rate from 1/2 to 5/16. The minimum distance of the length 8 code is four subsymbols. Hence, three arbitrary subchannels can be erased without causing errors, providing that the remaining subchannels are not in error.

10.4.3 Simulated Error Probabilities

Bit-error ratios (BER) and packet-error ratios (PER) for various delay spreads are depicted in Figure 10.6. For each mean E_b/N_o value, 40,000 ATM-cell transmissions have been simulated in Rayleigh fading channels, without antenna diversity. In all transmissions, a frequency offset of 40 kHz was simulated, which has to be estimated and compensated for by the receiver. Figure 10.6 clearly shows that the coded OFDM system is able to benefit from the frequency diversity, which is present for nonzero delay spreads.

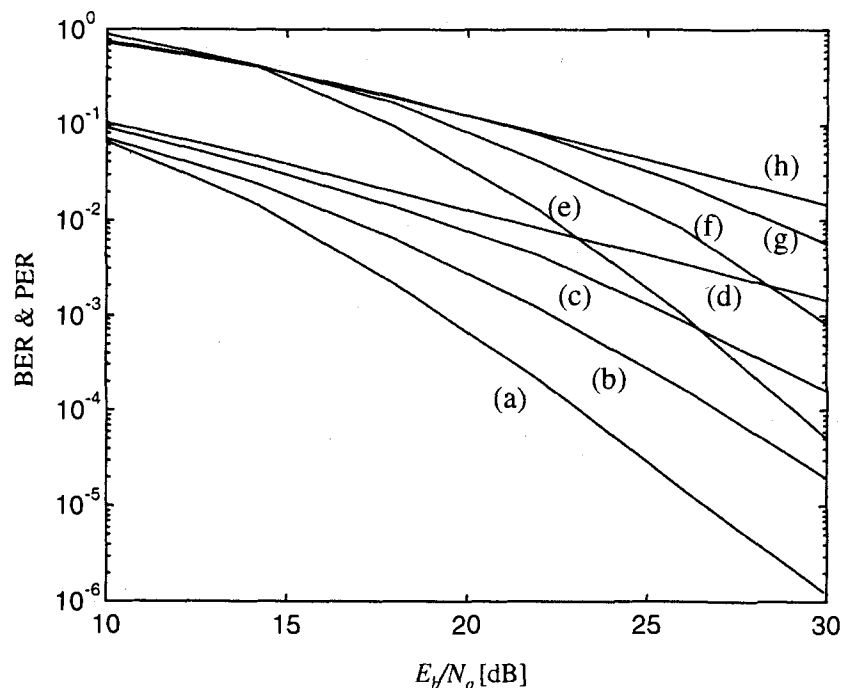


Figure 10.6 BER (a–d) and PER (e–h) versus mean E_b/N_o for delay spreads of (a,e) 50 ns, (b,f) 20 ns, (c,g) 10 ns, (d,h) 0.

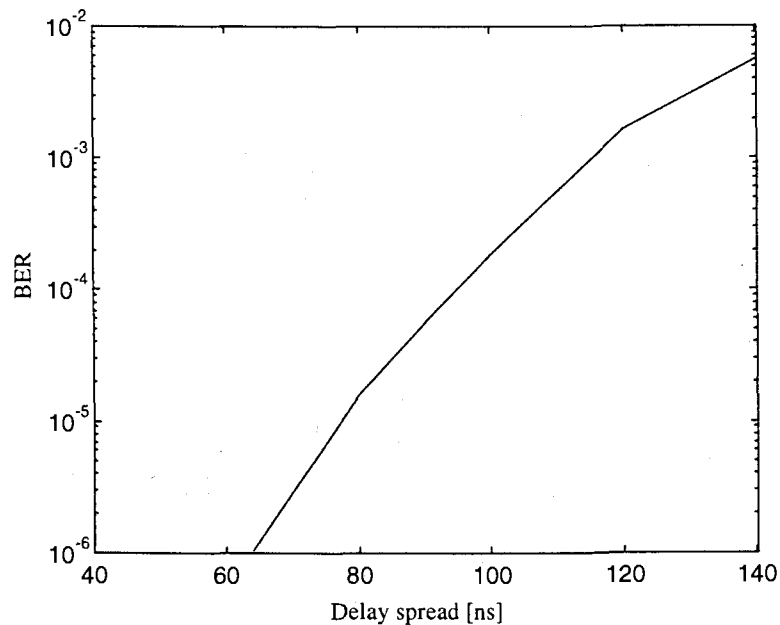


Figure 10.7 Irreducible BER versus delay spread for an exponential power delay profile.

For delay spreads larger than 50 ns, the error curves converge to some irreducible error floor, caused by intersymbol and intercarrier interference of multipath signals with excess delays larger than the guard time. In Figure 10.7, this irreducible BER is plotted versus the delay spread. Notice that an exponential power-delay profile is used in the simulations. For a two-ray model, for instance, the irreducible error floor arises only for delay spreads larger than half of the guard time (i.e., 200 ns for the prototype WAND modem). Thus, the exponential power delay profile gives much more pessimistic results in this respect. Conversely, the two-ray model is known to give less diversity gain, because there are only two independent fading paths.

10.4.4 Effects of Clipping

Despite the use of complementary coding in the WAND OFDM system, the transmitted signal still has a 6-dB PAP ratio. To make the efficiency of the transmitter power amplifier as high as possible, we have to accept a certain nonlinear distortion in the peaks of the OFDM signal. A crude analysis of this nonlinear distortion can be made by assuming a clipping transfer function. Figure 10.8 shows the BER in an AWGN channel for clipping levels of 0 to 4 dB below the maximum amplitude. It can be seen that significant degradation occurs only for a clipping level of more than 3 dB below the peak amplitude. Of course, such severe clipping is not allowed from a spectrum point of view, but the analysis at least shows that the OFDM transmission itself is relatively insensitive against clipping.

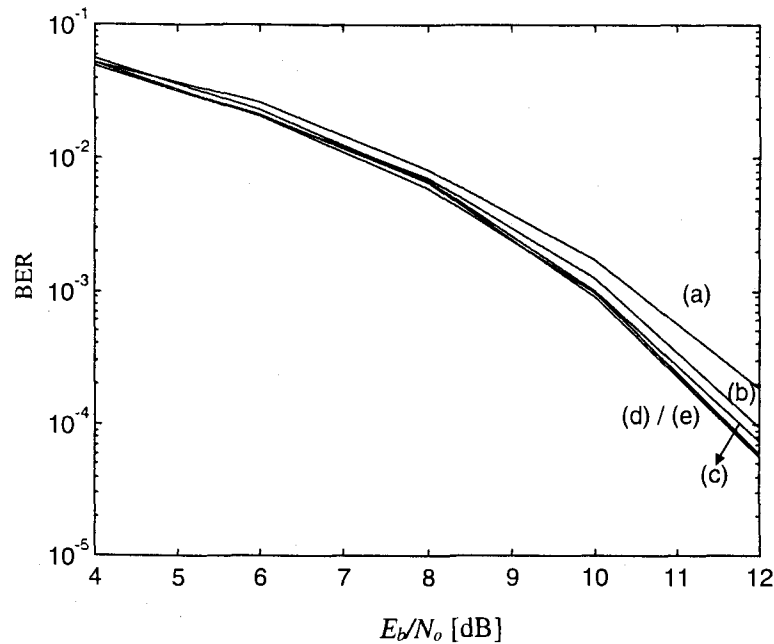


Figure 10.8 BER in AWGN with the transmitted OFDM signals clipped at (a) 4 dB, (b) 3 dB, (c) 2 dB, (d) 1 dB and (e) 0 dB below the maximum amplitude.

Clipping at the receiver is different from clipping at the transmitter, because the receiver does not know in advance what the peak amplitude is, contrary to the transmitter. Even after the initial training symbols, when the receiver freezes its AGC, the receiver does not know what the peak amplitude will be in the rest of the packet. Except for noise, this is caused by two effects: first, multipath fading channels change the peak-to-average power ratio of the OFDM signal and second, different symbols have different PAP ratios.

An OFDM receiver must freeze its AGC based on the observed amplitude level during training. The peak amplitude during training is most probably not the largest amplitude of the entire packet. Thus, the question is how to set the AGC level such that clipping effects are negligible. Based on the results from Chapter 6, the ideal AGC setting is such that the clipping level is about 6 to 10 dB above the average input power level. In this case, the interference caused by clipping is relatively small compared with the average signal power. If the clipping level is more than 10 dB above the average power level, then the risk exists that quantization noise starts dominating over clipping noise, as the most significant bits of the A/D converter are hardly used in this case.

10.4.5 Magic WAND Medium Access Control Layer

The MAC (Medium Access Control) and DLC (Data Link Control) layers of the WAND system have been combined in one layer, bearing the name MASCARA (Mobile Access Scheme based on Contention And Reservation for ATM). The underlying concept is based on the following set of ideas and requirements which are elaborated in the subsequent paragraphs.

- QoS-aware, reservation-based demand assigned protocol;
- Multiple virtual connections per terminal;
- Power efficiency;
- Cell transfer service for optimal interworking with ATM;
- Amortization of PHY overhead over multiple ATM cells;
- Contention-mode request and control channel; and
- ARQ (Automatic Repeat reQuest)-based cell loss recovery.

ATM is designed to offer service to wire-line users with a guaranteed quality of service. To extend ATM service to mobile terminals, the wireless access network needs to be QoS-aware as well. A centralized algorithm allotting transmission time to users on the basis of their explicit demands seems to be an obvious way to provide QoS and isolation among users' traffic streams. We note that the disadvantage over contention-based algorithms as used in wireless LANs and wireless PBXs is that they do not inherently support multicellular operation. To function correctly, they require a cellular frequency reuse topology, with perfect separation between radio cells with identical frequencies. As usual for wireless LANs, TDD between uplink and downlink is chosen, primarily to support traffic asymmetry.

As a multimedia terminal may have many simultaneous connections, most probably with different QoS requirements, the network must be able—besides addressing individual terminals—to distinguish separate connections of those terminals. Given the smaller number of users and the scarcity of bandwidth, the relatively large addressing overhead of ATM, being designed for large wire-line networks, must be avoided.

Mobile terminals draw power from batteries, and to extend battery-life the protocols need to be energy aware. A frame-based MAC, in which the access point notifies all associated terminals about their expected transmissions and receptions in the entire frame helps to conserve power: terminals switch on their radios only when necessary. From the energy perspective, the frame duration should be made as long as possible. QoS considerations, on the other hand, put a bound on the maximal frame length. For this scheme to work, a frame structure by itself is not sufficient. A common time base among terminals and access point is required as well. For practical reasons the granularity of time must be bounded. The unit of time in MASCARA is a timeslot, and all packet transmissions commence on a timeslot boundary.

To provide seamless interworking with the ATM backbone, and transparency to the user, packets must carry ATM cells. It makes sense to choose the slot duration equal to a cell's transmission time. The same length of time is imposed on the packet header (radio preamble and MAC header) as well. In the WAND system, the first half of the overhead slot is used for the preamble, the other half is used for the MAC header.

If each packet were to contain just one cell, the protocol efficiency would be merely 50%. To increase efficiency, a longer packet size can be adopted. On the other

hand, QoS-driven restrictions on cellization delay put an upper bound on packet length. In the case of 64 kbps speech traffic for instance, cellization delay is 6 ms per cell, which restricts the packet length to one or two cells. The logical decision is to allow packets of variable length, depending on the connection's delay requirements, with a payload of an integer number of cells.

Demand-assigned algorithms assign timeslots to terminals, based on terminal demand. Uplink packets contain fields in which a terminal can put its request. If a terminal cannot piggyback its request, because no timeslots were assigned to it (a deadlock situation), or because it cannot afford to wait for the next packet, the terminal can transmit its request in an unreserved timeslot. A contention period is scheduled at the end of every frame. Contention slots can be used for incidental control packets as well.

Adverse radio propagation conditions affect the cell loss ratio (CLR) QoS. By its nature, a radio network cannot provide the same QoS consistently. To sustain a negotiated CLR QoS as long as possible, the DLC layer adds ARQ capability to the system. ARQ can help to retain the agreed-on cell loss rate, at the cost of an increase in delay and data overhead.

Figure 10.9 depicts an example frame. Two mobile terminals (MT) and one access point (AP) are engaged in the exchange of packets. For instruction purposes, the frame duration is shorter than typically encountered in practice. The access point initiates every frame by broadcasting a frame header (FH), containing the slot map to all associated mobile terminals. The FH has a long preamble, allowing mobile terminals to synchronize to the access point. Subsequently, the access point sends its downlink data, one packet in this example. The channel remains idle for one slot to allow the access point to turn around its radio from transmitting to receiving. Then the mobile terminals are allowed to transmit their packets. In this example each mobile terminal transmits one. After the uplink period, a contention period is scheduled, which in this example is used by both terminals. Terminal 1 is transmitting two request packets and terminal 2 is transmitting a two-slot control packet. In the example, two packets collide, resulting in the loss of the control packet and one of the request packets. The second request packet is transmitted successfully in the third slot. After the contention period, and before the next frame, an idle slot is inserted to allow the mobile terminal radios to turn around.

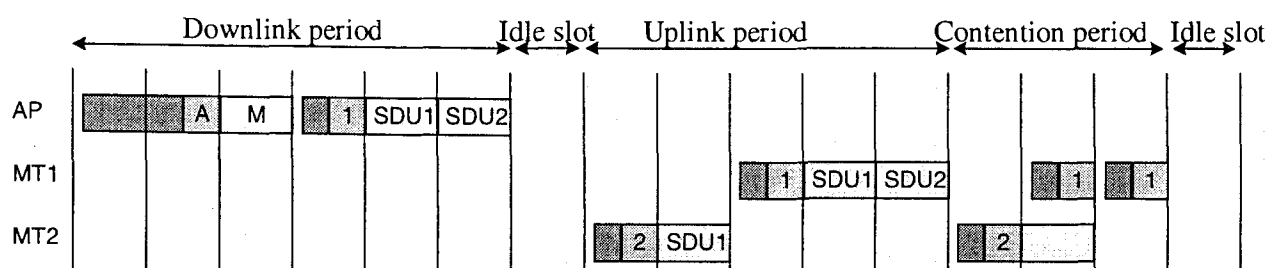


Figure 10.9 Magic WAND MAC frame.

The master scheduler, which must be able to schedule the transmissions of any mix of ATM traffic classes, employs a leaky-bucket-based scheme where the highest priority is given to constant bit-rate traffic, the second priority to variable bit rate, and so on. Tokens, which are generated at a constant rate, fill a bucket. The scheduler takes tokens from the bucket, and translates them in the allocation of slots in the slot map according to the connections' delay requirements. A traffic source can request slots (access points directly, mobile terminals use piggy-backed and contention requests) in excess of the mean rate. Depending on the negotiated burstiness of the source, which is reflected in a commensurate bucket depth, the scheduler grants the request. Effectively, the scheduler polices and shapes the traffic on the wireless link, to guarantee delay QoS compliance for all connections. See [7] for an extensive discussion of scheduling.

The second important measure of QoS, besides delay and delay jitter, is the connection's error performance over the wireless ATM link. In WAND, the radio physical layer provides a constant service that can meet typical real-time service requirements (e.g., for a voice service). TCP/IP-based data connections cannot tolerate high cell loss ($> 10^{-2}$) and these are protected by ARQ. Third, there are services such as video requiring real-time service with low error probability. The solution applied in WAND is to apply ARQ with a limited number of retransmissions.

10.5 IEEE 802.11, HIPERLAN/2 AND MMAC WIRELESS LAN STANDARDS

Since the beginning of the nineties, wireless local area networks (WLAN) for the 900-MHz, 2.4-GHz, and 5-GHz ISM (Industrial, Scientific, & Medical) bands have been available, based on a range of proprietary techniques. In June 1997, the Institute of Electrical and Electronics Engineers (IEEE) approved an international interoperability standard [8]. The standard specifies both medium access control (MAC) procedures and three different physical layers (PHY). There are two radio-based PHYs using the 2.4-GHz band. The third PHY uses infrared light. All PHYs support a data rate of 1 Mbps and optionally 2 Mbps. The 2.4-GHz frequency band is available for license-exempt use in Europe, the United States, and Japan. Table 10.3

lists the available frequency band and the restrictions to devices which use this band for communications.

Table 10.3
International 2.4-GHz ISM bands.

Location	Regulatory range	Maximum output power
North America	2.400–2.4835 GHz	1,000 mW
Europe	2.400–2.4835 GHz	100 mW (EIRP*)
Japan	2.471–2.497 GHz	10 mW

* EIRP = effective isotropic radiated power.

User demand for higher bit rates and the international availability of the 2.4-GHz band has spurred the development of a higher speed extension to the 802.11 standard. In July 1998, a proposal was selected for standardization, which describes a PHY providing a basic rate of 11 Mbps and a fall back rate of 5.5 Mbps. This PHY can be seen as a fourth option, to be used in conjunction with the MAC that is already standardized. Practical products, however, are expected to support both the high-speed 11- and 5.5-Mbit/s rates mode as well as the 1- and 2-Mbps modes.

A second IEEE 802.11 working group has moved on to standardize yet another PHY option, which offers higher bit rates in the 5.2-GHz band. This development was motivated by the adoption, in January 1997, by the U.S. Federal Communications Commission, of an amendment to Part 15 of its rules. The amendment makes available 300 MHz of spectrum in the 5.2-GHz band, intended for use by a new category of unlicensed equipment called Unlicensed National Information Infrastructure (UNII) devices [9]. Table 10.4 lists the frequency bands and the corresponding power restrictions. Notice that the maximum permitted output power depends on the emission bandwidth; for a bandwidth of 20 MHz, you are allowed to transmit at the maximum power levels listed in the middle column of Table 10.4. For a bandwidth smaller than 20 MHz the power limit reduces to the value specified in the right column.

Table 10.4
United States 5.2 GHz U-NII band.

Location	Maximum output power minimum of	
5.150–5.250 GHz	50 mW	4 dBm + $10\log_{10}B^*$
5.250–5.350 GHz	250 mW	11 dBm + $10\log_{10} B$
5.725–5.825 GHz	1,000 mW	17 dBm + $10\log_{10} B$

* B is the –26-dB emission bandwidth in MHz.

Like the IEEE 802.11 standard, the European ETSI HIPERLAN type 1 standard [10] specifies both MAC and PHY. Unlike IEEE 802.11, however, no HIPERLAN type 1 compliant products are available in the market place. A newly formed ETSI working group called Broadband Radio Access Networks (BRAN) is now working on

extensions to the HIPERLAN standard. Three extensions are under development: HIPERLAN/2, a wireless indoor LAN with a QoS provision; HiperLink, a wireless indoor backbone; and HiperAccess, an outdoor, fixed wireless network providing access to a wired infrastructure.

In Japan, equipment manufacturers, service providers and the Ministry of Post and Telecommunications are cooperating in the Multimedia Mobile Access Communication (MMAC) project to define new wireless standards similar to those of IEEE 802.11 and ETSI BRAN. Additionally, MMAC is also looking into the possibility for ultra-high-speed wireless indoor LANs supporting large-volume data transmission at speeds up to 156 Mbps using frequencies in the 30- to 300- GHz band.

In July 1998, the IEEE 802.11 standardization group decided to select OFDM as the basis for their new 5-GHz standard, targeting a range of data rates from 6 up to 54 Mbps [12, 13]. This new standard is the first one to use OFDM in packet-based communications, while the use of OFDM until now was limited to continuous transmission systems like DAB and DVB. Following the IEEE 802.11 decision, ETSI BRAN and MMAC also adopted OFDM for their physical layer standards. The three bodies have worked in close cooperation since then to make sure that differences among the various standards are kept to a minimum, thereby enabling the manufacturing of equipment that can be used worldwide.

The focus of this section is on the physical layer side. In the case of the IEEE 802.11 standard, the MAC layer for the higher data rates remains the same as for the currently supported 1- and 2- Mbps rates. A description of this MAC can be found in [11].

10.5.1 OFDM Parameters

Table 10.5 lists the main parameters of the draft OFDM standard. A key parameter that largely determined the choice of the other parameters is the guard interval of 800 ns. This guard interval provides robustness to rms delay spreads up to several hundreds of nanoseconds, depending on the coding rate and modulation used. In practice, this means that the modulation is robust enough to be used in any indoor environment, including large factory buildings. It can also be used in outdoor environments, although directional antennas may be needed in this case to reduce the delay spread to an acceptable amount and increase the range.

Table 10.5
Main parameters of the OFDM standard.

Data rate	6, 9, 12, 18, 24, 36, 48, 54 Mbps
Modulation	BPSK, QPSK, 16-QAM, 64-QAM
Coding rate	1/2, 2/3, 3/4
Number of subcarriers	52
Number of pilots	4
OFDM symbol duration	4 μ s
Guard interval	800 ns
Subcarrier spacing	312.5 kHz
-3-dB Bandwidth	16.56 MHz
Channel spacing	20 MHz

To limit the relative amount of power and time spent on the guard time to 1 dB, the symbol duration chosen is 4 μ s. This also determines the subcarrier spacing at 312.5 kHz, which is the inverse of the symbol duration minus the guard time. By using 48 data subcarriers, uncoded data rates of 12 to 72 Mbps can be achieved by using variable modulation types from BPSK to 64-QAM. In addition to the 48 data subcarriers, each OFDM symbol contains an additional four pilot subcarriers, which can be used to track the residual carrier frequency offset that remains after an initial frequency correction during the training phase of the packet.

To correct for subcarriers in deep fades, forward-error correction across the subcarriers is used with variable coding rates, giving coded data rates from 6 up to 54 Mbps. Convolutional coding is used with the industry standard rate 1/2, constraint length 7 code with generator polynomials (133,171). Higher coding rates of 2/3 and 3/4 are obtained by puncturing the rate 1/2 code. The 2/3-rate is used together with 64-QAM only to obtain a data rate of 48 Mbps. The 1/2-rate is used with BPSK, QPSK, and 16-QAM to give rates of 6, 12, and 24 Mbps, respectively. Finally, the 3/4-rate is used with BPSK, QPSK, 16-QAM, and 64-QAM to give rates of 9, 18, 36, and 54 Mbps, respectively.

10.5.2 Channelization

Figure 10.10 shows the channelization for the lower and middle UNII bands. Eight channels are available with a channel spacing of 20 MHz and guard spacings of 30 MHz at the band edges in order to meet the stringent FCC-restricted band spectral density requirements. The FCC also defined an upper UNII band from 5.725 to 5.825 GHz, which carries another four OFDM channels. For this upper band, the guard spacing from the band edges is only 20 MHz, as the out-of-band spectral requirements for the upper band are less severe than those of the lower and middle UNII bands. In Europe, a total of 455 MHz is available in two bands, one from 5.15 to 5.35 GHz and

another from 5.470 to 5.725 GHz. In Japan, a 100 MHz wide band is available from 5.15 to 5.25 GHz, carrying four OFDM channels.

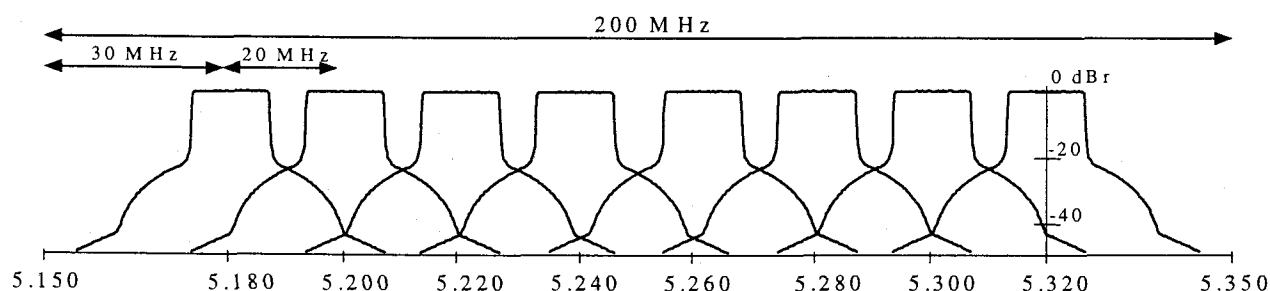


Figure 10.10 Channelization in lower and middle UNII band.

10.5.3 OFDM Signal Processing

The general block diagram of the baseband processing of an OFDM transceiver is shown in Figure 10.11. In the transmitter path, binary input data is encoded by a standard rate 1/2 convolutional encoder. The rate may be increased to 2/3 or 3/4 by puncturing the coded output bits. After interleaving, the binary values are converted into QAM values. To facilitate coherent reception, four pilot values are added to each 48 data values, so a total of 52-QAM values is reached per OFDM symbol, which are modulated onto 52 subcarriers by applying the IFFT. To make the system robust to multipath propagation, a cyclic prefix is added. Further, windowing is applied to attain a narrower output spectrum. After this step, the digital output signals can be converted to analog signals, which are then up-converted to the 5-GHz band, amplified and transmitted through an antenna.

The OFDM receiver basically performs the reverse operations of the transmitter, together with additional training tasks. First, the receiver has to estimate frequency offset and symbol timing, using special training symbols in the preamble. Then, it can do an FFT for every symbol to recover the 52-QAM values of all subcarriers. The training symbols and pilot subcarriers are used to correct for the channel response as well as remaining phase drift. The QAM values are then demapped into binary values, after which a Viterbi decoder can decode the information bits.

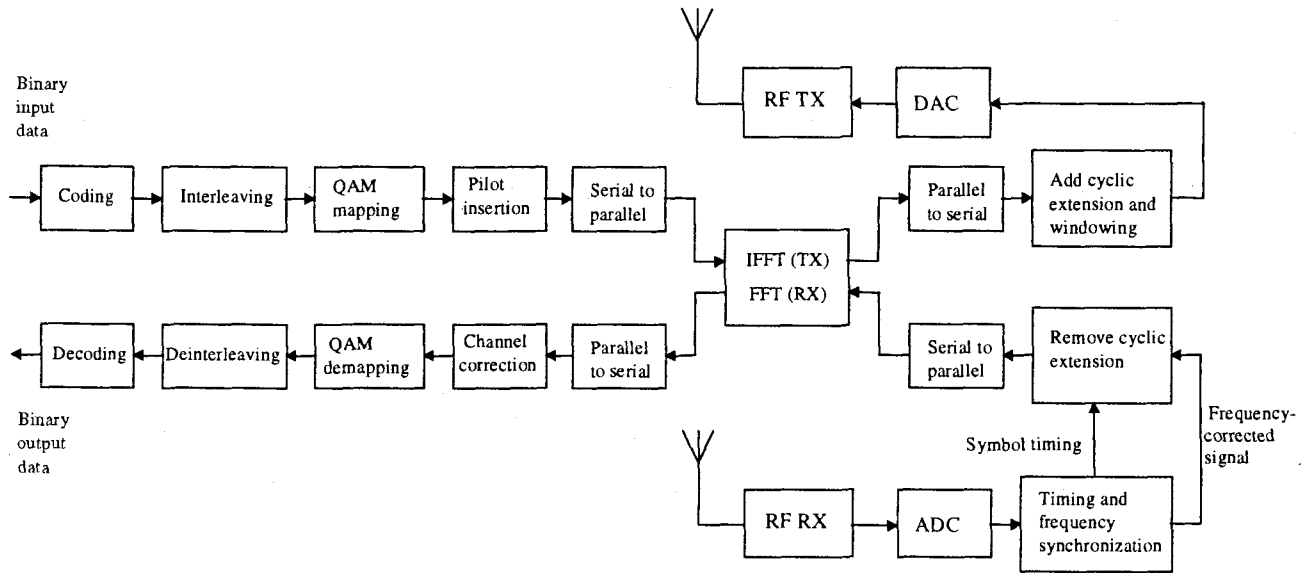


Figure 10.11 Block diagram of OFDM transceiver.

10.5.4 Training

Figure 10.12 shows the structure of the preamble that precedes every OFDM packet. This preamble is essential to perform start-of-packet detection, automatic gain control, symbol timing, frequency estimation, and channel estimation. All of these training tasks have to be performed before the actual data bits can be successfully decoded.

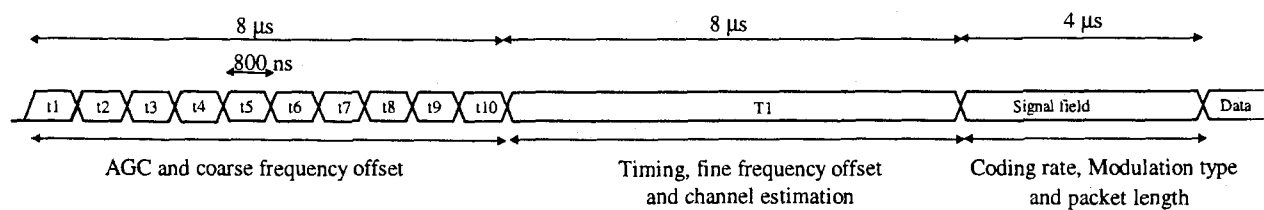


Figure 10.12 OFDM preamble.

The first part of the preamble consists of 10 repetitions of a training symbol with a duration of 800 ns each, which is only a quarter of the FFT duration of a normal data symbol. These short symbols are produced by using only nonzero subcarrier values for subcarrier numbers that are a multiple of 4. Hence, of all possible subcarrier numbers from -26 to $+26$, only the subset $\{-24, -20, -16, -12, -8, -4, 4, 8, 12, 16, 20, 24\}$ is used. There are two reasons for using relatively short symbols in this part of the training; first, the short symbol period makes it possible to do a coarse frequency offset estimation with a large unambiguous range. For a repetitive signal with a duration of T , the maximum measurable unambiguous frequency offset is equal to $1/(2T)$, as higher frequency offsets result in a phase change exceeding π from one symbol to another. Hence, by measuring the phase drift between two consecutive short symbols with a

duration of 800 ns, frequency offsets up to 625 kHz can be estimated. If training symbols with a duration equal to the FFT interval of 3.2 μ s were used, then the maximum frequency offset of only 156 kHz could be measured, corresponding to a relative frequency error of about 26 ppm at a carrier frequency of 5.8 GHz. The IEEE 802.11 standard specifies a maximum offset *per user* of 20 ppm, which means that the worst case offset as seen by a receiver can be up to 40 ppm, as it experiences the sum of the frequency offsets from both transmitter and receiver.

The second reason for using short symbols at the start of the training is that they provide a convenient way of performing AGC and frame detection. Detection of the presence of a packet can be done by correlating a short symbol with the next and detecting if the correlation magnitude exceeds some threshold. After each interval equal to two short symbol durations, the receiver gain can be adjusted after which detection and gain measuring can continue. Of course, this AGC algorithm could also be applied to long training symbols, but the advantage of short symbols is that we have more repetitions in the same amount of time, which makes it easier to do several measurements and gain adjustments during the training.

The short training symbols are followed by a long training symbol (T1) that contains 52 QPSK-modulated subcarriers like a normal data symbol. The length of this training symbol is twice that of a data symbol, however, which is done for two reasons. First, it makes it possible to do a precise frequency estimation on the long symbol. The long symbol is formed by cyclically extending the IFFT output signal to a length of 8 μ s. Thus, it contains two and a half times the original IFFT duration. The first 1.6 μ s serves as a guard interval, containing a copy of the last 1.6 μ s of the IFFT output. The long training symbol makes it possible to do a fine frequency offset estimation by measuring the phase drift between samples that are 3.2 μ s apart within the long training symbol. The second reason for having the long symbol is to obtain reference amplitudes and phases for doing coherent demodulation. By averaging the two identical parts of the long training symbol, coherent references can be obtained with a noise level that is 3 dB lower than the noise level of data symbols.

Both the long and short symbols are designed in such a way that the PAP ratio is approximately 3 dB, which is significantly lower than the PAP ratio of random OFDM data symbols. This guarantees the training degradation caused by nonlinear amplifier distortion to be smaller than the distortion of the data symbols. It also allows the use of a simple correlator implementation at the receiver as explained in Section 4.6.

After the preamble, there is still one training task left, which is tracking the reference phase. There will always be some remaining frequency offset that causes a common phase drift on all subcarriers. To track this phase drift, 4 of the 52 subcarriers contain known pilot values. The pilots are scrambled by a length 127 pseudonoise sequence to avoid spectral lines exceeding the average power density of the OFDM spectrum.

Figure 10.13 shows the time-frequency structure of an OFDM packet, where all known training values are marked in gray. It clearly illustrates how the packet starts with 10 short training symbols, using only 12 subcarriers, followed by the long training symbol and data symbols, with each data symbol containing four known pilot subcarriers.

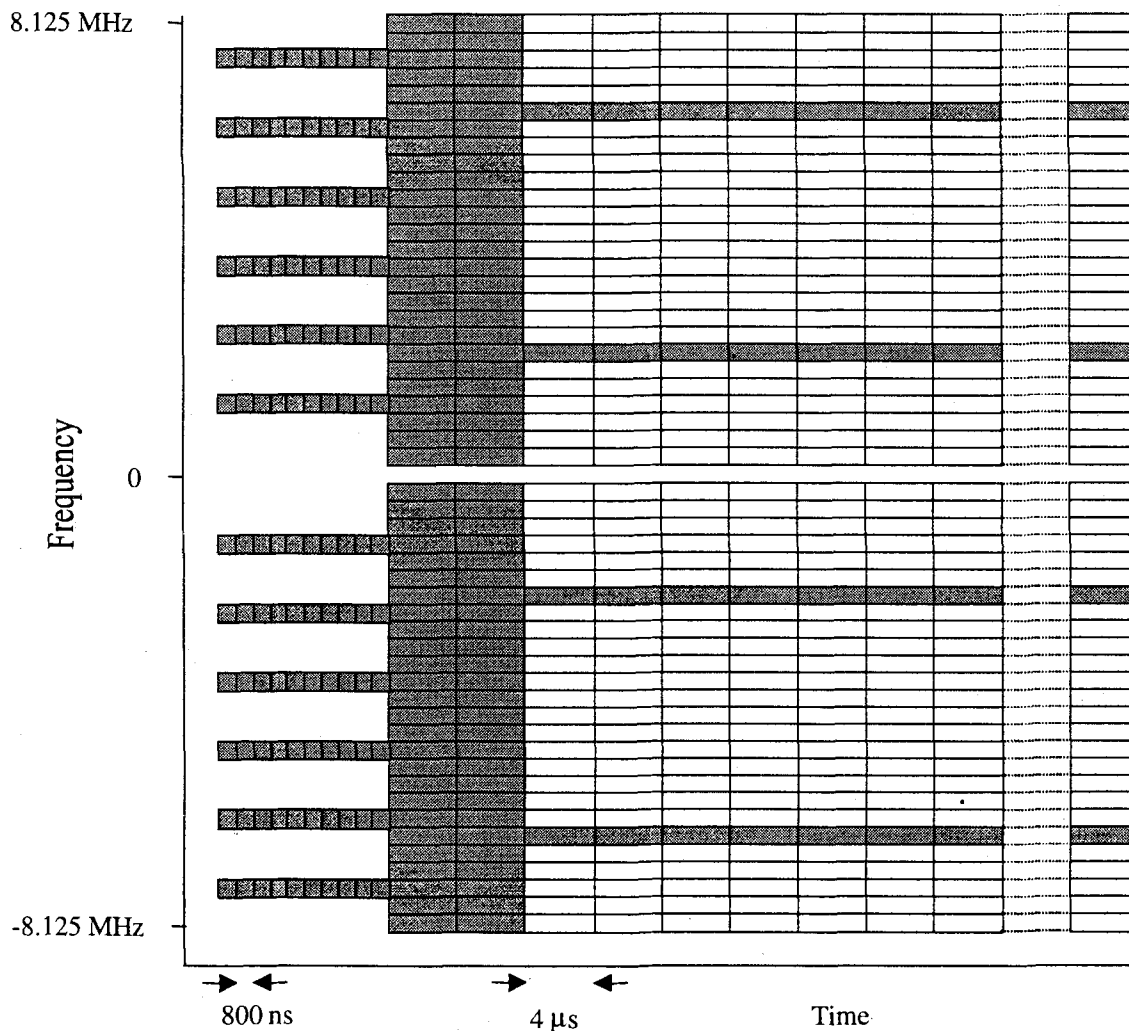


Figure 10.13 Time-frequency structure of an OFDM packet. Gray subcarriers contain known training values.

In the case of the IEEE 802.11 standard, at the end of the preamble a special OFDM data symbol at the lowest 6-Mbps rate is sent, which contains information about the length, modulation type, and coding rate of the rest of the packet. Sending this information at the lowest possible rate ensures that the dynamic rate selection is at least as reliable as the most reliable data rate of 6 Mbps. Further, it makes it possible for all users to decode the duration of a certain packet, even though they may not be able to decode the data content. This is important for the IEEE 802.11 MAC protocol, which specifies that a user has to wait until the end of any packet already in the air before trying to compete for the channel.

10.5.5 Differences Between IEEE 802.11, HIPERLAN/2 and MMAC

The main differences between IEEE 802.11 and HIPERLAN/2—which is standardized by ETSI BRAN [14]—are in the Medium Access Control (MAC). IEEE 802.11 uses a distributed MAC based on Carrier Sense Multiple Access with Collision Avoidance, (CSMA/CA), while HIPERLAN/2 uses a centralized and scheduled MAC, based on wireless ATM. MMAC supports both of these MACs. As far as the physical layer is concerned, there are a few relatively minor differences between IEEE 802.11 and HIPERLAN/2 which are summarized below:

- HIPERLAN uses different training sequences. The long training symbol is the same as for IEEE 802.11, but the preceding sequence of short training symbols is different. A downlink transmission starts with 10 short symbols as IEEE 802.11, but the first 5 symbols are different in order to detect the start of the downlink frame. The rest of the packets in the downlink frame do not use short symbols, only the long training symbol. Uplink packets may use 5 or 10 identical short symbols, with the last short symbol being inverted.
- HIPERLAN uses extra puncturing to accommodate the tail bits to keep an integer number of OFDM symbols in 54 byte packets. This extra puncturing operation punctures 12 bits out of the first 156 bits of a packet.
- In the case of 16-QAM, HIPERLAN uses a coding rate of 9/16 instead of 1/2—giving a bit rate of 27 instead of 24 Mbps—to get an integer number of OFDM symbols for packets of 54 bytes. The rate 9/16 is made by puncturing 2 out of every 18 encoded bits.
- Both IEEE 802.11 and HIPERLAN scramble the input data with a length 127 pseudo random sequence, but the initialization is different. IEEE 802.11 initializes with 7 random bits which are inserted as the first 7 bits of each packet. In HIPERLAN, the scrambler is initialized by {1, 1, 1} plus the first 4 bits of the Broadcast Channel at the beginning of a MAC frame. The initialization is identical for all packets in a MAC frame.
- HIPERLAN devices have to support power control in the range of -15 to 30 dBm with a step size of 3 dB.
- Dynamic frequency selection is mandatory in Europe over a range of at least 330 MHz for indoor products and 255 MHz (upper band only) for outdoor products. This means that indoor products have to support a frequency range from 5.15 to at least 5.6 GHz, covering the entire lower band and a part of the European upper band. Dynamic frequency selection was included to avoid the need for frequency planning and to provide coexistence with radar systems that operate in the upper part of the European 5 GHz band.

10.5.6 Simulation Results

Figure 10.14 shows the irreducible PER versus delay spread for a few different data rates. This is the minimum possible PER for a certain delay spread, for which all packet errors are caused by intersymbol interference because of path delays exceeding the guard time of the OFDM symbols. Hence, Figure 10.14 demonstrates the delay spread robustness for several data rates. For a 1% PER, the tolerable delay spread is close to 200 ns at 36 Mbps, while at 12 Mbps a delay spread of 450 ns can be tolerated. In practice, this means that the 36-Mbps rate can be used in most indoor environments, except some large factory buildings. The 54 Mbps rate can tolerate delay spreads up to about 120 ns, which is sufficient for most office buildings. The 12-Mbps rate can work in any indoor and even in outdoor environments. This is also true for the lowest rate of 6 Mbps, that is not included in Figure 10.14.

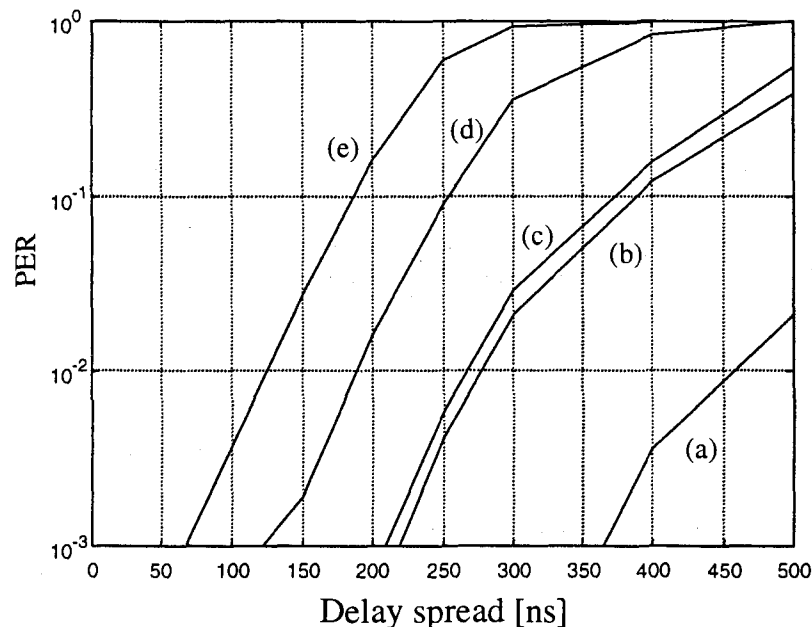


Figure 10.14 PER versus rms delay spread (no noise) for Rayleigh fading paths with an exponentially decaying power delay profile. Packet size is 64 bytes with data rates of (a) 12, (b) 18, (c) 24, (d) 36, and (e) 54 Mbps.

Figure 10.15 shows the PER versus E_b/N_o for a data rate of 24 Mbps in case of an AWGN channel and a Rayleigh fading channel with a delay spread of 100 ns. An E_b/N_o of about 18 dB is required to achieve a 1% PER in the fading channel, which is approximately 6 dB more than what is needed for an ideal Gaussian noise channel. Of course, other data rates have different requirements. Figure 10.16 shows the PER for various data rates as a function of the input power. We can see a difference of almost 18 dB in the signal power requirements of the lowest and highest data rates. This illustrates the importance of fallback rates; users who cannot use the highest rate because they are too far away or are in a bad multipath situation can at least obtain a data link at a lower rate.

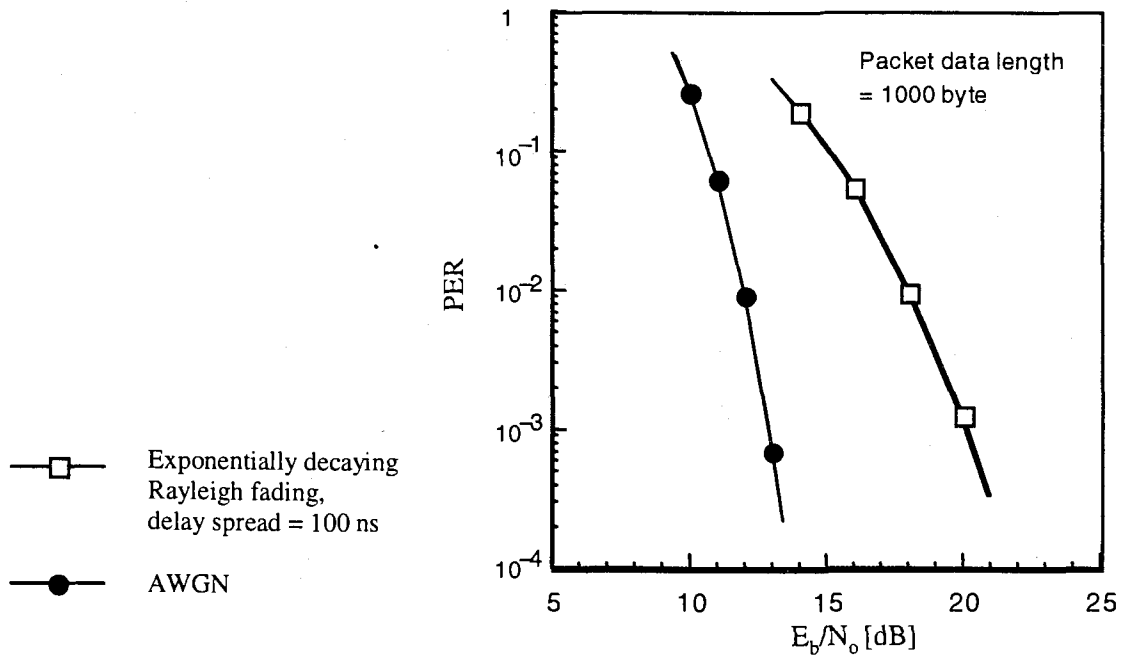


Figure 10.15 PER versus mean E_b/N_0 for AWGN and Rayleigh fading with a 100-ns delay spread and a bit rate of 24 Mbps.

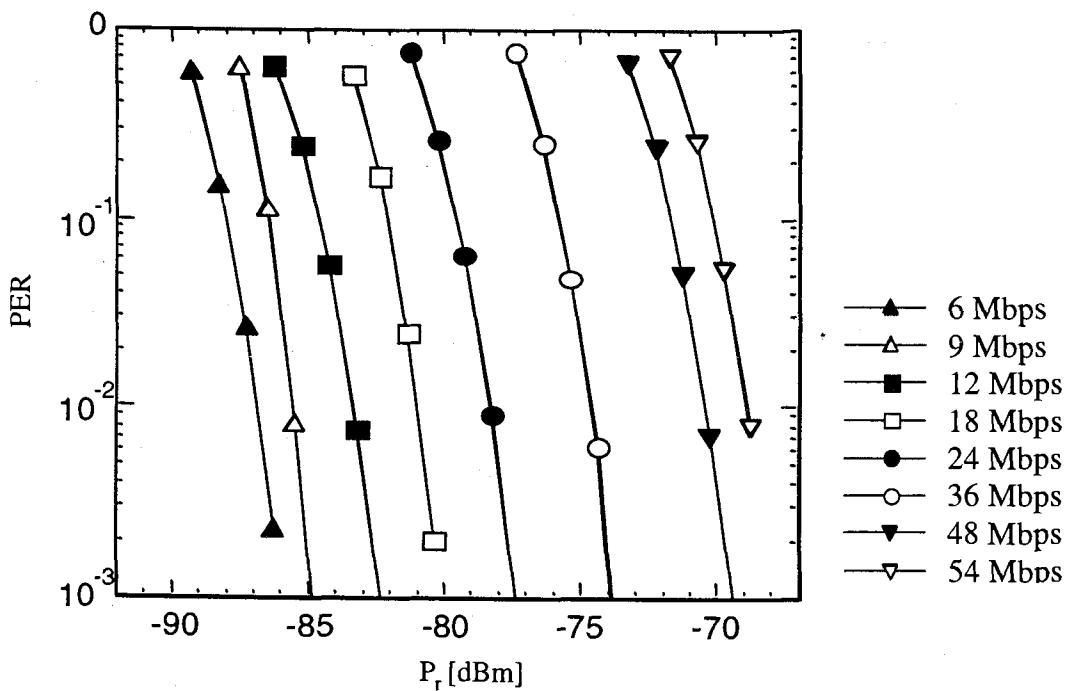


Figure 10.16 PER versus received power level for AWGN and various bit rates.

Figure 10.17 shows simulated spectra of an OFDM signal that is distorted by a nonlinear power amplifier with different backoff values. This is an important subject, because the susceptibility to nonlinear distortion and the need for large backoff values is often mentioned as a disadvantage of OFDM. As shown in [15], however, the effects of nonlinear distortion on the BER are negligible for backoff values of 6 dB or more, where the backoff is defined as the difference between the maximum (saturation) output power and the average output power in dB. The effects on the transmitted spectrum are illustrated in Figure 10.17. We can see that for a 7-dB backoff, the spectrum falls down very steeply after about 8 MHz, and only around 25 dB below the in-band density the spectrum starts to deviate significantly from an ideal undistorted OFDM signal. When the backoff is decreased to 5 dB, the out-of-band spectrum quickly grows toward the outer spectrum mask defined by IEEE 802.11.

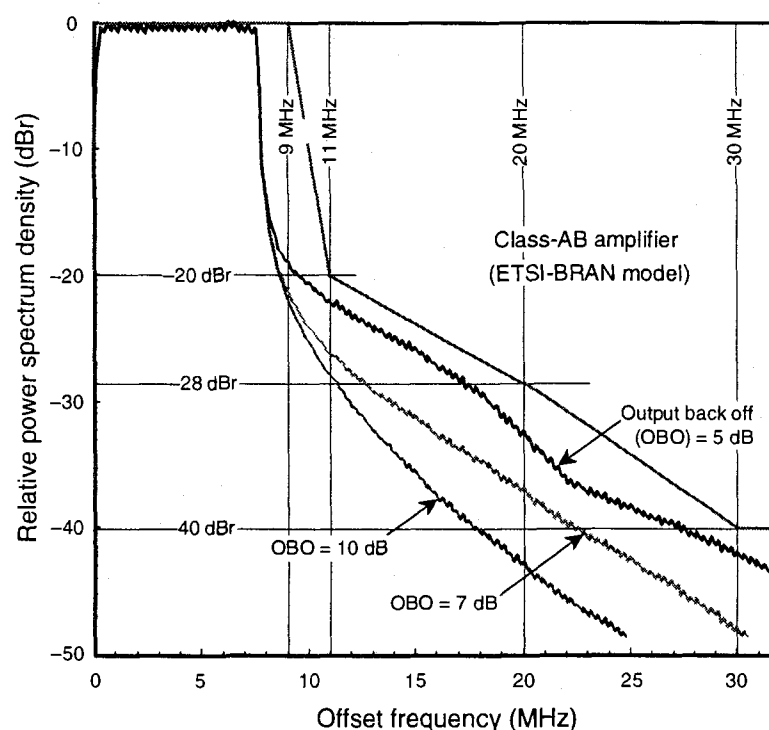


Figure 10.17 OFDM spectrum after a nonlinear power amplifier.

REFERENCES

- [1] ETSI, "Radio Broadcasting Systems: Digital Audio Broadcasting to Mobile, Portable and Fixed Receivers," European Telecommunication Standard, ETS 300-401, Feb. 1995.
- [2] Tuttlebee, W. H. W., and D. A. Hawkins, "Consumer Digital Radio: From Concept to Reality," *Electronics and Communication Engineering Journal*, Vol. 10, No. 6, pp. 263–276, Dec. 1998.

-
- [3] ETSI, "Digital Video Broadcasting: Framing Structure, Channel Coding, and Modulation for Digital Terrestrial Television," European Telecommunication Standard, EN 300-744, Aug. 1997.
 - [4] Reimers, U., "DVB-T: The COFDM-Based System for Terrestrial Television," *Electronics and Communication Engineering Journal*, Vol. 9, No. 1, pp. 28-32, Feb. 1997.
 - [5] Mikkonen, J., J. P. Aldis, G. A. Awater, A. Lunn, and D. Hutchinson, "The Magic WAND—Functional Overview," *IEEE JSAC*, Vol. 16, No. 6, pp. 953-972, Aug. 1998.
 - [6] Awater, G. A., and J. Ala-Laurila, "Wireless ATM Network Demonstrator," Presentation and Demonstration, *Demo '98 conference*, Berlin, Germany, Oct. 15, 1998.
 - [7] Passas, N., S. Paskalis, D. Vali, L. Merakis, "Quality-of-Service-Oriented Medium Access Control for Wireless ATM Networks," *IEEE Communications Magazine*, Vol. 35, No. 11, Nov. 1997.
 - [8] IEEE. 802.11, IEEE Standard for Wireless LAN Medium Access Control (MAC) and Physical Layer (PHY) specifications, Nov. 1997.
 - [9] FCC, "Amendment of the Commission's Rules to Provide for Operation of Unlicensed NII Devices in the 5-GHz Frequency Range," Memorandum Opinion and Order, ET Docket No. 96-102, June 24, 1998.
 - [10] ETSI, "Radio Equipment and Systems, High Performance Radio Local Area Network (HIPERLAN) Type 1," European Telecommunication Standard, ETS 300-652, Oct. 1996.
 - [11] Crow, B. P., I. Widjaja, J. G. Kim, and P. T. Sakai, "IEEE 802.11 Wireless Local Area Networks," *IEEE Communications Magazine*, pp. 116-126, Sept. 1997.
 - [12] Takanashi, H., and R. van Nee, "Merged Physical Layer Specification for the 5-GHz Band," IEEE P802.11-98/72-r1, Mar. 1998.
 - [13] IEEE, "Supplement to Standard for Telecommunications and Information Exchange Between Systems—LAN/MAN Specific Requirements—Part 11: Wireless MAC and PHY Specifications: High Speed Physical Layer in the 5-GHz Band," P802.11a/D7.0, July 1999.
 - [14] ETSI, "Broadband Radio Access Networks (BRAN); HIPERLAN Type 2 Technical Specification Part 1—Physical Layer," DTS/BRAN030003-1, Oct. 1999.
 - [15] Nee, R. van, "OFDM for High Speed Wireless Networks," IEEE P 802.11-97/123, Nov. 1997.

About the Authors

Richard D. J. van Nee was born in Schoonoord, the Netherlands, on January 17, 1967. He received an M.Sc. degree (cum laude) from Twente University of Technology, Enschede, the Netherlands, and a Ph.D. degree (cum laude) from Delft University of Technology, Delft, The Netherlands, in 1990 and 1995, respectively.

From December 1994, he worked as a private consultant to NovAtel Communications, Calgary, working on the design of multipath-robust GPS receivers, which were used in the reference stations of the United States Wide Area Augmentation System. In March 1995, he joined AT&T—now Lucent Technologies—Bell Labs in Utrecht, The Netherlands, where he is working in the area of high speed wireless communications. He was involved in the design of the OFDM modems for the European Magic WAND project. Together with NTT, he made the original OFDM-based proposal which lead to the IEEE 802.11 wireless LAN high-rate extension for the 5 GHz band. He was also one of the original proposers of the 11 Mbps IEEE 802.11 extension for the 2.4 GHz band. He holds several patents and published over 40 papers in the area of spread-spectrum tracking systems and OFDM.

Ramjee Prasad was born in Babhnaur (Gaya), Bihar, India, on July 1, 1946. He is now a Dutch Citizen. He received a B.Sc. (Eng) degree from Bihar Institute of Technology, Sindri, India and M.Sc. (Eng) and Ph. D. degrees from Birla Institute of Technology (BIT), Ranchi, India, in 1968, 1970 and 1979, respectively.

He joined BIT as a Senior Research Fellow in 1970 and became associate professor in 1980. While he was with BIT, he supervised a number of research projects in the areas of microwave communications and plasma engineering. During 1983 to 1988, he was with the University of Dar es Salaam (UDSM), Tanzania, where he rose to the level of professor of telecommunications at the Department of Electrical Engineering in 1986. At UDSM, he was responsible for the collaborative project “Satellite Communications for Rural Zones” with Eindhoven University of Technology, The Netherlands. From February 1988 to June 1999, he was with the Telecommunications and Traffic-Control Systems Group, Delft University of Technology (DUT), The Netherlands, where he was actively involved in the area of wireless personal and multimedia communications (WPMC). He was the Head of

the Transmission Research Section of IRCTR (International Research Center for Telecommunications - Transmission and Radar) and also Program Director of the Center for Wireless Personal Communications (CEWPC). Since June 1999, he has been with Aalborg University, Denmark as Co-director of Center for PersonKommunikation (CPK) and holds the Chair of Wireless Information and Multimedia Communications. He was involved in the European ACTS project FRAMES (Future Radio Wideband Multiple Access System) as a DUT Project Leader. He is Project leader of several international industrial funded projects. He has published over 300 technical papers, authored and co-authored three books "*CDMA for Wireless Personal Communications*," "*Universal Wireless Personal Communications*," and "*Wideband CDMA for Third Generation Mobile Communications*" published by Artech House, Boston. His current research interest lies in wireless networks, packet communications, multiple access protocols, adaptive equalizers, spread-spectrum CDMA systems, and multimedia communications.

He has served as a member of advisory and program committees of several IEEE international conferences. He has also presented keynote speeches, invited papers, and tutorials on WPMC at various universities, technical institutions, and IEEE conferences. He was the Organizer and Interim Chairman of the IEEE Vehicular Technology/Communications Society Joint Chapter, Benelux Section. He is now the Elected Chairman of the joint chapter. He is also founder of the IEEE Symposium on Communications and Vehicular Technology (SCVT) in the Benelux and he was the Symposium Chairman of SCVT'93.

He is the Co-ordinating Editor and Editor-in-chief of the Kluwer international journal on *Wireless Personal Communications* and also a member of the editorial board of other international journals, including the IEEE Communications Magazine and the IEE Electronics Communication Engineering Journal. He was the Technical Program Chairman of the PIMRC'94 International Symposium held in The Hague, The Netherlands, during September 19–23, 1994, and also of the Third Communication Theory Mini-Conference in conjunction with the GLOBECOM'94 held in San Francisco, CA, November 27–30, 1994. He was the Conference Chairman of IEEE Vehicular Technology Conference, VTC'99 (Fall), Amsterdam, The Netherlands held on September 19–22, 1999 and also the steering committee chairman of The Second International Symposium on Wireless Personal Multimedia Communications (WPMC), Amsterdam, The Netherlands held on September 21–23, 1999.

He is listed in the US Who's Who in the World. He is a fellow of the IEE, a fellow of the Institution of Electronics & Telecommunication engineers, a senior member of IEEE and a member of NERG (The Netherlands Electronics and Radio Society).

Index

- Additive white Gaussian noise (AWGN), 63, 69
- Advanced Communication Technologies and Services (ACTS), 3, 8, 233
- Air interface multiple access, 3
- Algorithm, 38, 239, 240, 247
- AM-PM conversion, 127
- Analog-to-digital conversion, 48
- ANDEFT, 23
- Antennas, 9, 10
- Anti-jamming, 159
- Asynchronous Transfer Mode (ATM), 1, 7, 12, 13, 14, 15, 229, 235, 237, 238, 239
 - adaptation layer, 14
 - network layer, 14
- Auto-covariance matrix, 98
- Automatic repeat request (ARQ), 243–245
- Available bit rate (ABR), 3, 4
- Averaging CDMA, 161
- Avoidance CDMA, 161
- AWACS, 3, 4

- Backoff, 125
- BAHAMA, 3
- Bandwidth, 47
- Battery, 9, 10
- Bessel function, 99
- Binary codes, 54
- B-ISDN, 7, 9, 12
- Bit error ratio (BER), 33, 66, 67
- Bit rate, 47
- Block codes, 54
- Block interleaver, 59
- BPSK, 6, 40, 62, 244
- Butterfly, 41, 145, 146

- CDMA era, 157
- CDMA, 25, 155–176

- Cell loss ratio (CLR), 243–245
- Channel
 - characterization, 2
 - coding, 220
 - estimate, 98
 - estimator, 96
 - model, 180–182
 - models, 16
- Clipping, 123–126
- Code sequence, 163–165, 170
- Coded modulation, 62–70
- Coding, 53–70
- Coherence time, 19, 20
- Coherent detection, 95–107
- Complementary code, 87
- Concatenated codes, 61
- Constant bit rate (CBR), 3
- Constellation, 41, 60, 57, 60, 62, 63, 66
- Convolutional codes, 55
- Convolutional interleaver, 59
- CORDIC algorithm, 50
- Correlation peak, 81, 86
- Correlation, 81
- Crest factor, 119
- Cross-covariance matrix, 98
- CSMA/CA, 6
- Cyclic extension, 39–42
- Cyclic prefix, 80, 81

- Data rate, 6, 8
- Decision feedback equalizer, 50
- DECT, 9
- Deep fades, 59
- Delay spread, 16–19, 33, 39, 43
- Delay, 39

- DFT, 22
- Differential amplitude and phase shift keying (DAPSK), 115

- Differential detection, 106–116
- Differential techniques, 48, 95, 106–116.
- Digital Audio Broadcasting (DAB), 23, 104, 233–235
- Digital filter, 45
- Digital Video Broadcasting (DVB), 104, 235–237
- Direct sequence (DS) CDMA, 160, 162–165, 182–184, 194
- Doppler shift, 19
- Doppler spread, 19, 33
- DS/FH CDMA, 161
- DS/TH CDMA, 161
- Dynamic channel allocation (DCA), 222, 229–232
- Effective guard time, 44
- Effective isotropic radiated power, 246
- Equal gain combining, 187
- Equalizer, 50
- Error floor, 67, 69, 70
- ETSI BRAN, 4, 5, 25, 229
- Fading channel, 68
- FDD, 4
- FFT, 22, 40, 47, 48
- FH/TH CDMA, 161
- Filtering, 45
- Forward-error correction coding, 33, 54–58
- Frame structure, 243
- FRAMES, 156
- Frequency division multiple access (FDMA), 213
- Frequency error standard deviation, 85
- Frequency hopping (FH) CDMA, 160, 165–168
- Frequency hopping OFDMA, 213–228
- Frequency
 - modulation (FM), 158
 - offset, 73, 77, 78
 - synchronization, 221
 - synchronization, 73, 75, 78
- Gaussian Minimum Shift Keying (GMSK), 49
- Global information village, 1, 2
- Gold codes, 197
- GSM, 7, 8, 9
- Guard time, 39–42
- Hamming distance, 54
- Hamming window, 124
- Handover, 173
- HDTV, 7, 23
- Health hazards, 2
- HIPERLAN, 5, 6, 7, 8, 241–251
- Hybrid
 - CDMA, 160
 - contention CDMA, 160
 - contentionless CDMA, 160
 - OFDM/CDMA, 160
- Ideal OFDM spectrum, 128
- IDFT, 36–39
- IEEE 802.11, 4, 5, 6, 7, 9, 25, 241–251
- IFFT, 33, 36–39, 43, 44, 47, 48
- Information bandwidth, 158
- In-phase component, 88
- Intercarrier interference (ICI), 39, 40, 44, 45, 46, 73
- Interference rejection, 159
- Interfrequency handover, 175
- Interleaving, 59
- Internet protocol (IP), 1
- Internet, 1
- Interpolation matrix, 98
- Intersymbol interference (ISI), 44, 45, 46, 73
- Irreducible packet error ratio, 70
- ISDN, 9
- ISM, 6
- Kaiser window, 124
- KATHRYN, 23
- KINEPLEX, 23
- Linear minimum mean square error (LMMSE), 176
- Lorentzian spectrum, 74
- Low probability of interception (LPI), 159
- Magic WAND, 3, 4, 25; 233–241
- Matched filter, 86
- Matrix inversion, 98
- Maximal ratio combining (MRC), 187
- Maximum delay spread, 18, 19
- Maximum likelihood decoding, 145–147
- MC-CDMA receiver, 188
- MC-CDMA transmitter, 188
- MEDIAN, 3, 4
- Medium access control (MAC), 242–252
- Minimum mean square error combining (MMSEC), 187
- MMAC, 4, 5, 241–251
- Mobile broadband systems (MBS), 5, 6, 12, 13, 14

- Mobile multimedia, 1
- Mobile telephony, 1
- Multi carrier (MC)-CDMA, 27, 160, 179–209, 215
- Multipath channel models, 16
- Multipath propagation, 15–20
- Multitone (MT)-CDMA, 160
- Multiuser detection (MUD), 175
- Multi-user detection, 155

- Narrowband CDMA, 157
- Network interface unit, 14, 15
- Non-binary codes, 54
- Non-ideal power amplifier, 127
- Normalized delay spread, 66, 68, 69
- Normalized Euclidean distance, 61, 69
- Normalized guard time, 67, 68
- Nyquist sampling, 96

- OFDMA, 213–228
- Offset synchronization, 222
- Optimal timing, 88
- Orthogonal Frequency Division Multiplexing (OFDM), 1, 3, 5, 20, 21, 22, 23, 33–51, 115, 233, 239, 241
 - preamble, 238, 244, 249–252
 - receiver, 95
 - symbol time, 41
 - transceiver, 48, 245
- Orthogonal restoring combining, 189
- Orthogonality, 35, 40, 41, 44, 89

- Packet error ratio (PER), 68, 69
- Packet transmission, 105
- PAP ratio distribution, 121–123
- PAP reduction codes, 138–150
- Parallel interference cancellation (PIC), 175
- Peak cancellation, 119, 130
- Peak windowing, 123–126
- Peak-to-average power (PAP), 121–156
- Phase
 - error, 84
 - estimation, 83
 - noise spectral density, 75
 - noise, 73
- Phase-locked loop (PLL), 76, 77
- Pilot estimates, 98
- Pilot subcarrier, 105
- Pilots, 97, 98, 236, 248, 251
- Postguard interval, 44

- Power
 - amplifier, 127
 - control, 172
 - delay profile, 17
 - spectral density, 134, 136
- Preguard interval, 44
- Privacy, 159
- Processing gain, 158
- PSK, 33, 95
- Pulse amplitude modulation (PAM), 60
- Pulse modulation (PM), 158
- Pure CDMA, 160

- QAM, 6, 33, 34, 35, 41, 46, 48, 53, 61–62
- QPSK, 6, 56, 60, 61, 62, 230, 232, 244
- Quadrature component, 88
- Quality of service (QoS), 243–245, 247
- Quantized OFDM signal, 87

- Radio interface unit (RIU), 14, 15
- Raised cosine, 45, 89
- RAKE receiver, 155, 171
- Random frequency hopping, 224
- Rapp's model, 127
- Rayleigh fading, 66, 68
- Reed-Solomon codes, 54
- Reference cancellation function, 131
- Repetition codes, 54
- Rolloff factor, 44, 45

- Safety considerations, 10, 11
- SAMBA, 3, 4
- Scrambling, 130, 150–152
- Sensitivity, 73
- Shift registers, 55
- Sidelobes, 81
- Signal processing, 47, 245
- Signal-to-noise ratio (SNR), 33, 46, 56–58, 96, 107, 232
- Single parity check, 54
- Single-carrier modulation, 49–51
- Single-sided spectrum, 74
- Smart antenna, 3
- Soft decision, 56, 58
- Soft handover, 173
- Spreading code, 157, 158, 160
- Spread-spectrum, 156
 - modulation, 158
 - multiple access (SSMA), 158
- Standard deviation, 81
- Subcarriers, 39

- Suboptimal decoding, 147
- Successive interference cancellation (SIC), 176
- SWAN, 3
- Symbol energy-to-noise density ratio (E_b/N_0),
56, 57, 59, 61, 62, 65
- Symbol scrambling, 150–152
- Symbol structure, 91
- Symbol time, 39, 44, 230, 235
- Synchronization, 73–92

- TDD, 4, 6
- TDMA, 4
- TDMA/CDMA, 161
- Time hopping (TH) CDMA, 160–170
- Time synchronization, 221
- Timing errors, 78–80
- Timing offset, 73
- Tracking loop bandwidth, 76
- Training symbol, 81
- Transmission bandwidth, 158
- Trellis coding, 62

- UMTS, 9
- UNII, 6

- Variable bit rate (VBR), 3
- Very large scale integration (VLSI), 23
- Very-High-Speed Digital Subscriber Line
(VDSL), 23
- Virtual channel identifier (VCI), 13
- Virtual path identifier (VPI), 13
- Viterbi decoding, 56
- Voltage controlled Oscillator (VCO), 76

- Walsh-Hadamard code, 197
- Walsh-Hadamard transform, 146, 147
- WATM, 3
- Wideband CDMA, 157
- Windowing, 42–46, 235, 245
- Wireless Broadband Mobile Communication
Systems, 12, 13, 14, 15
- Wireless Customer Premises Network
(WCPN), 2
- Wireless Local Area Network (WLAN), 1, 2, 6,
- Wireless Local Loop (WLL), 2

The Artech House Universal Personal Communications Series

Ramjee Prasad, Series Editor

CDMA for Wireless Personal Communications, Ramjee Prasad

OFDM for Wireless Multimedia Communications, Richard van Nee
and Ramjee Prasad

Third Generation Mobile Communication Systems, Ramjee Prasad,
Werner Mohr, and Walter Konhäuser, editors

Universal Wireless Personal Communications, Ramjee Prasad

Wideband for Third Generation Mobile Communications, Tero
Ojanperä and Ramjee Prasad, editors

For further information on these and other Artech House titles,
including previously considered out-of-print books now available
through our In-Print-Forever® (IPF®) program, contact:

Artech House
685 Canton Street
Norwood, MA 02062
Phone: 781-769-9750
Fax: 781-769-6334
e-mail: artech@artechhouse.com

Artech House
46 Gillingham Street
London SW1V 1AH UK
Phone: +44 (0)20 7596-8750
Fax: +44 (0)20 7630-0166
e-mail: artech-uk@artechhouse.com

Find us on the World Wide Web at:
www.artechhouse.com

Written by leading experts in the field of wireless communications, *OFDM for Wireless Multimedia Communications* is a practical guide to planning, designing, and using orthogonal frequency division multiplexing (OFDM). It offers you a thorough overview of OFDM signal processing techniques, and provides a solid base for assessing the performance of wireless OFDM systems.

Technical details of OFDM are provided, along with explanations of how OFDM signals are formed using the inverse fast Fourier transform, how windowing can limit out-of-band radiation, and how the cyclic extension mitigates the effects of modulation. You also learn how to assess the performance of OFDM-based systems in terms of SNR and delay-spread tolerance.

OFDM for Wireless Multimedia Communications contains a valuable investigation of the applications of OFDM, including digital audio and video broadcasting and wireless ATM. Plus, it helps you understand IEEE 802.11, MMAC, and HiperLAN standards for wireless LAN.

Richard van Nee, Ph.D., is a member of the technical staff at Lucent Technologies/Bell Labs in the Netherlands. He was among those who proposed the OFDM-based physical layer, which was selected for standardization in IEEE 802.11, MMAC, and ETSI HiperLAN. **Ramjee Prasad, Ph. D.**, is Wireless Information and Multimedia Chair and Co-Director of the Center for Person-Kommunikation at Aalborg University. He is the author of *CDMA for Wireless Personal Communications* and *Universal Wireless Personal Communications*, and coauthor of *Wideband CDMA for Third Generation Mobile Communications*, all published by Artech House.

